MEKELLE UNIVERSITY

COLLEGE OF NATURAL AND COMPUTATIONAL SCIENCES

FACULTY OF MINING AND GEOSCIENCES

A Thesis On

Enhancing Water Security through Water Harvesting and Groundwater Recharge in Arid and Semi-Arid Regions: A Case Study from Yechilla area, Tigray (Northern Ethiopia)

Submitted to the Faculty of Mining and Geosciences in Partial Fulfillment of the Requirements for the Degree of Master of Science in Geological Engineering

By

Hailay Gebreslassie Berhe

Under the supervision of

Dr. Gebremedhin Berhane (Associate professor)

And

Dr. Tesfamichael Gebreyohannes (Associate professor)

March, 2026

Mekelle, Ethiopia

APPROVAL SHEET

MEKELLE UNIVERSITY

COLLEGE OF NATURAL AND COMPUTATIONAL SCIENCES

FACULTY OF MINING AND GEOSCIENCES

Enhancing Water Security through Water Harvesting and Groundwater Recharge in Arid and Semi-Arid Regions: A Case Study from Yechilla area, Tigray (Northern Ethiopia)

SUBMITTED BY:

Hailay Gebreslassie Berhe ID.No. CNCS/PRG001/13 _____ 27/04/2026
Signature Date

APPROVED BY:

Dr. Gebremedhin Berhane Advisor	Signature	27/04/2026 Date
Dr. Fthanegest Weldemariam Faculty Head	Signature	07/05/2026 Date
Mr. Tesfahunegn Abera Chairperson	Signature	27/04/2026 Date
Dr. Asmelash Abay Internal Examiner	Signature	27/04/2026 Date
Dr. Ashenafi Zeabreha External Examiner	Signature	27/April/2026 Date

Declaration

I, the undersigned, declare that this thesis entitled **"Enhancing Water Security through Water Harvesting and Groundwater Recharge in Arid and Semi-Arid Regions: A Case Study from Yechilla area, Tigray (Northern Ethiopia)"** is my original work and has not been presented for any other award, and that all sources of materials used in this thesis are duly acknowledged. This thesis was carried out under the supervision of my principal advisor Dr. Gebremedhin Berhane and co-advisor Dr. Tesfamichael Gebreyohannes, Faculty of Mining and Geosciences, College of Natural and Computational Sciences, Mekelle University in the academic year of 2025/2026.

Hailay Gebreslassie

Signature _____

This thesis has been submitted for examination with my approval as university **advisor/co-advisor**.

Name of the advisor Dr. Gebremedhin Berhane

Signature of the Advisor with date: _____

Name of the co-advisor: Dr. Tesfamichael Gebreyohannes

Signature of the co-advisor with date: _____

Mekelle University, Mekelle, Ethiopia

Date of submission: *07/05/2026*

ACKNOWLEDGMENT

I would like to express my sincere gratitude to Adigrat University and Mekelle University for granting me the opportunity to pursue my postgraduate studies at Mekelle University.

This MSc research was supported by the VLIR-UOS funded project (ET2023SIN389A103), a collaborative initiative between Ghent University (Flemish Government) and Mekelle University (Registration No. RDPD/MU/EXTERNAL/004/2023), for which I am deeply grateful. I also acknowledge the additional financial support provided by Mekelle University through the Ethiopian Ministry of Education. Furthermore, I extend my sincere appreciation to the Faculty of Mining and Geosciences at Mekelle University for their unwavering support throughout every stage of this research.

My deepest gratitude goes to my advisor, Dr. Gebremedhin Berhane, for his unwavering guidance, invaluable advice, constructive feedback, and continuous encouragement throughout my thesis work. I sincerely appreciate his insightful discussions, limitless support at every stage, and his generosity in suggesting and providing essential reference materials. Above all, I am truly grateful for his approachable and supportive demeanor, which greatly enriched my research journey.

I would like to express my deep thanks to my co-advisor, Dr. Tesfamichael Gebreyohannes, for his hands-on guidance in hydrogeological fieldwork and for teaching me GIS and Remote Sensing, which played a crucial role in my research. I am also deeply grateful to Prof. Miruts Hagos for his invaluable support in geological and structural assessments during my field data collection. Additionally, I extend my thanks to Dr. Abdelwassie Hussien for his expert advice on hydrogeological data collection techniques in the field.

I would also like to extend my sincere appreciation to my colleagues for their invaluable contributions to my thesis work. Special thanks go to Mr. Hailemikael Hans for his assistance with GIS, Mr. Gebremariam Mesele for his help in geological cross-section preparation and Global Mapper, Mr. Misgan Mola, Mr. Yohannes Berhanu and Mr. Hagos Hiluf for their help in sharing essential reference materials and moral support, and Mr. Ashenafi Fitsum for his support in laboratory sieve analysis. Their expertise and generosity greatly facilitated the progress of my research.

I would like to extend my heartfelt gratitude to the community of Yechilla town and its surrounding areas for their kindness and invaluable assistance during my fieldwork. Their warm hospitality and support made my research experience both productive and memorable.

Last but not least, I wish to express my deepest appreciation to my wife, Amit Gereziher, for her continuous moral support throughout my studies. Special thanks to my beloved daughter Rodas for her patience during my extended fieldwork absences. I am very grateful to all my family members.

TABLE OF CONTENTS

LIST OF FIGURES

LIST OF TABLES

LIST OF ABBREVIATIONS AND SYMBOLS

λ:	Joint frequency
Δt:	Time interval
ΔV:	volume of liquid used during time interval to maintain constant head in the infiltrometer ring
AGWR:	Artificial Groundwater Recharge
AHP:	Analytical Hierarchy Process
ANS	Arabian-Nubian Shield
AR:	Artificial Recharge
A_r:	Internal Area of infiltrometer ring
ASTER:	Advanced Space borne Thermal Emission and Reflection Radiometer
ASTM:	American Standard Testing and Materials
Av.:	Average
B:	Bedding
CHRS:	Center for Hydrometeorology and Remote Sensing
DD	Drainage Density
deg.:	degree
DEM:	Digital Elevation Model
EIGS:	Ethiopian Institute of Geological Survey
ENMA	Ethiopian National Meteorological Agency
Ethio:	Ethiopian
E-W:	East-West
F:	Foliation
FWH:	Flood Water Harvesting
GIS:	Geographic Information System
GWH:	Groundwater Harvesting
GWR:	Groundwater Recharge
IAEG:	International Association for Engineering Geology and the Environment
IDW:	Inverse Distance Weighting
I_r:	Infiltration rate
ISRM:	International Society for Rock Mechanics
J1:	Joint set 1
J2:	Joint set 2
J3:	Joint set 3

JCS:	Joint Compressive Strength
J_v:	Volumetric joint count
L:	Sample length measured perpendicular to the adjacent joint intersections in joint spacing measurement
LD	Lineament Density
LULC:	Land Use/Land Cover
Ma:	Mega annum (Million years ago)
MCDM	Multi-Criteria Decision Making
MS:	Meta-Sediment
Mts.:	Mountains
MV:	Meta-Volcanic
MVC:	Meta-Volcanic Clast
n:	Number of joints
NGWR:	Natural Groundwater Recharge
NNE-SSW:	North Northeast-South Southwest
NW:	Northwest
NW-SE:	Northwest-Southeast
PWCM	Pairwise Comparison Matrix
RF:	Rainfall
RMR:	Rock Mass Rating
RQD:	Rock Quality Designation
RWH:	Rain Water Harvesting
Sh:	Shear
TRB:	Tekeze River Basin
UCS:	Uniaxial Compressive Strength
USGS:	United States Geological Survey
UTM:	Universal Transverse Mercator
WH:	Water Harvesting
WTF:	Water Table Fluctuation

APPENDICES

Appendix A: Infiltration Test Data for 10 Selected Site Locations of the Study Area

Appendix B: Discontinuity Measurements

Appendix C: Uniaxial Compressive Strength (Schmidt hammer) tests

Appendix D: Laboratory Soil Texture Analysis

ABSTRACT

Water scarcity in arid and semi-arid regions, aggravated by climate change and population growth, poses significant challenges to sustainable development, particularly in Sub-Saharan Africa. Groundwater depletion, driven by overexploitation and reduced recharge, threatens water security, food production, and ecosystem stability. Water harvesting (WH) and groundwater recharge (GWR) strategies offer viable solutions to enhance water availability and resilience. This study focuses on the geological, hydrogeological, and engineering geological characterization of Yechilla, Central Tigray, Northern Ethiopia, to assess its suitability for WH and artificial recharge (AR) aimed at improving water security and sustainability. The study area is situated within the Tekeze River Basin (TRB) and encompasses seven lithologic units: metavolcanic, metasediments, granite intrusions, sandstone, trap basalt, dolerite sills, and alluvial deposits. Detailed field data collection including soil sampling and description, infiltration test, discontinuity measurements and UCS (Schmidt hammer test) were done during the extended research study. Laboratory soil textural analysis, employing sieve and hydrometer methods, was used to classify soils based on hydrologic soil groups (HSG). A GIS-based multi-criteria decision-making method was employed to identify potential WH and GWR zones, utilizing eight criteria: lithology, soil texture, slope, elevation, drainage density, lineament density, rainfall, and land use/land cover (LULC). The relative importance of each factor was determined through pairwise comparisons using the Analytical Hierarchy Process (AHP). Suitability classes were assigned to all parameters, followed by weighted overlay analysis in ArcGIS 10.8 to generate integrated suitability maps, which were validated using field data and high-resolution Google Earth imagery with ROC-AUC curve analysis. Results indicate that fluvial soils, composed of over 97% sand, exhibit high infiltration rates and low runoff potential, whereas residual soils formed from in-situ weathering display varied textures—including clay, sand, and loam—that influence water retention and runoff properties. Infiltration tests revealed rates ranging from 0.2 cm/hour (slow) in clay soils to 4.7 cm/hour (medium) in sandy soils. The final suitability map classified WH zones as 14.20% (very high), 29.50% (high), 22.00% (moderate), 22.40% (low), and 11.90% (unsuitable), while GWR yielded 11.30%, 24.34%, 33.90%, 26.85%, and 3.64%, respectively. With AUC values of 80.10% (WH) and 84.30% (GWR), the study demonstrates that the AHP method, combined with field validation, effectively identifies appropriate potential zones. These findings offer decision-makers and planners a robust framework for developing effective water management strategies by pinpointing optimal sites for water harvesting and groundwater recharge, thereby promoting sustainable water sources in Yechilla and similar water-scarce regions.

***Keywords**: AHP, Arid semiarid regions, GIS, Groundwater Recharge, Water harvesting, Water scarcity, Yechilla*

CHAPTER ONE

1. INTRODUCTION

1.1. Background of the study

Water is a vital resource for human and animal survival, as well as for economic development (Berhane, 2016; Haile & Suryabhagavan, 2019; Mahmood et al., 2020). Arid and semi-arid regions encompass roughly 43% of the world's land surface, and these areas are defined by limited water availability, elevated temperatures, and reduced precipitation (Perez-Aguilar et al., 2021). Many countries in Sub-Saharan Africa (SSA) face significant challenges related to low water productivity and high rainfall variability, which is often worsened by the impacts of climate change, creating a complex web of environmental and socio-economic difficulties (Woldearegay et al., 2018).

Water security and management play an essential role in ensuring food security, impacting every stage of the food supply chain, and fostering sustainable agricultural practices (Manisha et al., 2024). To address these issues, implementing effective water harvesting (WH) structures and groundwater recharge GWR) are essential for enhancing water security and mitigating the impacts of climate change on water availability (Al-Adamat, 2008). One of the significant implications of water harvesting is for groundwater recharge and overall groundwater management (Adhikari et al., 2013; Alataway and El Alfy, 2019; Dillon et al., 2019; Hussain et al., 2019 ;Huang et al., 2021; Ertop et al., 2023).

A brief review of the literature reveals that groundwater supplies drinking water to approximately 50% of the world's population and accounts for 43% of all water used for irrigation. In addition, it is estimated that a total of 2.5 billion people rely solely on groundwater resources to meet their basic daily water needs (Lall et al., 2020; Barthel et al., 2021). However, over-pumping and/or overexploitation of aquifers to satisfy various competing water uses, climate change, etc., are causing groundwater levels to decline. Groundwater depletion has several effects, including (a) lowering of the water table; (b) reduction in water in streams and lakes; (c) ground subsidence; (d) increased costs to the user; (e) deterioration of water quality and ecological damage, etc. Excessive groundwater depletion affects large regions of North

Africa, the Middle East, South and Central Asia, Northern China, North America, and Australia, as well as in various local areas around the world (Lall et al., 2020; Barthel et al., 2021). The groundwater depletion rate is accelerating around the world, and the consequences are continually worsening, highlighting the need for an objective analysis of the problem and consideration of possible solutions. As a result, the depletion of groundwater is an issue of global interest.

In many developing countries, such as those in sub-Saharan Africa (e.g., Ethiopia, Kenya, etc.), groundwater serves as a main source of drinking water for many urban dwellers estimated at 30% (Chakava et al., 2014) due to its better quality and minimal treatment needs (Jebamalar et al., 2012). However, urbanization increases/accelerates groundwater demand while reducing the groundwater recharge areas (Abd-Elaty et al., 2024), leading to the decline and complete extraction of groundwater (Noori and Singh, 2023). This issue is particularly severe in arid and semi-arid regions, which make up over 40% of the Earth's surface, causing significant groundwater depletion globally (Adhikari et al., 2013; Wang et al., 2021; Ahmed et al., 2023). Recharge is essential to sustain water resources and build resilience against climate change and shifting water demands (Barthel et al., 2021). Among the internationally proposed measures to tackle the problem are groundwater recharge (GWR) and surface water harvesting. This can be conducted both naturally through rainfall and artificially through human intervention.

According to Yannopoulos et al. (2019), rainwater harvesting systems are being increasingly adopted by African countries. However, despite the rapid expansion of these systems, progress remains slow due to several factors: (a) low and seasonal rainfall, (b) a limited number and size of impervious roofs, (c) the high cost of constructing catchment systems relative to typical household incomes, (d) a lack of cement and properly graded sand in certain regions of Africa, and (e) insufficient water resources for the construction industry, which adds to the overall costs. Water harvesting (WH) systems are increasingly expanding in Africa (e.g., Kenya, Ethiopia, South Africa, Mali, etc.) (Chakava et al., 2014).

WH is the collection, storage, and use of rainwater or surface runoff to supplement or replace other water sources (Prinz, 1996; Denison and Wotshela, 2012). It involves capturing water via systems like rooftop catchments or small dams, storing in tanks or reservoirs, and distributing it

for drinking, irrigation, livestock, or groundwater recharge (Ertop et al., 2023). WH plays a key role in groundwater recharge and management (Adhikari et al., 2013; Alataway and El Alfy, 2019; Dillon et al., 2019; Hussain et al., 2019; Huang et al., 2021; Ertop et al., 2023). Captured surface runoff percolates into the ground, replenishing aquifers and helping maintain groundwater levels, especially in overexploited areas. By reducing reliance on groundwater for domestic, agricultural, and industrial uses, it slows groundwater depletion and supports aquifer recovery. Rainwater harvesting, in particular, offers relatively clean water for recharge, diluting contaminants and improving the groundwater quality. Integrating WH into management strategies promotes resource sustainability, supports ecosystems, and maintains stream flows and wetlands.

The effectiveness of WH for GWR depends on local hydrogeology, system design, and regional water management practices (Abu-Taleb, 2003). When well-implemented, it supports integrated water resource management by enhancing groundwater availability, quality, and sustainable use.

In case of Ethiopia, particularly in Tigray, various water harvesting and groundwater recharge activities have been implemented, aiming to improve water security and support sustainable livelihoods (Woldearegay et al. 2018). One example of successful activity in the region is the Abreha-We Atsbeha, Kilete-Awlaelo Wereda; eastern Tigray (Gebru et al. 2021). The study area (Yechilla, central zone, Tigray, Northern Ethiopia) is affected by water scarcity due to low rainfall, high temperature and population growth. In addition to this, the Ethio-Tigray war worsened the situation in the area. Hence, this study was concerned on the geological, hydrogeological and engineering geological characterization of the area for water harvesting and groundwater recharge suitability.

1.2. General description of the study area

1.2.1. Location and Accessibility

The research area is located around Yechilla (Tigray), Northern Ethiopia. It is about 115km to the southwest of Mekelle city, the capital of Tigray Regional state. The area is part of Tekeze River Basin specifically located southwest to south to southeast catchment of the Yechilla town with geographic location bounded by 494714m to 508138m E longitude and 1458791m to 1469753m N latitude (figure 1.1) and an elevation ranging from 1491 to 2265 m above mean sea

level. The areal coverage of the catchment is about 81 km^2. The area is accessed by a major gravel road, N-S crossing the Yechilla town, which is running to Amhara region to the south and connected to the Abi-Adi-H/selam asphaltic road (Agbe town) to the north. Another dry gravel road is to the west reaching to Tekeze dam and to the east through Gijet connected to Samre-Mekelle main road.

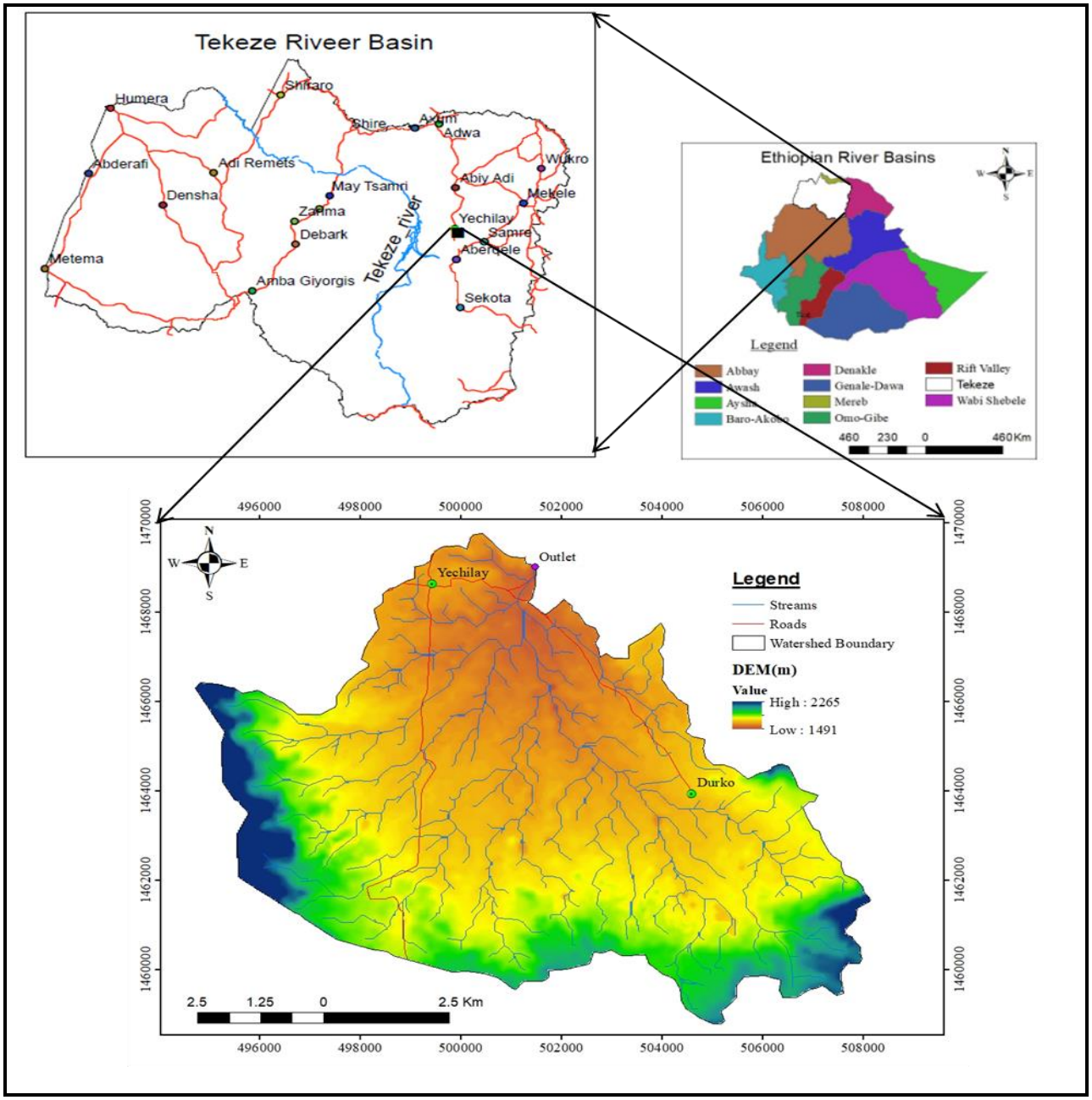

Figure 1.1: Location map of the study area with reference to Ethiopian River Basins (from Ethio-GIS dataset), the specific target area (extracted from Tigray_DEM and processed in ArcGIS 10.8)

1.2.2. Physiography and Drainage pattern

Yechilla area is bounded by mountainous and rugged topography to the east, southeast, south, southwest and west and gentle to flat topography to the north and northwest directions (Figure 1.2). Mostly the gentle to flat topography is an agricultural farmlands and the steeply sloped and hilly area is rocky. The catchment area is dominantly characterized by dendritic type of drainage pattern (Figure 1.1). The small streams flowing from SW, S and SE directions are gradually joining to the main river at various angles, and then running to NW direction.

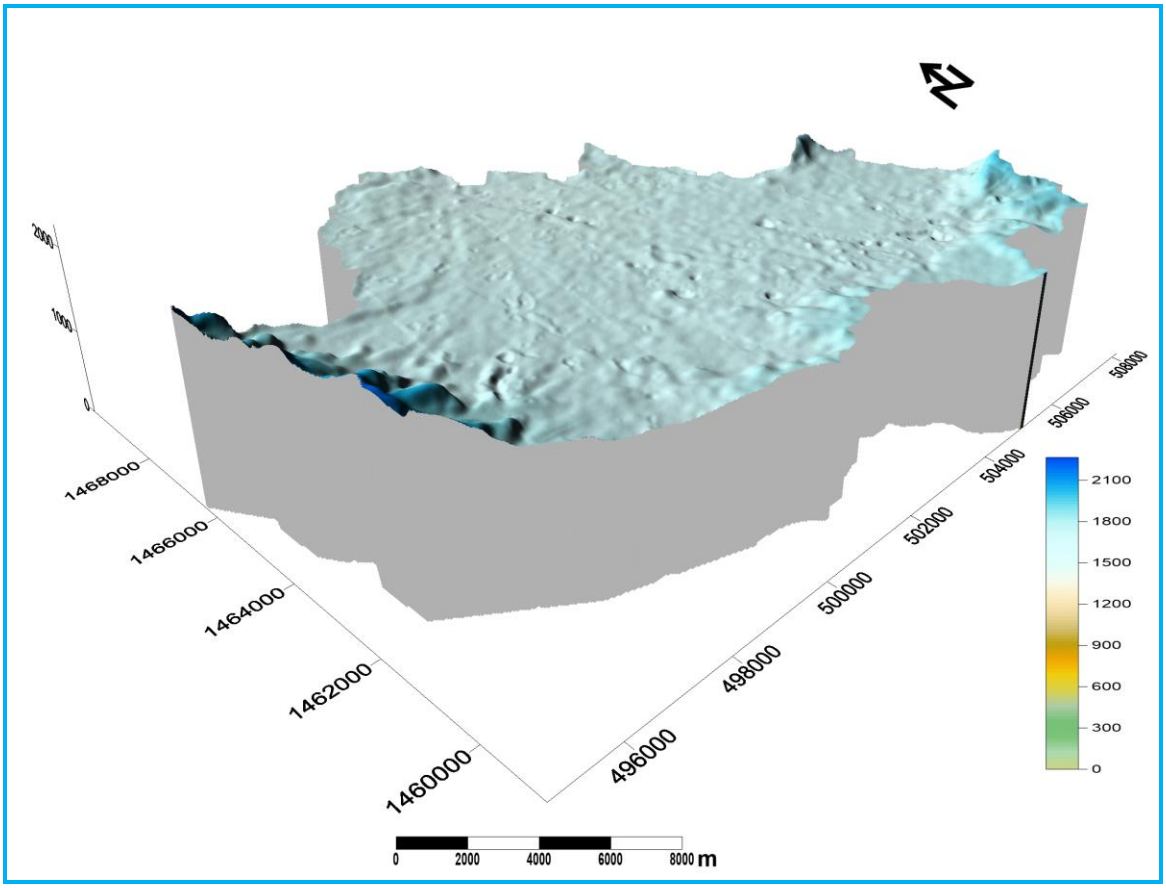

Figure 1.2: Physiographic map of the study area

1.2.3. Climatic condition and Vegetation

The area is part of semi-arid region as of very low vegetation cover, low rainfall patterns and high temperature. The mean monthly rainfall in the main rainy season (June-September) ranges from 59 mm in September to 239 mm in July and the annual rainfall ranges from 206 mm to 1402 mm with an average of approximately 700 mm (data recorded for the period of 1991-2024 from CHRS and https://power.larc.nasa.gov/data-access-viewer/). The mean minimum and

maximum annual temperature of the area varies from 17-20.4^{o}C and 30-35.4^{o}C respectively (data from Ethiopian National Meteorological Agency and https://power.larc.nasa.gov/data-access-viewer/).

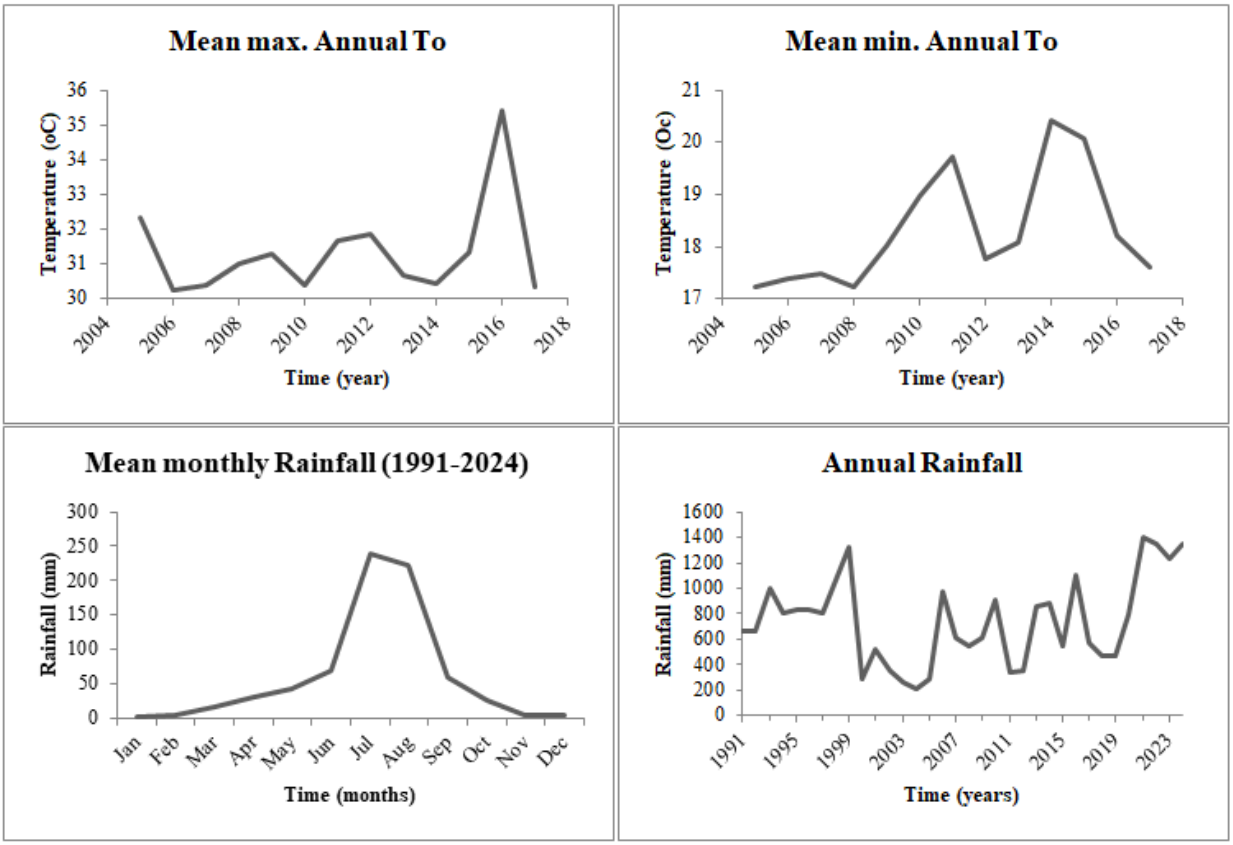

Figure 1.3: Rainfall and Temperature conditions of the Yechilla area (data sourced from ENMA and https://power.larc.nasa.gov/data-access-viewer/)

1.3. Statement of the problem

Water scarcity is a critical challenge in arid and semi-arid environments of Tigray, significantly affecting agricultural productivity, drinking water supply, and overall community well-being. The Ethio-tigray war, which broke out in November 2020 is another problem compounding the drought in the region. The war and siege on Tigray has been waited for more than two years and all the infrastructures including the water sector are destroyed by the Ethiopian and Eritrean armies. The study area (Yechilla) is one of the war battles, which is called *"shewate hugum war"*. So, this area is degraded due to the war in addition to erratic rainfall patterns leading to severe socio-economic consequences for local populations. There were no any water supply constructions and maintenances because of the war for the last four years.

Figure 1.4: Water scarcities in the area; (a) damaged and dried hand pump well, (b) the community used untreated and polluted water, (c) Water shortage for livestock due to poor water harvesting structures, and (d) Poor water harvesting technique that causing insufficient water for irrigation

The study area currently lacks sufficient scientific research on its geological framework, engineering geological properties, and hydrogeological characteristics, which are critical for effective WH and GWR initiatives.

Field assessment revealed that more than 10 of the 19 wells in the study area were dried. The data gathered from the local people by questionnaires and interviews indicated that most of the

wells are dried in short period of time. For reconstruction insights in these problems, implementation of water harvesting techniques and groundwater recharge methods becomes essential in the area. Some WH techniques are practiced by the community such as ponds, stone bunds and sand dams. However, geological, hydrogeological and engineering geological studies are fundamentally needed to select the suitable site for the WH and GWR methods.

The current research aims to address the research and existing knowledge gap surrounding the efficacy and applicability of these methods in the study area. By investigating the potential of WH and GWR in enhancing water security, this study seeks to contribute to sustainable water management practices tailored to the climatic and war challenges faced in Yechilla area, Tigray, Northern Ethiopia.

1.4. Objectives of the study

1.4.1. General Objective

The general objective of the study is to assess and select effective water harvesting and groundwater recharge potential sites in Yechilla area, central Tigray, Northern Ethiopia aimed at improving water security and sustainability.

1.4.2. Specific Objectives

The specific objectives of the study are to:

- Analyze and characterize discontinuity and strength of the rock exposures of the area as relevant to water permeability and stability
- Constrain the permeability of the soils through infiltration test and soil textural classification
- Produce detail geological map of the area at the scale of 1:25,000
- Select the WH and GWR potential sites using geology, soil texture, slope, elevation, drainage density, lineament density, rainfall and LULC assessments
- Formulate policy and institutional recommendations for sustainable adoption of WH and GWR technologies, addressing gaps in governance, community participation, and maintenance frameworks.

1.5. Hypothesis/Research questions

The following research questions were addressed:

- ✓ What are the current water scarcity challenges faced by communities in Yechilla, Tigray, Northern Ethiopia?
- ✓ What are the existing water harvesting and groundwater recharge methods being employed in the study area?
- ✓ What geological and hydrogeological conditions in the selected sites influence the effectiveness of water harvesting and groundwater recharge techniques?
- ✓ What best practices can be identified from successful case studies of water harvesting and groundwater recharge in similar climatic regions?
- ✓ What policy frameworks and institutional support are necessary to promote sustainable water management in arid and semi-arid regions?

1.6. Significance of the study

The study aims to provide practical solutions to the critical water scarcity issues faced by communities in Yechilla. By identifying suitable sites and effective water harvesting and groundwater recharge techniques, the research can help improve water availability for agricultural and domestic use, thereby enhancing food security and livelihoods. This research promotes sustainable water management practices fitted to the unique climatic, geological and hydrogeological conditions of the area. The findings can guide policymakers and local authorities in developing strategies that preserve and optimize water resources.

CHAPTER TWO

2. LITERATURE REVIEW

2.1. Overview

Water scarcity is a global problem recognized by the World Economic Forum as one of the most significant threats facing the world today (World Economic Forum 2011). According to AL-Shammari et al. (2021), Water scarcity can be classified as either physical or economic. Physical water scarcity refers to a limited availability of water in regions, particularly in arid and semiarid areas. Economic water scarcity arises from inadequate investment in water resources or insufficient capacity to meet water demands, even in regions that may have abundant water supplies.

WH systems are critical for improving water resources worldwide, in general, and in arid and semi-arid regions in particular (Bhattacharya, 2010; Jebamalar et al., 2012; Gontia and Patil, 2012; Adhikari et al., 2013; Lasage and Verburg, 2015; Nachshon et al., 2016; Alataway and El Alfy, 2019; Hussain et al., 2019; Yannopoulos et al., 2019; Tamagnone et al., 2020; Huang et al., 2021; Ertop et al., 2023; Noori and Singh, 2023; Raimondi et al., 2023; Umukiza et al., 2023; Wartalska et al., 2024). Techniques like percolation tanks and check dams (dams on small gully) enhance GWR and improve water quality, particularly in semi-arid regions (Bhattacharya, 2010; Jebamalar et al., 2012). Alataway and El Alfy (2019) emphasized that rainwater harvesting (RWH) and GWR strategies are effective in mitigating water scarcity in arid environments facing rising demands and climatic challenges. Similarly, Ertop et al. (2023) addressed growing water scarcity caused by population growth, climate change, and unplanned industrialization, advocating RWH as a practical solution for irrigation and domestic uses of water management.

RWH offers multiple benefits, including cost-effectiveness, flood mitigation, GWR, and supporting sustainable agriculture (Huang et al., 2021). Huang et al. (2021) advocate for globally systematic RWH implementation, emphasizing the use of local knowledge and materials to develop decentralized, community-based systems as alternatives to centralized water supplies. Hussain et al. (2019) highlight RWH through recharge wells as a solution for urban flooding and groundwater depletion. Lasage and Verburg (2015) analyze various WH methods, examining

their physical, economic, and governance characteristics. They propose a decision-making framework for selecting suitable techniques based on local conditions, concluding that larger structures are more cost-effective but require complex governance, while smaller systems are easier to implement but may incur higher costs per unit of water stored.

Water turbidity has a significant effect on the efficiency of GWR in reservoirs. Increased turbidity levels result in higher sedimentation rates within sand columns, infiltration ponds, micro-dam reservoirs, etc., used for recharge, which in turn reduces the flow rate of water infiltrating into the aquifer (Azis et al., 2015). This highlights the necessity for utilizing high-permeability sand columns in recharge reservoirs and implementing strategies to prevent turbid water from entering these systems. By doing so, optimal GWR rates can be maintained, helping to alleviate problems such as land subsidence and seawater intrusion that arises due to excessive groundwater extraction.

Gwenzi and Nyamadzawo (2014) discuss the hydrological impacts of urbanization and roof water harvesting in water-limited catchments, with a focus on sub-Saharan Africa. They highlight how urbanization alters hydrological processes, increases surface runoff, and reduces GWR. Researches on GWR methods, both natural and artificial, have been extensively explored by several studies (Abu-Taleb, 2003; Brown and Signor, 1974; Hashemi et al., 2013; Mukherjee, 2016). GWR estimation techniques are examined in works like (Gee and Hillel, 1988; Sibanda et al., 2009; Islam et al., 2015; Singh et al., 2019; Cambraia Neto and Rodrigues, 2020; Sun et al., 2024). These studies employ various methods based on factors such as hydrological and climatic conditions, hydrogeological conditions (soil and geological characteristics), land use patterns, data availability, scale of study (e.g., local or regional and short-term or long-term), and research objectives. The diversity in approaches reflects the complexity of GWR processes and the need to adapt methods to specific environmental and study area contexts.

Gee and Hillel (1988) explore the complexities of estimating natural GWR in arid regions, emphasizing the variability of recharge rates, limitations of common methods, and significance of the vadose zone. Recharge variability depends on factors like climate, soil type, vegetation, and topography, which can lead to inaccuracies if estimates are based solely on average precipitation. Traditional methods, such as water balance calculations and simulation models,

often yield unreliable results due to challenges in measuring components like evapotranspiration and soil moisture. The vadose zone, lying between the soil surface and the water table, plays a critical role in recharge, with water sometimes moving rapidly through narrow pathways and bypassing larger volumes of soil. This creates concentrated recharge events that are difficult to predict. Gee and Hillel (1988) advocate for direct measurement techniques such as lysimetry and tracer tests, to improve accuracy over traditional methods.

Other studies have evaluated various methods, tailoring them to hydrogeological conditions and data availability. Sibanda et al. (2009) used techniques like chloride mass balance, water table fluctuation (WTF), Darcian flownet computations, and groundwater age dating. Similarly, Islam et al. (2015) employed methods including WTF, water budget, Darcy's law, empirical relationships, groundwater models, and tracer techniques. Sun et al. (2024) and Cambraia Neto and Rodrigues (2020) assessed methods such as base-flow separation, WTF, and sequential water balance, highlighting their ease of use, data accessibility, and robustness. These studies underline the importance of selecting appropriate estimation techniques based on the specific context of the region and the reliability of input data.

2.2. Water Harvesting Types and Techniques

WH refers to the process of collecting and storing rainwater or surface runoff on the ground, underground, in the soils, or in reservoirs for future use (Ertop et al., 2023). This practice can be implemented at various scales, from small household levels to large-scale municipal or watershed projects. The primary objective of WH is to capture and conserve water for purposes such as drinking, irrigation, GWR, and other needs, particularly in regions experiencing water scarcity or regions having longer periods of dry seasons. WH offers a range of benefits (Umukiza et al., 2024) including (a) drought mitigation, (b) efficient water use, (c) flood management, (d) soil conservation, (e) groundwater improvement, and (f) energy conservation. Zhao et al. (2024) also pointed numerous benefits in the form of economic, environmental, technological, and social advantages.

WH, a time-honored practice, encompasses three key components that are essential for effectively capturing and utilizing rainwater or runoff (Ertop et al., 2023). These components are the collection system, transportation system and a storage system. Collection System is the part

of the system where rainwater or surface runoff is initially gathered. This system typically includes surfaces such as rooftops or catchment areas that direct water into a designated collection point. Once the water is collected, it must be transported to a storage location, which is facilitated by a transportation system that often involves pipes, channels, or gutters to guide the water from the collection point to the storage unit (Ertop et al., 2023). The final component is the storage system, where the water is stored for later use; this can be in tanks, cisterns, or other reservoirs that hold the water until it is needed for drinking, irrigation, or other purposes.

WH can be classified into three main types: (1) rainwater harvesting, (2) flood harvesting, and (3) groundwater harvesting, which involve both surface and subsurface storage reservoirs. The primary WH structures employed include short term options such as contour bunds, trapezoidal bunds, semi-circular hoops, rock catchments, and ground catchments. Additionally, long term structures like dugout ponds, farm ponds, irrigation dams, silt/sand detention dams, percolation dams are commonly practiced, alongside subsurface dams. These systems collectively enhance water resource management and contribute to sustainable water use, particularly in areas facing water scarcity.

2.2.1. Rainwater Harvesting (RWH)

RWH is the process of capturing and storing rainwater from precipitation, specifically rain that falls directly onto rooftops, surfaces, or catchment areas (Yannopoulos et al., 2019). This practice involves a systematic collection method, utilizing components such as gutters, downspouts, and storage tanks to gather and store rainwater efficiently. The primary objective of RWH is to provide a sustainable water supply for a variety of uses, including domestic needs, irrigation, and other applications, particularly during dry periods or regions with water scarcity.

The design of RWH systems typically targets smaller, more frequent rainfall events, emphasizing adequate storage capacity and effective filtration mechanisms to ensure water quality. These systems are versatile and can be implemented in both urban and rural areas, adapting to varying rainfall patterns. In urban areas, RWH focuses on localized collection from rooftops and impervious surfaces, reducing reliance on municipal water supplies and mitigating urban flooding. In rural areas, the techniques are often employed to enhance agricultural productivity and provide consistent water access for communities.

RWH also plays a critical role in water resource management and climate change adaptation strategies (Teston et al., 2022). By capturing rainwater at its source, it helps reduce surface runoff, prevents soils erosion, and supports GWR. Moreover, it contributes to building resilience in regions prone to droughts and water shortages. The adoption of RWH systems is increasingly encouraged as a sustainable solution for addressing global water challenges, promoting efficient water use, and supporting environmental conservation (Yannopoulos et al., 2019; Nandi et al., 2022; Teston et al., 2022).

2.2.2. Flood Water Harvesting (FWH)

FWH involves the collection and management of excess water from flooding events, such as heavy rainfall, storm surges, or river overflows. This method employs various structures such as check dams, percolation tanks, and infiltration ponds to temporarily store and regulate large volumes of floodwater. The primary objectives of FWH include mitigating the adverse impacts of flooding, managing surplus water, and enhancing GWR during and after flood events (Qadir et al., 2003; Alam t al., 2021).

Unlike RWH, FWH systems are designed to handle significantly larger and more rapid inflows of water. As a result, these structures often require robust engineering and durable materials to withstand the high pressures and dynamic conditions of flood events. For example, check dams help slow down water flow and allow it to percolate into the ground, while percolation tanks are used to store floodwater for infiltration into aquifers, improving GWR (Sharma et al., 2021). Additionally, FWH pits are implemented to collect and contain water temporarily, preventing uncontrolled runoff that can cause soil erosion and damage infrastructure.

This method is particularly relevant in regions prone to seasonal flooding or areas with intense and erratic rainfall patterns. FWH often involves large-scale landscape management, requiring coordinated efforts at both community and governmental levels. Beyond mitigating flood risks (Jamali et al., 2020), this technique provides numerous benefits, such as improving water availability during dry periods, enhancing soil moisture for agriculture, and restoring ecological balance in flood-prone areas (Kebede et al., 2024). FWH is increasingly recognized as a valuable climate adaptation strategy in the face of changing rainfall patterns and extreme weather events caused by climate change. By capturing and managing floodwaters effectively, this approach not

only addresses immediate water-related challenges but also contributes to long-term water security and sustainability (Fathy et al., 2021).

2.2.3. Groundwater Harvesting (GWH)

GWH involves the extraction and sustainable utilization of water stored in underground aquifers, typically accessed through wells, boreholes, or springs. This method is an essential part of water resource management, particularly in arid and semi-arid regions where surface water is scarce (Fathy et al., 2021). GWH also includes the use of specialized techniques and structures such as subsurface dams, Qanat systems (combination of shaft and tunnel system) and specialized wells, to enhance GWR and ensure long-term water availability (Ahmed and Umar, 2008; Remini et al., 2014).

Subsurface dams are built within riverbeds to obstruct the flow of ephemeral streams during seasonal rains, by trapping water in the sediment below the ground surface. Subsurface dams reduce water loss from evaporation and provide a sustainable source of water for aquifer recharge. The stored water can then be accessed later through wells or other extraction methods, making it a reliable source for drinking, irrigation, and other uses (Fathy et al., 2021). Qanat systems are used in the Middle East and North Africa and are remarkable engineering systems consisting of a series of underground tunnels and vertical shafts. These structures transport groundwater from higher elevation aquifers to the surface using gravity alone, eliminating the need for mechanical pumps. Qanats are highly efficient in regions with sloping terrains and help deliver water to arid plains for agriculture, drinking, and domestic use (Remini et al., 2014). Specialized wells such as infiltration wells and recharge wells are designed to facilitate the percolation of surface water into the underground aquifers (Fuentes et al., 2020).

These wells enhance GWR by capturing rainwater or runoff and directing it into the aquifer system. In regions with declining water tables (Islam et al., 2015), recharge wells are increasingly used to replenish groundwater reserves and prevent further depletion (Fuentes et al., 2020; Shemer et al., 2023). By minimizing water loss through evaporation and improving water storage efficiency, GWH contributes to sustainable water management practices. Despite its advantages, GWH faces challenges such as over-extraction, contamination, and the need for proper maintenance of harvesting structures. Sustainable management practices, such as

monitoring water levels, regulating extraction, and promoting aquifer recharge, are crucial to ensure the long-term viability of groundwater resources (Sharma et al., 2021).

2.3. Groundwater Recharge

2.3.1. Benefits of Groundwater Conservation

Groundwater conservation is essential for both the environment and society due to its far-reaching impacts on sustainable water supply, agricultural support, ecosystem conservation, and drought resilience. Additionally, it plays a critical role in preventing land subsidence, protecting water quality, adapting to climate change, preserving cultural and social values, and enhancing GWR. As a vital resource, groundwater supports numerous livelihoods, ecosystems, and communities, making its conservation a top priority in water resource management.

One of the most effective strategies for groundwater conservation is GWR (Kebede et al., 2024), which involves replenishing aquifers to maintain their sustainability and functionality (Abraham and Mohan, 2015). This can occur naturally, through precipitation and infiltration, or artificially, by directing water into aquifer systems through recharge structures (Abraham and Mohan, 2015; Kebede et al., 2024).

The identification of areas suitable for artificial recharge is crucial and should be based on specific factors (among others), areas such as (1) declining groundwater levels, (2) de-saturated aquifers, (3) inadequate water supply (wells and hand pumps fail to provide sufficient water), and (4) poor ground water quality.

By focusing on these factors (in addition to geological and hydrogeological factors), GWR efforts can enhance (1) the availability and quality of groundwater, (2) support long-term environmental sustainability, (3) mitigate subsidence, and (4) improve human well-being (Fathy et al., 2021). Additionally, such measures contribute to climate change adaptation (Kebede et al., 2024), providing resilience against the increasing challenges posed by changing precipitation patterns and water scarcity (Burnett and Wada, 2014). Groundwater conservation and recharge are integral to protecting this critical resource and ensuring its availability for future generations (Shemer et al., 2023).

2.3.2. Water Sources for GWR

GWR is a process that replenishes underground aquifers through both natural and artificial means. To ensure effective recharge, it is crucial to identify and evaluate the availability of adequate water sources. These sources serve as the foundation for designing recharge systems, particularly in regions facing water scarcity or aquifer depletion. The primary sources of water for GWR include (1) rainfall; (2) rainwater collected from rooftops, (3) surplus water from natural streams and springs, and (4) properly treated municipal and industrial wastewater.

Rainfall or precipitation is the most common natural source of GWR. Rainwater percolates through the soil and gradually replenishes aquifers, making it an integral part of the hydrological cycle. However, the effectiveness of precipitation as a recharge source depends on several factors, such as land slope, soil type, geology, vegetation cover, and rainfall intensity. While in situ precipitation occurs naturally at all locations, it may not always provide enough water for effective recharge, especially in arid or semi-arid regions where rainfall is infrequent or insufficient.

In urban and densely populated areas, rainwater collected from large roof surfaces can significantly contribute to GWR. Rooftop RWH systems collect and channel rainwater into recharge structures such as pits, trenches, or wells. This method is particularly effective in areas with limited open land for natural infiltration and helps reduce surface runoff, which often causes waterlogging and urban flooding. By utilizing roof areas, rainwater can be captured and redirected to replenish aquifers, making it a valuable strategy for urban water management.

Natural streams, rivers, and other surface water bodies are another important source of water for GWR. During periods of high flow or seasonal surpluses, water from these sources can be diverted into recharge systems like check dams, percolation tanks, or infiltration basins. This diverted water helps replenish aquifers while minimizing surface water wastage. However, it is essential to ensure that the diversion of water does not violate the rights of downstream users or disrupt aquatic ecosystems. Proper planning and stakeholder engagement are necessary to balance recharge activities with other competing water needs.

In addition to natural sources, properly treated municipal and industrial wastewater can be utilized for GWR (Shemer et al., 2023). Advanced wastewater treatment processes remove

harmful contaminants, making the water safe for recharge purposes. Treated wastewater can be directed into aquifers through recharge wells or basins, providing a sustainable way to reuse water and reduce pressure on freshwater resources. This approach is particularly beneficial in urban and industrial areas where water demand is high, and alternative sources are limited.

In regions where rainfall and natural water sources are inadequate for effective recharge, alternative water sources can be explored and transported to recharge sites. For example, surplus water from nearby reservoirs, rivers, or other catchments can be conveyed through pipelines or canals to areas needing recharge. While this solution enhances recharge efficiency, it requires careful infrastructure planning to minimize water losses during transportation and ensure cost-effectiveness (Shemer et al., 2023). Kebede et al. (2024) pointed out that globally, GWR projects are increasing by around 5% each year.

2.4. Groundwater Recharge Methods

2.4.1. Natural Groundwater Recharge (NGWR)

NGWR is a process through which water from precipitation and other surface sources infiltrates the ground, replenishing underground aquifers (Hashemi et al., 2013). This occurs when rainwater or melted snow seeps into the soil and permeable rock layers, gradually making its way to the groundwater table. The efficiency and rate of natural recharge are influenced by a variety of factors, including soil type, geology, land cover, topography, groundwater table, vegetation and climate conditions (Barthel et al., 2021). Favorable conditions for natural recharge include permeable soils, fractured rock formations, perennial rivers and streams, forest cover, and relatively level land with minimal slope, all of which enhance the infiltration of water into the subsurface.

However, NGWR can be significantly reduced or obstructed due to a variety of factors, many of which are driven by human activities and environmental changes. Urbanization is one of the main contributors to reduced recharge, as the expansion of impervious surfaces such as roads, pavements, and buildings prevent water from infiltrating into the soil. Instead, water flows off these surfaces into storm drains, reducing the amount of water available for aquifer replenishment (Patel and Chaudhari, 2023). The presence of vegetation plays a crucial role in facilitating natural recharge. Trees and plants promote infiltration by allowing water to percolate

through the soil, while their roots create pathways that enhance soil permeability. When vegetation is reduced, for example, through deforestation or land clearing, there is a significant reduction in the amount of water absorbed into the ground, leading to lower recharge rates. Similarly, certain agricultural practices, such as excessive tillage, can compact soil, decreasing its ability to absorb water. The use of chemical fertilizers and pesticides further degrades soil health and reduces permeability, impeding the natural recharge process (Hashemi et al., 2013). In addition, excessive groundwater extraction can outpace natural recharge rates, leading to a decline in the water table. Over-extraction can also reduce the effectiveness of recharge, as deeper groundwater levels make it harder for infiltrating water to reach aquifers. Climate change further exacerbates these challenges by altering precipitation patterns and intensities. For instance, an increase in the frequency and intensity of droughts, along with shifts in rainfall distribution, can reduce the overall availability of water for recharge. Areas that experience heavy rainfall over short periods may see more surface runoff than infiltration, further limiting the water that reaches the aquifer.

Another critical factor affecting natural recharge is the discharge of polluted water into natural waterways. Polluted water can block soil pores with impurities, reducing the soil's infiltration capacity. Industrial discharges, untreated wastewater, and contaminated surface water flows prevent water from percolating effectively into the ground, thereby hindering natural recharge processes (Raimondi et al., 2023).

2.4.2. Artificial Groundwater Recharge (AGWR)

AGWR is a method of replenishing groundwater reservoirs by deliberately modifying the natural movement of surface water, treated wastewater, rainwater, etc., using appropriate civil/hydraulic engineering techniques (Gontia and Patil, 2012; Hussain et al., 2019). This process is typically implemented in situations where natural recharge is insufficient to meet groundwater demand throughout the year and store water for later use. By employing artificial recharge, water managers can enhance the sustainability of aquifers and ensure the availability of groundwater for various uses.

The primary objectives of artificial recharge techniques are to (Abu-Taleb, 2003) (1) enhance natural recharge: replenishing aquifers by capturing and directing precipitation and surface

runoff into the ground; (2) stabilize aquifer levels: contributing to maintaining consistent groundwater levels; (3) control contamination of water supplies: protect groundwater quality and reduce the risk of pollutants infiltrating aquifers (recharged water quality is controlled); and (4) prevent freshwater degradation: minimize salt water intrusion in coastal areas.

These techniques are especially valuable in areas with high water demand, limited natural recharge, or increasing pressure on groundwater resources due to climate change, urbanization, and population growth.

Groundwater levels can be improved through various artificial recharge methods, including spreading, recharge/injection wells, and the induced infiltration method (see Table 2.1). According to Mukherjee (2016), the first two methods—spreading and recharge/injection wells—are classified as direct techniques, with spreading involving the application of water directly to the surface, while recharge/injection wells operate below the surface. In contrast, the induced infiltration method falls under the indirect category, as it utilizes the natural processes of infiltration from nearby water sources to enhance GWR. Examples of induced infiltration method include induced recharge, aquifer modification, and groundwater conservation structures (Bhattacharya, 2010; Mukherjee, 2016). Zhang et al. (2020) presented an in-depth review and analysis on historical development, the current situation, and perspectives of managed aquifer recharge.

I. Direct Methods

a) Surface Spreading Method

The surface spreading method is a widely used technique for artificial GWR (Bouwer, 2002). In this approach, water is diverted from streams or released from reservoirs into shallow basins or trenches. Recharged water then infiltrates through the bottom of these basins or trenches, percolating through the unsaturated zone (vadose zone) and gradually migrating to the water table. The rate of recharging is influenced by several factors, including (1) the permeability of the material between the basin bottom and the water table, (2) the depth of water table in the basin, and (3) the biological, geochemical, and physical changes occurring within the materials through which the water moves (Brown and Signor, 1974). For optimal recharge efficiency, the area chosen for the surface spreading method have gently sloping terrain that avoids significant

gullies or ridges. Additionally, the vadose zone—the soil and rock above the water table—should be permeable and free from clay lenses, as these can obstruct water movement and reduce infiltration. The permeability of the geological formation plays a critical role in ensuring that water easily reaches the aquifer.

Several sub-techniques are commonly employed within the surface spreading method. These include (Bouwer, 2002; Mukherjee, 2016; Saha et al., 2022) Flooding, Ditches and Furrows, Recharge Basins, Run-off Conservation Structures (Bench Terracing, Gully plugs, Contour bunds, Contour trenches, Percolation tanks, etc.), Stream Channel Modification, and Surface Irrigation. The surface spreading method is particularly effective in areas with high permeability in the vadose zone and is a cost-efficient solution for enhancing groundwater resources when natural recharge is insufficient (Mukherjee, 2016).

b) Sub surface method

The subsurface method is employed in regions where the soil exhibits low vertical permeability, which hinders natural infiltration of water into the ground (Brown and Signor, 1974; Mukherjee, 2016). This technique involves the construction of structures such as injection wells, recharge wells, dug wells, shafts, and pits that are placed below the surface (Hussain et al., 2019). These structures facilitate the direct recharge of groundwater by allowing water to be introduced into the subsurface layers, overcoming the limitations posed by the surrounding soil conditions. As a result, the subsurface method is particularly effective in areas where traditional surface recharge techniques may not be viable due to insufficient permeability.

II. Indirect Methods

a) Induced Recharge

Induced recharge is an indirect method of artificial GWR that involves pumping water from an aquifer that is hydraulically connected to surface-water sources. By creating a flow gradient, this process encourages the surface water to infiltrate and recharge the groundwater reservoir. One of the notable benefits of induced recharge is the natural filtration effect: as surface water passes through the aquifer materials, its quality often improves before being discharged from the pumping well, provided the hydrogeological conditions are favorable. This natural filtration

process can significantly enhance the overall quality of the groundwater (Mukherjee, 2016). A few examples of induced recharge are described below (Azis et al., 2015).

Pumping Wells: An induced recharge system typically pumping wells strategically located near perennial streams that are hydraulically linked to an aquifer through permeable materials in the stream channel. A prime location for a well is often at the outer edge of a bend, where the hydrological conditions are particularly conducive to recharge. However, a critical consideration in this system is the chemical quality of the surface water source, as it directly impacts the effectiveness and safety of the recharge process (Mukherjee, 2016).

Collector Wells: These are used to extract significant water from riverbed or lakebed deposits and waterlogged areas. In cases where the phreatic aquifer (unconfined aquifer) near the river has limited thickness, horizontal wells are often more effective than vertical wells. Collector wells equipped with horizontal laterals and infiltration galleries can considerably enhance induced recharge from the stream, making them a preferable option for maximizing water extraction in suitable locations (Azis et al., 2015; Mukherjee, 2016).

Infiltration Gallery: Infiltration galleries are specialized structures designed to access groundwater reservoirs beneath riverbed strata. These galleries consist of horizontal perforated or porous pipes with open joints, enclosed in a gravel filter envelope (Bouwer, 2002; Mukherjee, 2016). They are installed in permeable, saturated layers with a shallow water table and a continuous source of recharge. Typically positioned at depths of 3 to 6 m (Mukherjee, 2016), infiltration galleries collect water through gravity flow. Key considerations when designing an infiltration gallery include the desired yield and economic feasibility of the project (Mukherjee, 2016; Kumar et al., 2017).

b) Aquifer Modification Techniques

Aquifer modification techniques aim to enhance the physical characteristics of aquifers, improving their ability to store and transmit water. While these methods are primarily used to augment water yield rather than serving as traditional artificial recharge structures, they are increasingly recognized as effective approaches for boosting groundwater storage within aquifers (Azis et al., 2015; Mukherjee, 2016).

Bore Blasting is an effective technique for hard crystalline and consolidated strata (Kumar et al., 2017; Kumar et al., 2021). Through detailed hydrogeological investigations, suitable sites are identified where aquifers are underperforming or drying up. In this method, blasting holes are drilled to the required depth of the aquifer—whether it is unconfined or confined. Explosive charges are arranged in rows or circular patterns and detonated simultaneously to maximize the impact. The controlled blasts increase the secondary porosity and permeability of the aquifer, allowing for greater water infiltration and storage capacity (Brown and Signor, 1974; Mukherjee, 2016).

Hydro-Fracturing is a modern alternative to traditional blasting methods, particularly in cases where blasting has yielded inconsistent results. This technique is designed to enhance secondary porosity in hard rock formations by applying hydraulic pressure to a specific zone within bore wells. The process involves injecting high-pressure water into the borehole to initiate and expand fractures in the rock. Additionally, it clears clogged fissures and improves connectivity with nearby water-bearing strata, significantly increasing water flow and accessibility. Hydro-fracturing is particularly effective for improving the hydraulic properties of aquifers in areas with limited natural recharge potential.

c) Groundwater Conservation Structures

Groundwater conservation structures are essential for ensuring that artificially recharged water remains available for use when needed. Once water is recharged into the aquifer, it becomes subject to natural groundwater flow regimes, which may lead to its movement away from the desired area. Conservation techniques aim to slow or control this flow, enhancing sustainable management of groundwater resources and improving long-term water availability (Burnett and Wada, 2014).

Subsurface Dams/Underground Barriers are structures built across streams, or other flow paths to slow the natural flow of groundwater and create subsurface storage. By impeding the movement of groundwater, these dams increase the storage capacity within the aquifer and allow water to be retained during peak usage periods. The primary objective of a subsurface dam is to prevent the outflow of groundwater from the sub-basin while simultaneously enhancing the aquifer's storage

potential. This method is particularly effective in areas where aquifers experience rapid depletion or where seasonal water demand is high (Fuentes et al., 2020).

The Fracture-Sealing Cementation Technique is a specialized groundwater conservation method used in arid and semi-arid regions. In these areas, boreholes may initially provide good yields but often dry up by the end of the winter or summer due to limited groundwater storage along preferential flow paths. This method involves sealing fractures in the rock with specially formulated cement to reduce water loss through these pathways. In addition to conserving groundwater, this technique is highly effective in preventing the intrusion of saline or polluted water from known sources, thereby protecting the quality of the aquifer. It is particularly useful in regions with challenging topography or aquifer conditions where water management is critical (Fuentes et al., 2020).

Table 2.1 Summary of artificial GWR techniques and types (gathered from the reviewed papers)

<table>
<tr><td colspan="9">Artificial GWR Methods</td></tr>
<tr><td colspan="6">Direct Methods</td><td colspan="3">Indirect Methods</td></tr>
<tr><td>Main Type</td><td>Sub-Type</td><td>Example *</td><td>Main Type</td><td>Sub-Type</td><td>Example</td><td>Main Type</td><td>Sub-Type</td><td>Examples *</td></tr>
<tr><td rowspan="7">Surface</td><td rowspan="7">Spreading (In-and Off Channel)</td><td>Flooding</td><td rowspan="7">Subsurface</td><td rowspan="7">Injection well</td><td>Recharge Well</td><td rowspan="7">Induced infiltration</td><td rowspan="3">Induced Recharge</td><td>Pumping Well</td></tr>
<tr><td>Ditches and Furrows</td><td>Dug Well</td><td>Collector Well</td></tr>
<tr><td>Recharge Basins</td><td>Recharge Shaft (Vadose zone wells)</td><td>Infiltration Gallery</td></tr>
<tr><td>Run-off conservation structures</td><td>Recharge Pit</td><td rowspan="2">Aquifer Modification Techniques</td><td>Bore Blasting</td></tr>
<tr><td>Stream-channel modification</td><td>Connector wells</td><td>Hydro-fracturing</td></tr>
<tr><td>Surface Irrigation</td><td></td><td rowspan="2">Groundwater Conservation Structures</td><td>Subsurface dam</td></tr>
<tr><td></td><td></td><td>Fracture Sealing/Cementation Technique</td></tr>
</table>

** Note: Terminologies related to artificial GWR techniques are not standardized. In the reviewed papers terminologies vary from region to region and within a country.*

2.4. Water harvesting practices in Arid and Semi-arid regions of the world

WH has been practiced for thousands of years in various parts of the world particularly in arid and semiarid regions of Asia and Africa (Ertop et al., 2023). Several water harvesting techniques

have been implemented in the Asian countries like Israel, Syria, Iran, Iraq, Afghanistan, India, Saudi-Arabia, Yemen, China, Pakistan and Jordan (Prinz, 1996). In the Negev Desert of Israel, where annual rainfall is just 100 mm, tanks are used to store runoff from hillsides for both agricultural irrigation and residential use (Ertop et al., 2023). Large bunds were constructed in west Rajastan (India) in the early 15th century to accumulate runoff (Prinz, 1996). In Ghana, water harvesting has been utilized for decades to meet various needs, including domestic use whereas in South Africa, conservation practices and water harvesting have played a great role in supporting agricultural production for over a century (Denison and Wotshela, 2012). The research conducted by Barry et al. (2008) in West African countries such as Niger, Mali, Burkina Faso, and Senegal found that integrated water harvesting can effectively rehabilitate degraded land, retain moisture, restore vegetation cover, and enhance crop growth.

Table 2.2 Examples of water harvesting practices in the Asian and African countries

S.N	Country	Source	WH practice	Objective
1	Kenya	Umukiza et al. (2023) Aroka, (2010)	sand dams in underground sand reservoirs	To combat deforestation and improve water availability
2	South Africa	Denison and Wotshela, (2012), Umukiza et al. (2023)	Tanks installation for rooftop RWH	For domestic use
3	Ethiopia	Umukiza et al. (2023) Vema et al., (2018)	Tassa tank, stone bunds	For reliable water supply, manage runoff and soil erosion, recharging groundwater, supporting agricultural productivity
4	Senegal	Barry et al. (2008) Umukiza et al. (2023)	small-scale reservoirs and pans	To irrigate vegetable gardens and improve food security in rural areas
5	Morocco	Ouali et al., (2022)	Small dams, cisterns, and underground reservoirs (khettaras)	For irrigation and domestic use
6	Burkina Faso	Barry et al. (2008)	digging of small planting pits	For vegetation growth
7	Somalia	Oduor and Gadain, (2007) Oweis et al., (2012) Prinz, (1996)	Barkads (small underground reservoirs lined with water-proof masonry walls), caag system (larger earthen bunds to harvest runoff water in sloping and flat lands	To settle and ensure a reliable water supply for domestic use and livestock, for flood control
8	Mauritania	Ahmed et al., (2007)	Jassour (small stone	For irrigation and livestock

			embankment built across dry riverbeds)	watering during prolonged dry spells
9	Chad	Nijhof et al., (2010) Prinz, (2013)	Zarai system (constructing small shallow basins in the soil	To promote water infiltration and reduce evaporation, making it an effective method for small-scale farmers
10	Mali	Umukiza et al. (2023)	Zai (digging small pits or basins in the soil)	To infiltrate the soil, promoting plant growth and better water retention in the root zone
11	Egypt	Prinz, (1996)	Tanks installation for Rooftop Collection, Micro-catchments, Wadi Systems, mulching and conservation tillag	For domestic use, enhancing groundwater recharge, irrigation,
12	India	Bhattacharya et al., (2011) Bhattacharya, (2015)	Khadins (earthen embankments constructed across hill slopes) Kunds (saucer-shaped catchment areas with a central circular underground well) Taankas (cylindrical, paved underground pits)	For artificial groundwater recharge
13	Iran	Ghanbarpour et al., (2007) Alemohammad & Gharari, (2017) Abadi et al., (2023)	Qanat Systems	For irrigation and domestic use.
14	Iraq	Abdullah et al., (2020)	Cisterns, tanks, ponds, Qanat and Karez Systems, Check Dams and Barriers	For domestic use, irrigation, groundwater recharge
15	Jordan	Abdulla, (2020) Alkhaddar, (2003)	Roof catchment systems and cisterns, Ponds and Pools	For domestic use , irrigation
16	Israel	Ertop et al., (2023)	Tank installation, check dams, bunds	For agricultural irrigation, residential use
17	China	Zhou et al., (2023)	Terracing, Check Dams, Recharge pits, Shuijiao Water Cellars	To combat erosion and enhance water retention
18	Pakistan	Asif et al., (2024)	Check Dams, Percolation Tanks, and Agricultural Ponds	For groundwater recharge
19	Saudi Arabia	Abdelaziz et al., (2006)	Large basins and dams, Wadi Systems, Water spreading dykes	For agricultural irrigation

CHAPTER THREE

3. METHODOLOGY

3.1. Data Collection

3.1.1. Soil Sampling and field description

Soil samples were collected by zoning based on variations in soil characteristics across the catchment. The cliff and rocky area (34 km^2 area coverage) is not considered for sampling due to its unsuitability for both WH and GWR. A total of 20 soil samples were taken during the dry season, comprising 10 samples from residual deposits and 10 from fluvial deposits (stream deposits). The samples were collected randomly from the zoned area, which covered 58% (47 km^2) of the total catchment. The samples were extracted from shallow excavations at 15 cm depth using a hand borer and were carefully described during the sampling process based on Regen Network Development Soil Sampling Guide (2021).

3.1.2. In-situ Soil Infiltration tests

Soil infiltration rates were measured at different points throughout the catchment using ASTM standard method of 30 cm diameter single ring infiltrometer. The double ring infiltrometer is preferable for specific sites that required for engineering design (e.g., recharge basins, percolation tank, etc.). For wide area assessment, single ring is needed due to its cost-effectiveness for rapid assessments across many locations. The test sites were homogenous soil texture and structure where lateral flow effects are minimal. This method is useful to identify high infiltration zones and low infiltration zones of watershed areas. The infiltration test was measured at different locations representing various soil types, land use land cover types and topographic positions. A total of 10 measurements were carried out in the dry season at the flat to gentle slope part of the watershed. The test is conducted by cleaning soil surface and vegetation. Next, the single ring infiltrometer is installed by penetrating about 7.5 cm below the surface based on ASTM standards. After the soil is saturated with water, measurement record is followed using constant head (in the sand soil) and falling head (in the silt and clay soils) water level.

The infiltration rate is calculated using the formula (ASTM Standard Test Method):

$I_r = \frac{\Delta V}{(A_r \times \Delta t)}$ *Where,* I_r = *tested infiltration rate (cm/hr)*

ΔV = *volume of liquid used during time interval to maintain constant head in the ring* (cm^3)

A_r = *internal area of ring* (cm^2)

Δt = *time interval (hr)*

3.1.3. Discontinuity Measurements

A number of field observations and discontinuity measurements were recorded at the entire catchment of the study area in accordance with the suggested method of the International Society of Rock Mechanics (ISRM 1978). The condition of joints relative to hydrogeology largely controls permeability. A total of 30 joint measurements were recorded from rock exposures within the relatively lower elevation and gentle terrain (50 km²), which represents the most suitable area for WH and GWR potential sites. The spacing, aperture, persistence and infillings are measured using tape meter and their orientation (strike and dip) is using Brunton compass for each joint sets. Discontinuity orientations were processed using a RockWorks17 linear rose diagram (RockWare Inc. 1983-2020). Joint spacing is measured perpendicular to the adjacent joint intersections with the measuring scanline. For volumetric joint count (Jv), a sampling length of 5m or 10m (depending on the rock exposure) is used and the number of joints for each set are counted perpendicular along the relevant joint set. The average joint spacing, frequency, volumetric joint count and RQD are calculated (Hudson and Harrison, 1997) as:

Discontinuity frequency, $\lambda = n/L$, discontinuity spacing average is the reciprocal of the frequency, i.e. $\bar{x} = L/n$

Where, L = length of the sampling line (m) and n = number of discontinuities it intersects

J_v is the sum of the number of joints per meter or the sum of the reciprocal of average spacing for each joint set present and RQD is calculated from the volumetric joint count as;

$$RQD = 115 - 3.3J_v \quad , \quad RQD = 100 \; for \; J_v \leq 4.5$$

The aperture is the opening discontinuities and measured using tape meter. Types of discontinuities filling materials, filling thickness, roughness and weathering conditions are measured and recorded in the field observations carefully. The persistence is the size or areal extent of a discontinuity within a plane. It is measured using the tape meter and visual estimation

(for more than 20 m length) depending on the exposure; measured in the direction of dip and strike for three-dimensional exposure and in the direction of visual joint length for planar exposure. Rock mass rating (RMR, Bieniawski 1989) was calculated from the measured and recorded surface exposure rock discontinuity conditions to characterize general rock mass quality of the area.

3.1.4. Uniaxial compression test/Schmidt hammer test

L-type Schmidt hammer is conducted in the field by applying vertically perpendicular to the rock surfaces for at least 20 single impact readings in a given one intact rock according to the suggested method of the International Society of Rock Mechanics (ISRM 1978a). From the 20 single impact readings, the upper 50% values were accepted by averaging them. This correction is needed because of the presence of hidden cracks. About 30 selected sites were carried out for the Schmidt hammer test depending on the variations of the rocks in visual eye observation.

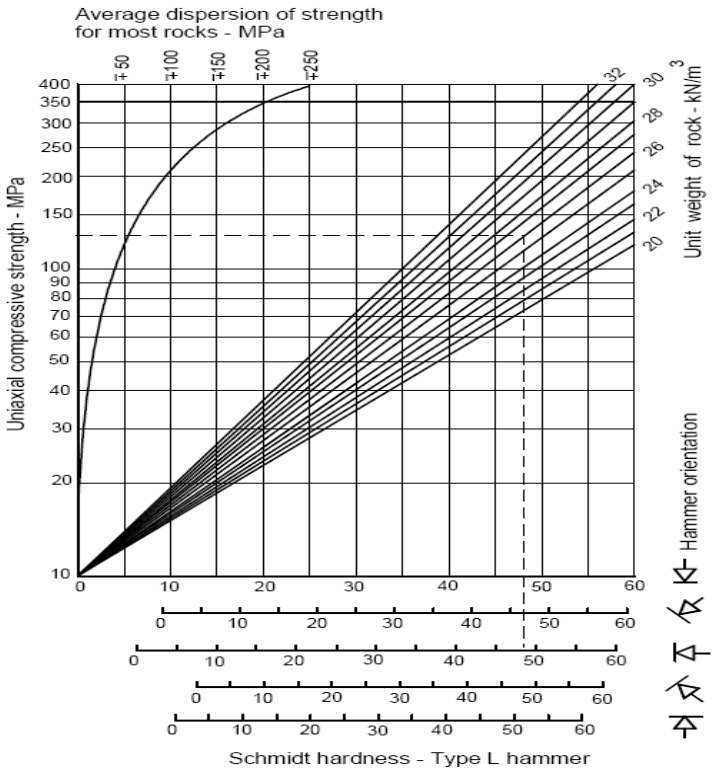

Figure 3.1: Schmidt Hammer Test JCS estimation chart showing Correlation between Schmidt hammer rebound number, hammer orientation, UCS and Rock density (Deere and Miller, 1966)

The rebound number is converted in to the Uniaxial Compressive Strength (UCS) by the Schmidt Hammer Test JCS estimation chart (Figure 3.1).This test was applied to evaluate the weakness and degree of weathering of the rocks and resulting general stability and permeability condition of the rock mass of the area.

3.2. Laboratory Soil Textural Analysis

A total of 20 soil samples (10 from residual and 10 from fluvial deposits) were collected from the study area and carefully transported to the laboratory for grain size analysis using U.S. standard sieves. The sieve analysis was conducted following the American Society for Testing and Materials (ASTM D422) standard.

To determine the particle-size distribution of the soil samples, two methods were employed: sieve analysis for particles larger than 0.075 mm (retained on the No. 200 sieve) and hydrometer analysis for particles smaller than 0.075 mm. For the hydrometer analysis, sodium hexametaphosphate ($NaPO_3$), commonly known as Calgon, was used as a dispersing agent to ensure proper separation of fine particles. The particle-size classification was based on ASTM guidelines, with the following ranges: >4.75 mm (No.4) gravel; 4.75 – 0.075 mm (No.200) sand; 0.075 – 0.002 mm silt and < 0.002 mm clay.

The results of this analysis were used to classify the hydrologic soil groups of the area, which helped estimate water retention, infiltration, and permeability. Clay soils exhibit high water retention and low permeability, allowing them to hold water for extended periods. This makes them well-suited for water harvesting. In contrast, sandy soils have low water retention and high permeability, causing water to drain quickly. While this characteristic is less favorable for water harvesting, it can be beneficial for groundwater recharge.

3.3. Criteria identification and Preparation of Thematic Maps

The two broad categories of criteria used for WH and AR site selection are biophysical and socioeconomic factors (Oweis et al., 1998; FAO, 2003). The biophysical criteria include slope, soil texture, drainage system, rainfall, agronomy and LULC. The socioeconomic parameters are people's priorities, people's experiences, water laws, land tenure, workforce, population density, accessibility, and related costs. The socioeconomic considerations are assessed during field study and mostly fulfill the standards. Here in this study, the biophysical criteria are focused to produce WH and artificial groundwater recharge suitability map. Hence, 8 parameters are selected and prepared as thematic layers in ArcGIS. These attributes are lithology, soil texture, slope, elevation, drainage density, lineament density, rainfall and LULC. These attributes are

implemented successfully in the selection of WH and AR suitable sites in arid and semi-arid regions of the world, especially Africa and Asia (Ahmed et al. 2023).

The geological map of the area is done using systematically arranged North-South and East-West parallel traverse lines. Most of the traverse lines have been projected North-South direction along the streams to counter various lithologies. Many observation points and measurements have taken in every traverse line to produce detail geological map.

Soil data in a raster format at a spatial resolution of 1:250 m were sourced from the "SoilGrids.org" data portal. The data were accessed with 5-15 cm depth. This soil data were used to create a soil map that depicts the distribution and types of soils present in the study area. Understanding soil characteristics is essential for site selection of water harvesting structures and artificial recharge zones, as it influences the processes of water surface runoff, water retention capacity, and permeability (Patel & Chaudhari, 2023; Hassan et al., 2025a, 2025b).

Slope, elevation, drainage density and lineament density were generated from the Advanced Space borne Thermal Emission and Reflection Radiometer (ASTER) digital elevation model (DEM) with a spatial resolution of 30 m in raster format. This dataset was downloaded from the United States Geological Survey (USGS). These maps offer essential terrain-related information that enhances in understanding of landscape characteristics and hydrological processes (Patel and Chaudhari, 2023).

Rainfall data were collected as distributed data with a spatial resolution of 1:4 km in raster format. This data was sourced from the Center for Hydrometeorology and Remote Sensing (CHRS) for the years 2003 to 2024. The average annual rainfall over the 22-years period was calculated, resulting in a map that illustrates the spatial distribution of rainfall in the study area. This map was generated using the inverse distance weighting (IDW) spatial interpolation technique. Understanding precipitation patterns is crucial for assessing water availability and drought conditions.

LULC map was derived from cloud free Landsat-8 satellite image with a spatial resolution of 30 m in raster format, which sourced from the United States Geological Survey (USGS). This map provides valuable information about the land cover types in the study area.

3.4. AHP Technique

The present study utilizes the Analytic Hierarchy Process (AHP), a well-established method for multi-criteria decision-making (MCDM) introduced by Saaty (1980). AHP is renowned for its effectiveness in assigning weights to various factors through a preference matrix, where all relevant criteria are systematically compared against one another using reproducible preference factors. In this methodology, the selected factors are deemed significant for the decision-making process. Each factor is evaluated in a pairwise comparison matrix, which facilitates the expression of relative preferences among them (Şener et al., 2010). To quantify these preferences, numerical values are assigned to reflect the relative importance of one factor over another. These preferences are articulated through a set of descriptors proposed by Saaty, as outlined in Table 3.1 below.

Table 3.1 Scale for pairwise comparison (Saaty, 2008)

Intensity	Importance	Explanation
1	Equal importance	Two activities contribute equally to the objective
2	Equal to moderate importance	
3	Moderate importance	Experience and judgment slightly favor one activity over another
4	Moderate to strong importance	
5	Strong importance	Experience and judgment strongly favor one activity over another
6	Strong to very strong importance	
7	Very strong importance	An activity is favored very strongly over another, its dominance demonstrated in practice
8	Very to extremely strong importance	
9	Extreme importance	The evidence favoring one activity over another is of the highest possible order of affirmation
Reciprocal	Values for Inverse Comparison	

The Analytic Hierarchy Process (AHP) technique utilizes mathematical and expert knowledge to provide a systematic framework for organizing and analyzing complex decisions. By simplifying intricate judgments through pairwise comparisons and evaluating the results, AHP helps determine both the subjective and objective aspects of a decision (Dweiri et al., 2016). Since these comparisons are based on subjective or personal perceptions, some degree of inconsistency

is inevitable. To ensure the reliability of these perceptions, the AHP method incorporates a useful tool for assessing the consistency of the decision-maker's judgments by calculating the consistency ratio (CR), thereby minimizing decision-making bias.

The consistency ratio measures the degree of coherence among pairwise comparisons of different criteria, which is one of the most significant advantages of AHP (Kurttila et al., 2000; Benitez et al., 2012; Emrouznejad & Ho, 2017; Kubler et al., 2018). The basic AHP procedure involves defining the goal, identifying and analyzing the factors or criteria influencing the final decision, and assigning judgments to these criteria using Saaty's scale. To compute the weights using the AHP method (Saaty 1980), the first step involves normalizing the elements of the relative importance matrix using the cumulative eigenvectors. This can be expressed as follows:

$$N_{ij} = \frac{a_{ij}}{\sum_{i=1}^{n} a_{ij}} \qquad \textit{Where,} \quad \begin{array}{l} N_{ij} - \textit{Normalized element in row i and column j} \\ a_{ij} - \textit{Original element in row i and column j} \\ n - \textit{Total number of rows (or columns) in the matrix} \end{array}$$

The weight of each factor is then calculated from the normalized matrix using the following formula:

$$Weight = \frac{\sum_{j=1}^{n} N_{ij}}{n}$$

To verify the consistency of the assigned weights, the consistency ratio, as proposed by Saaty (1980), is calculated as:

$$CR = \frac{CI}{RCI} \qquad \textit{Where,} \quad \begin{array}{l} \textit{CI - consistency index} \\ \textit{RCI - random consistency index} \end{array}$$

The consistency index (CI) is given by the equation:

$$CI = \frac{\lambda_{max} - n}{n-1} \qquad \textit{Where,} \quad \begin{array}{l} \lambda_{max} \textit{ - the principal eigenvalue} \\ n \textit{ - the number of criteria} \end{array}$$

The random index (RI) is an estimate of the average consistency index derived from a sufficiently large number of randomly generated matrices of size n (Table 3.2). To ensure consistency in decision-making, the calculated consistency ratio (CR) should be less than 0.10;

otherwise, the assigned weights must be re-evaluated. If the CR is below 0.10, the judgments are considered consistent and acceptable for AHP analysis (Saaty, 1980).

Table 3.2 The values of RCI for different orders of matrix (Saaty, 1980, 2000)

Size of matrix (n)	1	2	3	4	5	6	7	8	9	10
RCI	0	0	0.58	0.90	1.12	1.24	1.32	1.41	1.45	1.46

After assigning the weights, all the eight thematic layers were incorporated into the weighted overlay analysis. Each layer was assigned a specific weight based on its hydrological influence, while ranks were determined by classifying and evaluating its relative contribution to watershed characteristics. This systematic approach enabled the identification of optimal zones for water harvesting (WH) and GWR within the study area.

All thematic maps were converted to raster format using the Spatial Analyst tool in ArcGIS 10.8. During the conversion, cell size was carefully considered to ensure high accuracy and realism. Subsequently, the rasterized layers were classified and assigned appropriate weights based on their suitability. The final integrated map was generated by combining these weighted layers through either additive or multiplicative overlay techniques.

For both the water harvesting (WH) and groundwater recharge (GWR) maps, each thematic unit was ranked using a knowledge-based hierarchy, with scores ranging from 1 to 5. In this ranking system, a score of 1 represents poor potential, while 5 indicates excellent prospects, reflecting the relative significance of each unit.

3.5. Validation

The produced suitability map was cross-validated using field and Google Earth data. Several existing WH and GWR structures such as sand dams, check dams, ponds, and hand dug wells were gathered and placed over the final potential map of the study area. The Receiver Operating Characteristics (ROC) and Area Under the Curve (AUC) validation methods were used to verify the precision of the delineated potential zone map (Ozdemir and Altural, 2013; Naghibi et al., 2015, 2016). In the ROC method, the AUC measures model accuracy, with values ranging from 0.5 to 1.0 (Nandi & Shakoor, 2009). An AUC close to 1.0 indicates an ideal model, while a value

near 0.5 suggests poor accuracy (Fawcett, 2006). The qualitative relationship between AUC and prediction accuracy is categorized as follows (Pourghasemi et al., 2013a):

Table 3.3 The Range of AUC values and their Test Quality

AUC Values	Test Quality
0.9 – 1.0	Excellent
0.8 – 0.9	Very good
0.7 – 0.8	Good
0.6 – 0.7	Satisfactory
0.5 – 0.6	Unsatisfactory

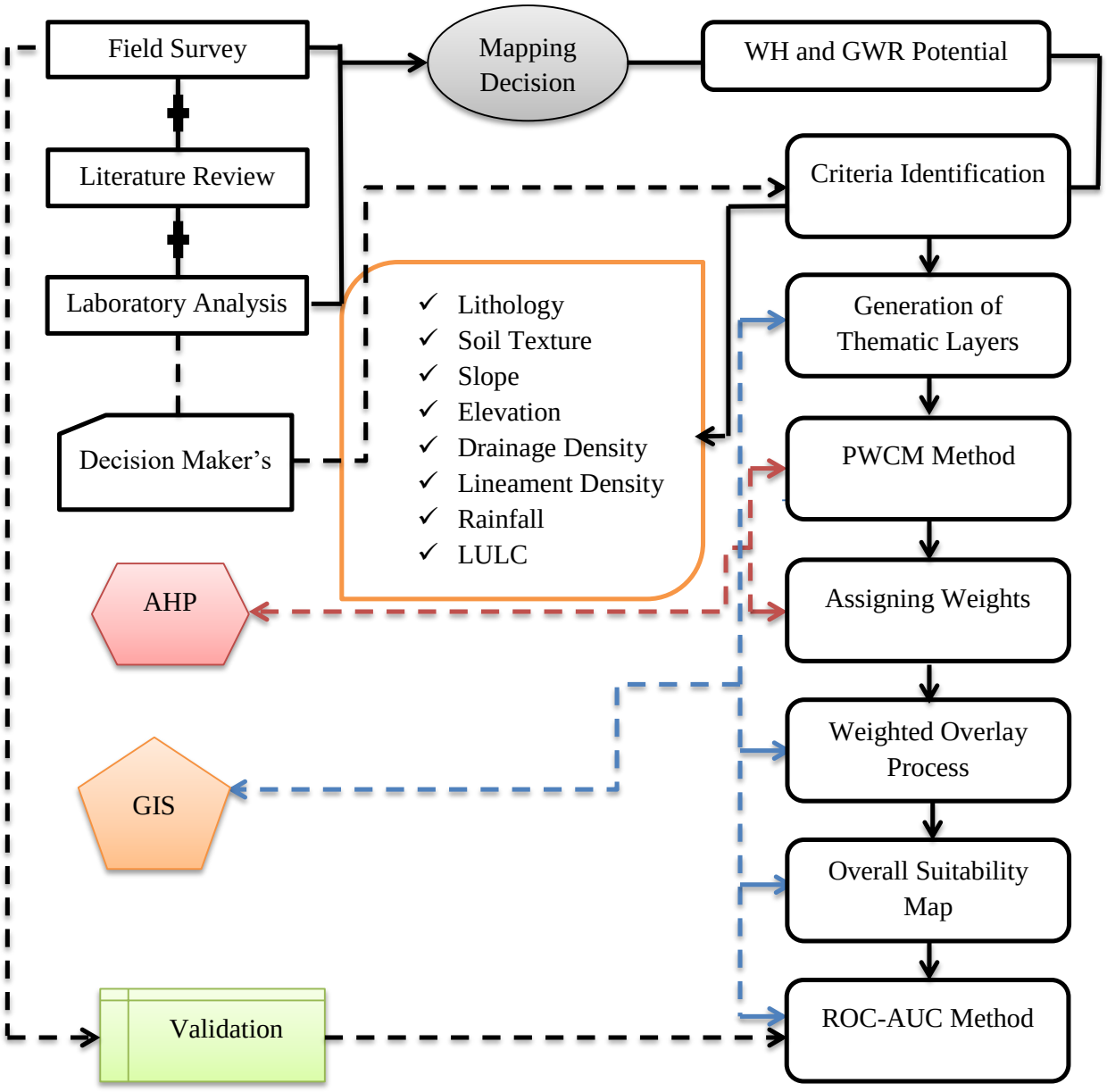

Figure 3.2: Flowchart of the methodological approach for the Research study

CHAPTER FOUR

4. GEOLOGY AND HYDROGEOLOGY

4.1. Regional Geology

The Tekeze River basin (TRB), situated in northern Ethiopia, is a remarkable geographical feature encompassing an area of approximately 82,000 square kilometers. It is bounded by the Simien Mountains range to the west and south, the western escarpment of the Afar Depression to the east and the Ethiopia-Eritrea border to the north.

The geology of the region consists of a Precambrian basement that is unconformably overlain by a sequence of Paleozoic and Mesozoic sedimentary rocks, which are capped by Tertiary volcanic formations. This geological framework is deformed by a range of tectonic structures, including folds, faults; shear zones, and lineaments, resulting from Neoproterozoic to present-day tectonic activity (Sembroni et al., 2017). The stratigraphic succession of Tekeze River basin including northern Ethiopia can be classified into 10 units; from the oldest to the youngest as Precambrian basement, Enticho Sandstones, Edaga Arbi Glacial, Adigrat Sandstones, Antalo Limestone, Agula Shale, Amba Aradam Formation, Trap series, Mekelle Dolerites and Axum-Adwa Plugs (Sembroni et al., 2017).

The Precambrian basement of northern Ethiopia is part of the southern extension of the grand Arabian–Nubian Shield (ANS) (Stern, 1994; Alene, 1998; Alene et al., 2000, 2006; Gebreyohannes et al., 2010: Hagos et al., 2020). It is composed of two major sequences (Beyth, 1972a; Garland, 1980): the older MV/MVC sequence (Tsaliet Group) and the younger MS sequence (Tambien Group) (Alene et al. 2006 and references therein). These sequences are intruded by syn- to post tectonic intrusions (granite). The Tsaliet group contains intermediate to felsic and pyroclastic (welded tuffs, lapilli and agglomerates) (Beyth, 1972a; Beyth et al., 2003). The Tambien group is composed of meta-sediments slates, phyllites, meta-limestone/dolostone and pebbly slates (Hagos et al., 2020). Arkosic metasandstones and conglomerates are observed in the upper part of Shiraro plains (Beyth, 1972a).

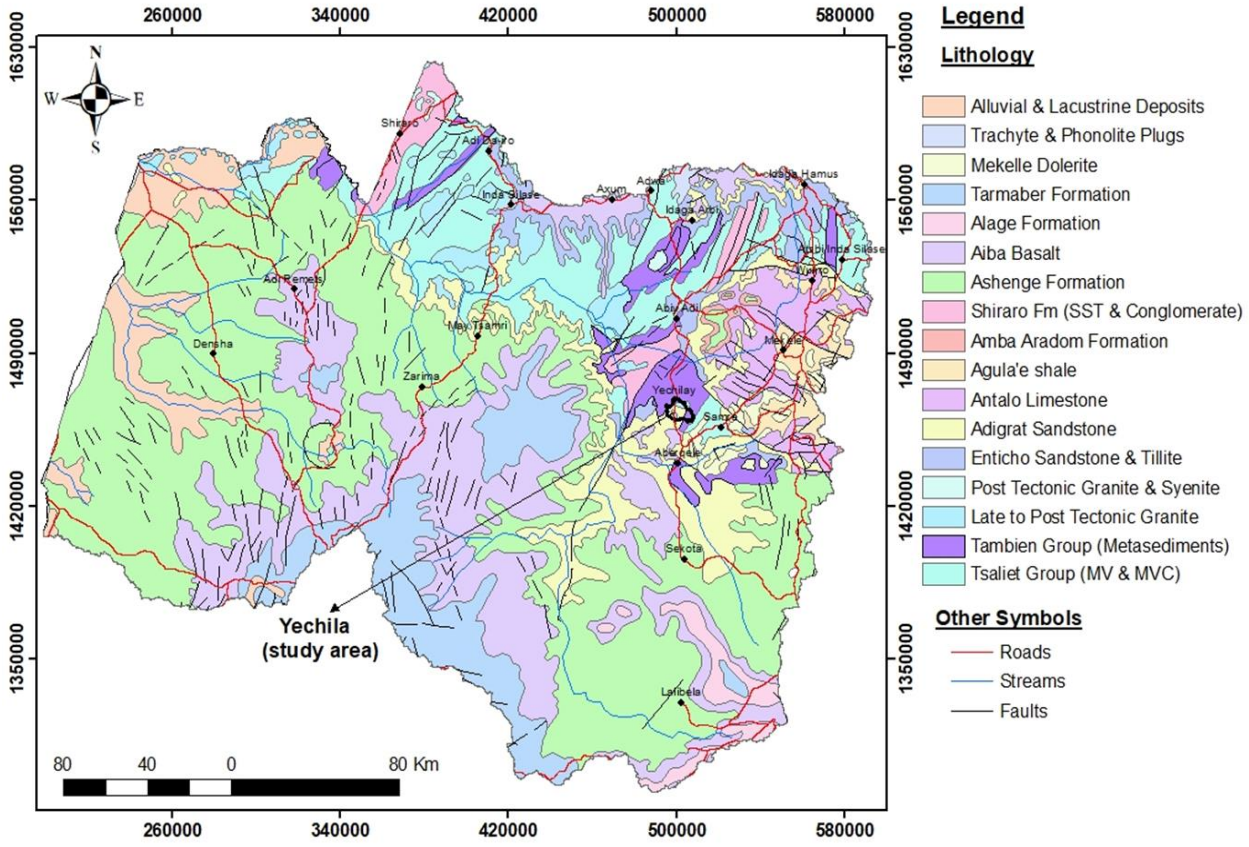

Figure 4.1: Geological map of Tekeze River basin showing fault lines and stratigraphic formations from the Tsaliet and Tembien groups (older) to the Alluvial and Lacustrine deposits (younger) (after Sembroni et al., 2017)

After prolonged deformation and peneplanation, parts of northern Ethiopia were covered by Paleozoic sedimentary deposits, forming the region's oldest preserved undeformed sedimentary succession (Hagos et al., 2020). The basal contact of the formation with the basement is angular unconformity. The Paleozoic sediments in northern Ethiopia comprise two distinct facies: a sandstone facies (Enticho Sandstone) and a tillite facies (Edaga Arbi glacial deposits) (Beyth, 1972b; Lewin et al., 2017 and references therein). These two facies are laterally interfingering to each other (Sacchi et al., 2007). The Enticho Sandstone is characterized by cross-stratified quartz arenite, interbedded with white, calcareous, coarse-grained polymictic conglomerate. The conglomerate contains sub-rounded to well-rounded clasts ranging from pebbles to cobbles and boulders. Dispersed erratic's, mainly granite and gneiss are common in the formation (Beyth, 1972b). The Edaga Arbi Tillite is deposited by glacial process that contains shale and siltstone up to pebbles and boulders. The Mesozoic sedimentary sequences - comprising the Adigrat

Sandstone, Antalo Limestone, Agula Shale, and Amba Aradom Sandstone formations - are predominantly exposed in the eastern and northern part of the basin. The Adigrat sandstone is unconformably overlain the Paleozoic sediments (Getaneh, 2002 and references therein). It is characterized by well sorted, friable its upper section, transitioning to fine-grained, lateritized deposits in its central portion (Hagos et al., 2020). Its thickness is about 670m in Abi Adi area and thinning westward over a short distance to about 80m above the Tekeze River and disappearing completely north of Adigrat – Axum Road (Beyth, 1972a). The Antalo limestone, Agula shale and Amba Aradom sandstone are exposed in the eastern part of Tekeze basin (Mekelle outlier). The Antalo limestone is conformably overlain the Adigrat sandstone and it consists intercalations of limestone, marl and shale units. The Agula shale is composed of finely laminated gray to black shale, marl and limestone with some evaporites (gypsum). The contact between the Antalo Limestone and Agula Shale formations is gradational, with no distinct lithological boundary (Hagos et al., 2020). Above the Agula shale Amba Aradom sandstone is deposited by angular unconformity (Beyth, 1972b). It is coarse grained with conglomeratic lenses in its upper part and lateritized siltstone of lower part. This formation is exposed in Amba Aradom ridge and Hagere Selam massif (Hagos et al., 2020).

The flood basalts were unconformably covered the lateritized Amba Aradom sandstone formation and some on deeply eroded basement complexes (Hagos et al., 2010 and references therein). The huge tertiary volcanic rocks were erupted during the Oligocene period 31 – 29 Ma; Hofmann et al., 1997). Extensive regions of northern Ethiopia, Eritrea, and Yemen were overlain by successive lava flows, along with minor pyroclastic falls and flows, reaching a cumulative thickness of ~2000m (Hagos et al., 2019). Hence, the northwestern Ethiopia flood basalt was emplaced over the past 30Ma, making it the youngest known flood basalt province on Earth (Hagos et al., 2010). The Traps (flood basalts) are covered the southeastern, southern and western areas of the Tekeze River basin (Figure 4.1). The Mekelle dolerites are clearly observed in the eastern sector of the basin (Sembroni et al., 2017). These sills and dykes are characterized by aphanitic to phaneritic texture with basaltic to gabbroid composition (Gebreyohannes et al., 2010) and trending SW-NE direction (Hagos et al., 2020). The Axum-Adwa Plugs are composed of silica- deficient volcanic to hypabyssal rocks, primarily phonolite and trachyte (Hagos et al.,

2010b), dating back 7 to 3 million years (Beyth, 1972a). The plugs overlie the Trap basalts and in places intrude and deform the underlying basaltic flows (Sembroni et al., 2017).

4.2. Hydrogeology

The TRB features a diverse array of rock types spanning Precambrian, Paleo-Mesozoic, and Tertiary periods. These rocks have undergone multiple episodes of deformation and intrusion, resulting in a complex hydrogeological framework. To fully grasp this intricate system, extensive scientific research is essential. A thorough review of various previous hydrogeological studies has been conducted, aiming to develop a comprehensive conceptual model of the hydrogeological system in the region.

According to Ermias Hagos et al. (2015), the aquifer types in the basin are confined, semi-confined and unconfined. The former two aquifers are the dominant types, constituting the shallow aquifers that are most frequently utilized. These aquifers span various rock types and are situated across diverse physiographic regions, making them vital sources of groundwater for multiple uses.

In the northern and northeastern regions of the TRB, the metamorphic and intrusive rocks present a complex hydrogeological environment, shaped by their geological history. These rocks typically exhibit low primary porosity and permeability. However, processes such as weathering and fracturing have developed notable secondary porosity and permeability, which can vary significantly both spatially and with depth. The lack of extensive, uniformly permeable lithological units across large areas suggests that extensive aquifers are absent in this region. This variability in groundwater storage and flow characteristics poses challenges for water resource management and underscores the need for detailed hydrogeological assessments to better understand the aquifer systems in these complex rock formations.

The massive to weakly foliated metavolcanic rocks flanking the synformal folds create distinctive hilly landforms. Due to their geomorphological characteristics and hard, compact nature, these rocks primarily function as runoff zones. Groundwater primarily occurs within fault zones, fractures, and joints of these rock units, as well as along contact zones with aplitic dikes and granitic plutons. In the open synformal structures of the basement complex, groundwater flow is controlled by the dip of the metasedimentary strata and the orientation of the folds.

Narrow valleys that run along the cores of these folds—composed of slates and phyllites and covered with thin alluvial sediments—tend to be more productive. Many of the productive hand-dug wells and shallow boreholes in these metamorphic terrains are situated within these valleys. Conversely, between these valleys, metadolomites and metalimestones create elongated ridges that resemble the metavolcanic hills. However, these ridges typically have minimal groundwater storage capacity due to their limited recharge areas, steep slopes, and the low permeability of the rocks. This results in a challenging landscape for groundwater management and resource extraction.

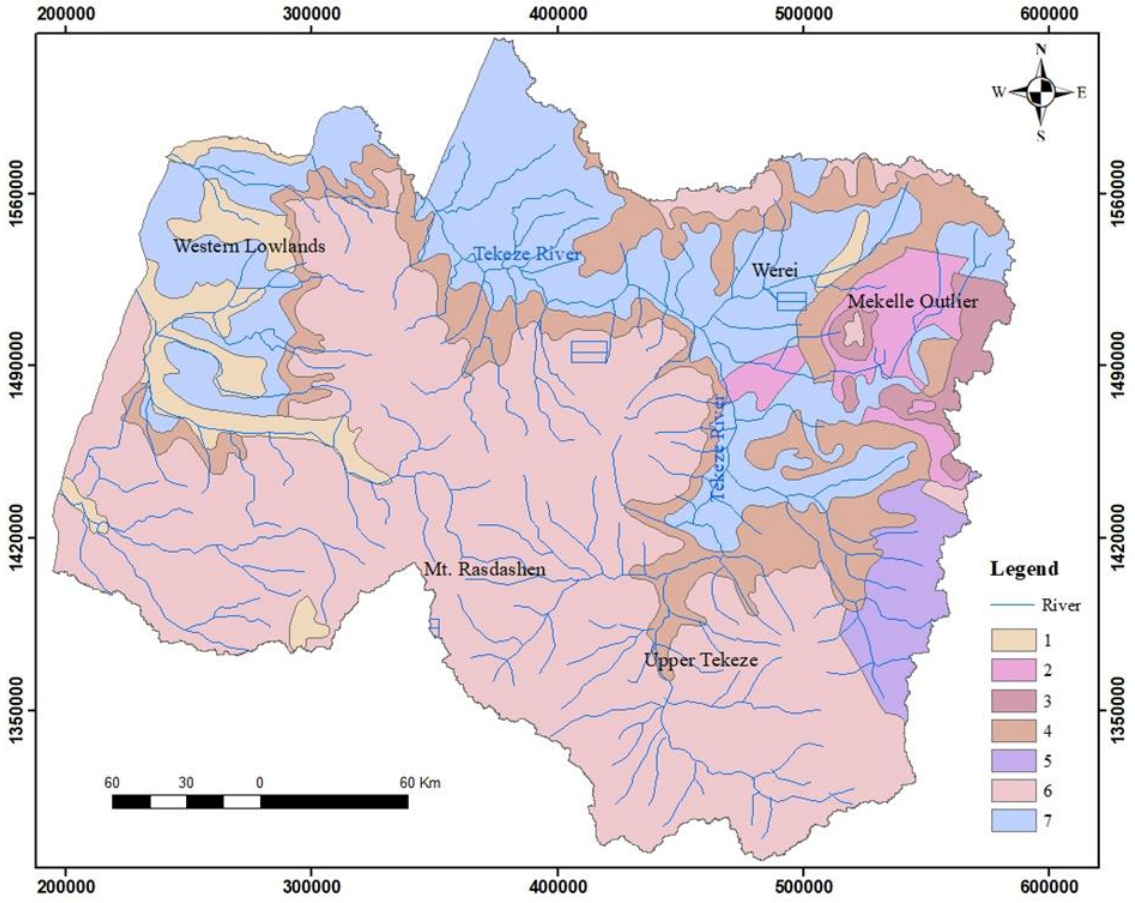

Figure 4.2: Simplified hydrogeological map of the TRB (modified from Tesfaye Chernet, 1988; Ermias Hagos et al., 2015)

Note: the colors on the map are presented in the legend with the numbers for: 1 = moderate productivity aquifers in the Quaternary sediments; 2 = high productivity aquifers in the Mesozoic sedimentary rocks; 3 = low productivity aquifers in the Mesozoic sedimentary rocks; 4 = moderate productivity aquifers in the Mesozoic sedimentary rocks; 5 = high productivity aquifers in the Cenozoic volcanics; 6 = moderate productivity aquifers in the Cenozoic volcanics; 7 = low productivity aquifers in the Neoproterozoic basement rocks

Groundwater occurrence and flow within the Edaga Arbi tillites is highly localized primarily confined to the thin upper weathered and fractured zone along stream channels. Occasionally, perched aquifers can be found within more permeable horizons at greater depths, but these tend to pinch out over short distances. The discontinuity of joints and fractures, both laterally and vertically, arises from significant variations in lithology throughout the tillites. Additionally, the poorly sorted and unstratified nature of this geological unit limits groundwater accumulation, resulting in a slow rate of flow and recharge. This combination of factors creates challenges for effective groundwater management and resource utilization in the area.

The Enticho Sandstone unit forms distinctive dome-shaped hills and flat-topped plateaus, unconformably overlying the basement rocks. The lower section of the unit is characterized by white, medium to coarse-grained sandstone with coarsely cross-bedded structures, silty beds, and some ferruginous layers. In contrast, the upper part features calcareous sandstone, interspersed with lenses of polymictic conglomerates, pebbles, and large granite boulders. In places, this unit is discontinued by faults and erosion which forms Mesa structures. The storage capacity of Enticho sandstone is low due to high permeability and limited lateral extent of the aquifer.

The Adigrat Sandstone formation is characterized by double porosity, encompassing both intergranular and fracture porosity, and primarily hosts confined regional aquifers (Ermias Hagos et al., 2015). This confinement is attributed to inter-beds of less permeable siltstones and mudstones between the sandstone layers. In the Antalo Super-sequence, groundwater primarily moves through fractures, dissolution cavities, and along bedding planes found in the thinly bedded layers. The marl units exhibit a greater intensity of fracturing compared to the limestone beds. However, the fractures in the limestone beds tend to have wider openings. The Agula Shale and dolerite formations are marked by shallow and localized groundwater flow systems (Berhane, 2016).

Within the Tekeze River Basin (TRB), the Adigrat Sandstone and Antalo Limestone formations constitute the most productive semi-regional aquifers. In contrast, the Amba Aradom Sandstone, Agula Shale, Paleozoic sediments, and Proterozoic basement complex host only shallow, localized groundwater systems, primarily functioning as recharge zones for the deeper underlying aquifers. Semi-regional aquifers are present in the fractured and weathered volcanic

rock that creates elevated plateaus, as well as in alluvio-colluvial sediments found in intermountain depressions, river valleys, and lowland plains. In the highlands, thick pyroclastic deposits, buried paleo-valleys, and volcanic rocks situated along structural discontinuities are recognized as some of the basin's most effective aquifers (Tesfaye Chernet, 1993; EIGS, 1993).

4.3. Geology of the Study Area

The study area (Yechilla Catchment) is covered with mainly seven distinct lithological units. These units are listed from the oldest to the youngest as MV, MS, Granite intrusion, Sandstone, Trap Basalt, Dolerite sill and alluvial sediment.

4.3.1. Basements

The MV rock is the oldest unit that of classified under Tsaliet group (Beyth, 1972) and characterized by low grade metamorphic rock with gray to greenish color. It is exposed mainly due to removal of all the overlain younger rocks by erosion and small local faults. Locally, this rock unit is exposed in the northern part of the catchment. This unit is highly sheared near to the main river with N15^{o}E-N60^{o}E orientation of foliations. The MS, belonging to Tambien group, is exposed as small local ridge exposures to the southern part of the study area. These are dominantly composed of meta-carbonates, slates, phyllites and greywacke with NNE-SSW foliation orientation.

4.3.2. Granite intrusion

The granite intrusion in the area is emplaced within the metavolcanic (MV) rocks and exhibits relatively low deformation, except for minor local shearing near the contact zones. The rock displays a distinctive pinkish hue, attributed to the abundance of potassium feldspar (K-feldspar), along with clearly visible coarse-grained minerals such as quartz and feldspar. Quartz-filled veins crosscut the granite, indicating late-stage hydrothermal activity or residual melt crystallization. Small amounts of biotite and/or amphibole are also present in some localities. The rock is moderately to highly weathered, with feldspars often altered to kaolinite or sericite, giving a chalky appearance in some areas.

The main granite body is mostly undeformed, but localized shear zones near the contacts suggest minor post-emplacement tectonic activity. Fractures and joints are present; some filled with

secondary minerals such as quartz and loosen materials. The intrusion exhibits a sharp to slightly diffuse contact with the surrounding metavolcanic rocks.

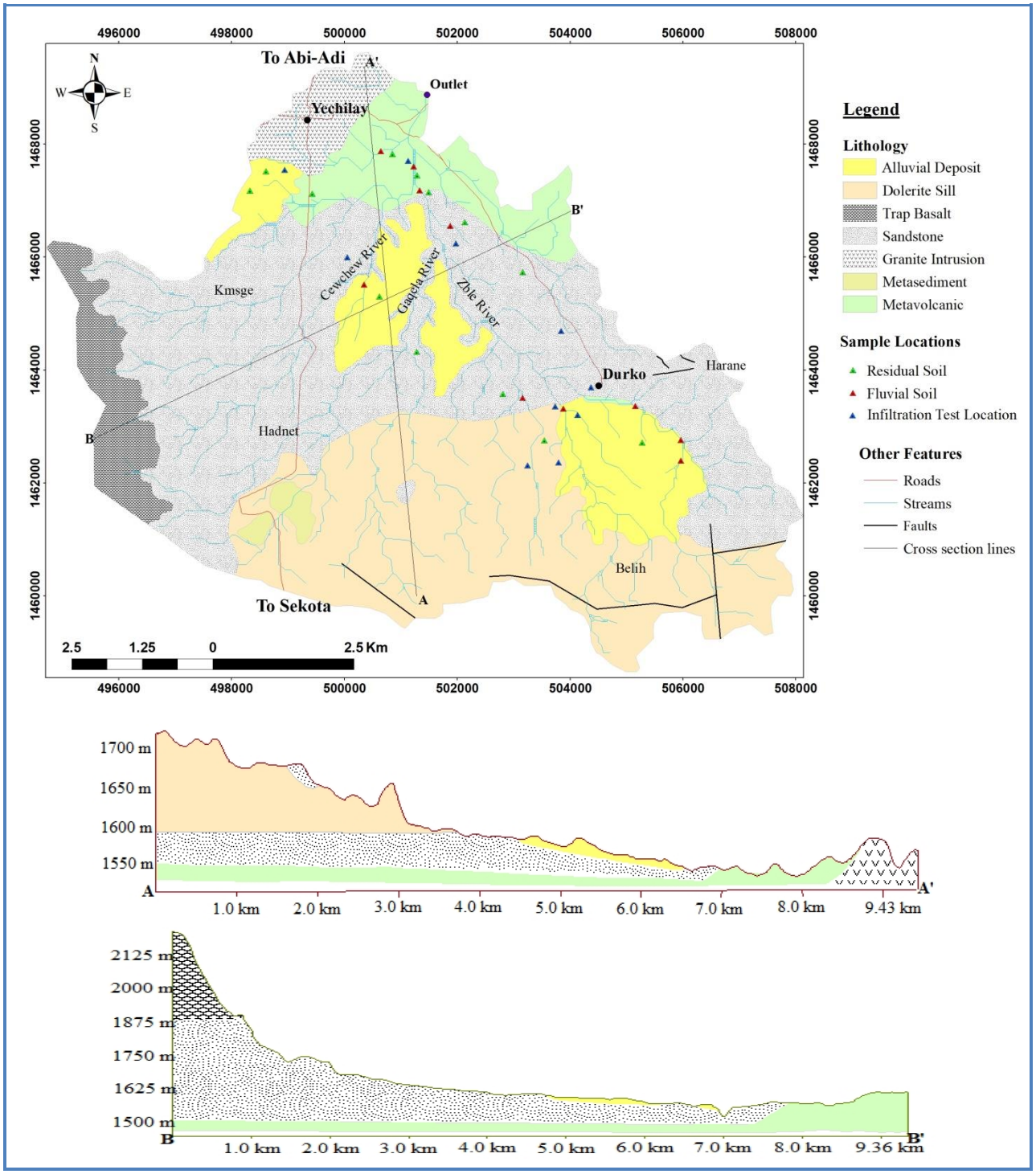

Figure 4.3: Geological map of the study area and schematic cross section along line A-A' and B-B' on the map that shows the major lithology and land forms

Figure 4.4: (a) highly sheared MV observed in river exposure, (b) less sheared MV observed near to the river exposure , (c) highly sheared and exposed by erosion, and shows existing concrete sand dam with 7 gates (at the main river), (d) Meta-carbonates (meta-dolomite and marble), from the southern part of the study area, (e) Slate-Phyllite rock of ridge exposure from southern part of the study area, and (f) Fractured granite near contact with MV

4.3.3. Sandstone

Sandstone represents one of the most widespread rock units in the area. It is described as whitish to reddish color with very hard iron staining localities. The sandstone is predominantly massive and thickly bedded, exhibiting frequent large-scale cross-bedding. It is typically fine- to medium-grained and well-sorted, though localized coarse-grained point bar deposits occur intermittently. Generally this rock shows an intercalation of shale, siltstone, laterite and dark gray alterations. This type of sandstone is regionally correlated with the Adigrat sandstone and exactly overlain the basement in the area. Other locally unique sandstone is also observed in the southern part of the study area. The distinctive sandstone unit is highly indurated and exhibits a light gray color (Figure 4.5c). It is a small ridge that remained from erosion with columnar exposure that shows dolomitic nature at the top and the local people use for construction material as masonry.

Figure 4.5: (a) Sub-horizontal Adigrat Sandstone, intercalation of variegated colors of shale-siltstone-sandstone exposure and wide river bed with thick sand deposit, from eastern part of the study area; (b) Reddish sandstone with clear deformational band, from eastern part of the study area); (c) Distinct ridge forming hard sandstone exposure with columnar feature, from southern part of the study area

4.3.4. Trap Series

Trap basalts are prominently exposed across the southwestern to western sectors of the study area, where they form a distinctive unconformable capping over underlying sandstone formations. These volcanic units predominantly occur at higher elevations within the catchment, creating characteristic dome-shaped landforms that dominate the local topography. This unit is olivine dominated basalt with subophitic to intergranular texture and well developed columnar jointing (Arkine et al., 1971).

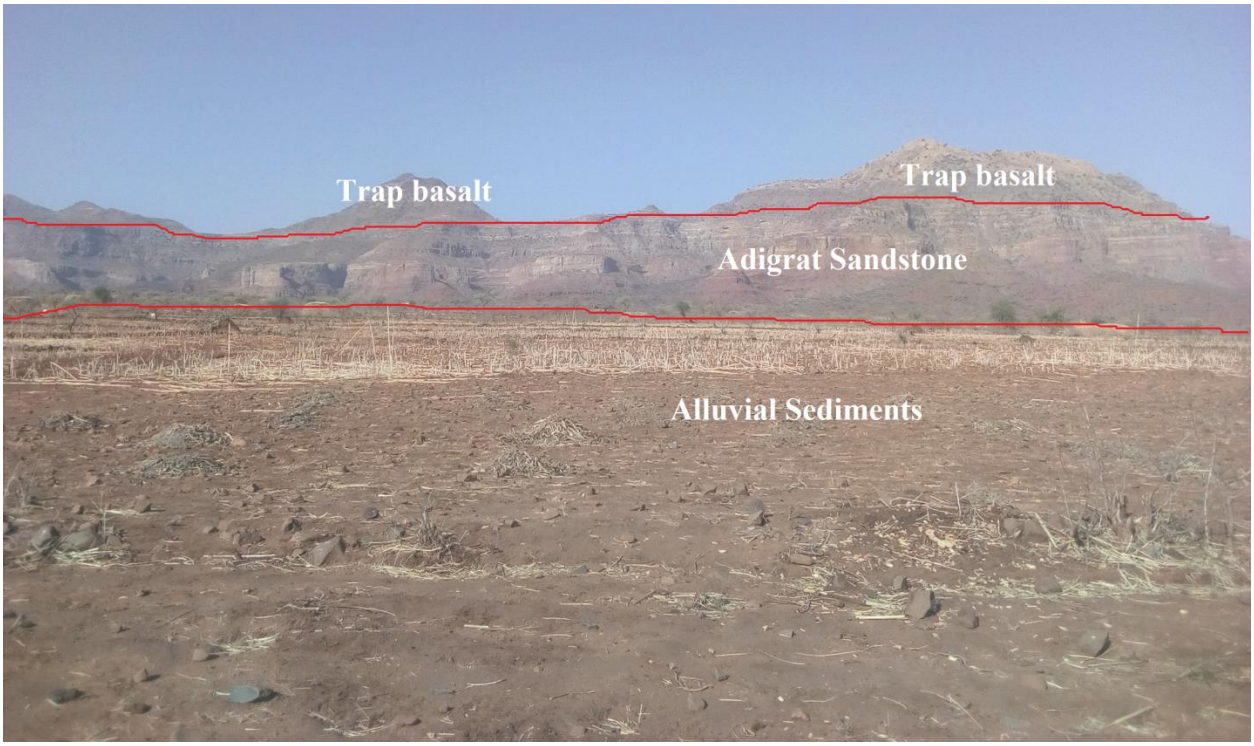

Figure 4.6: Trap Basalt underlain by Adigrat Sandstone from the southwestern to western part of the catchment

4.3.5. Dolerite Sill

The dolerite unit in the study area primarily occurs as tabular sills intruding both sandstone and meta-sedimentary (MS) sequences. These intrusions exhibit variable textures ranging from aphanitic (fine-grained) margins to phaneritic (coarse-grained) interiors, reflecting differences in cooling rates. The dolerite displays basaltic to gabbroic mineralogy, dominated by plagioclase feldspar, with minor olivine and other minerals. Irregular fractures and spheroidal weathering are prominent, leading to rounded boulder outcrops. Sills predominantly follow a NW-SE trend, consistent with regional structural controls.

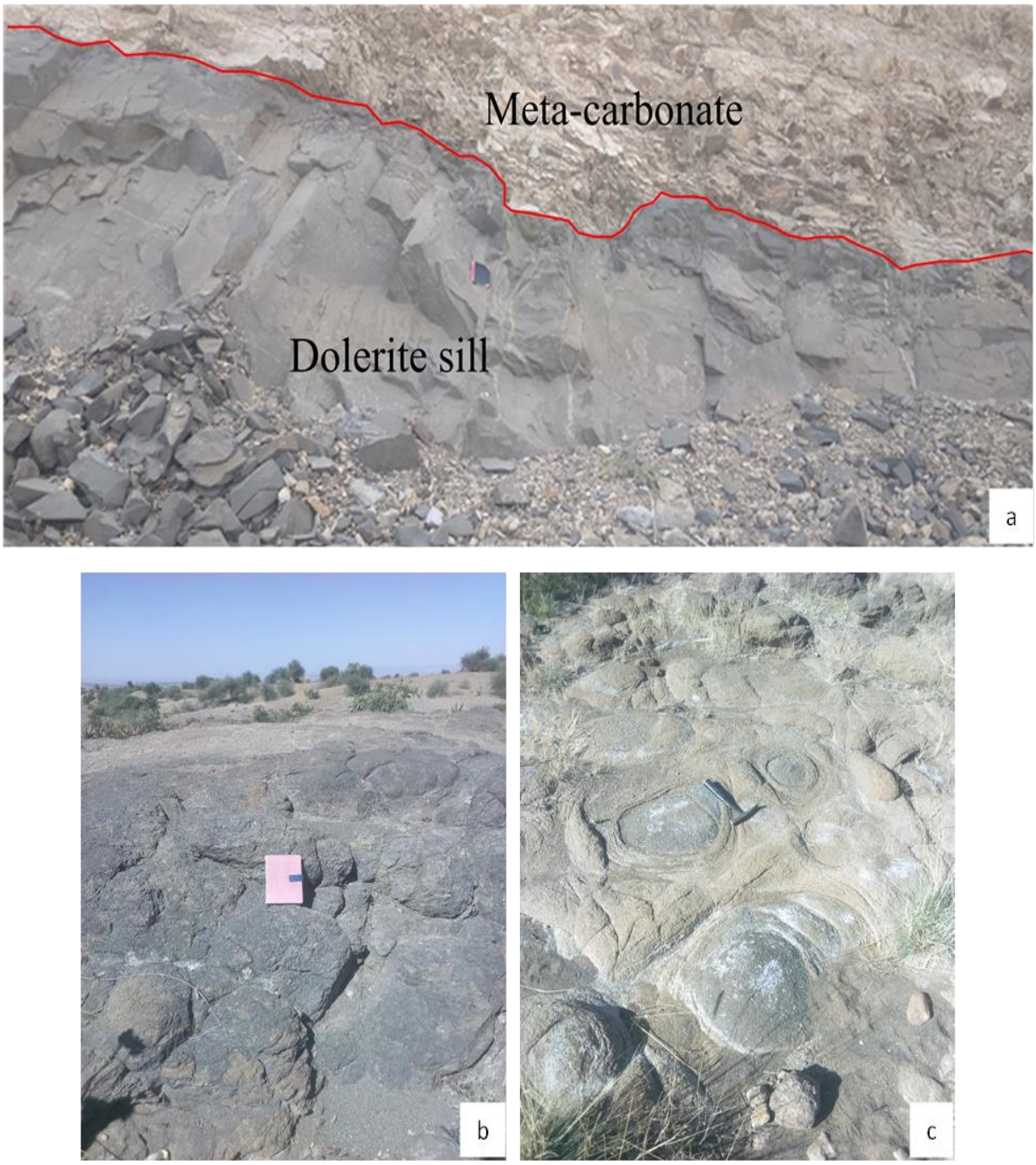

Figure 4.7: Dolerite outcrops from the southern part of the catchment; (a) Aphanitic texture and intruded as a sill in the MS, (b) Highly weathered, Phaneritic texture with dominant dark minerals, (c) Exfoliation weathering, Phaneritic texture with dominant light minerals

4.3.6. Alluvial Deposit

The study area is characterized by extensive alluvial deposits that primarily cover agricultural farmlands and active stream channels. These deposits consist of sand, clay, silt and gravel

sediment mixtures. The stream bed deposits exhibit light to dark-colored sand layers, reflecting variations in sediment source and organic content. Thick deposit is found in the southeastern, central and western parts of the study area.

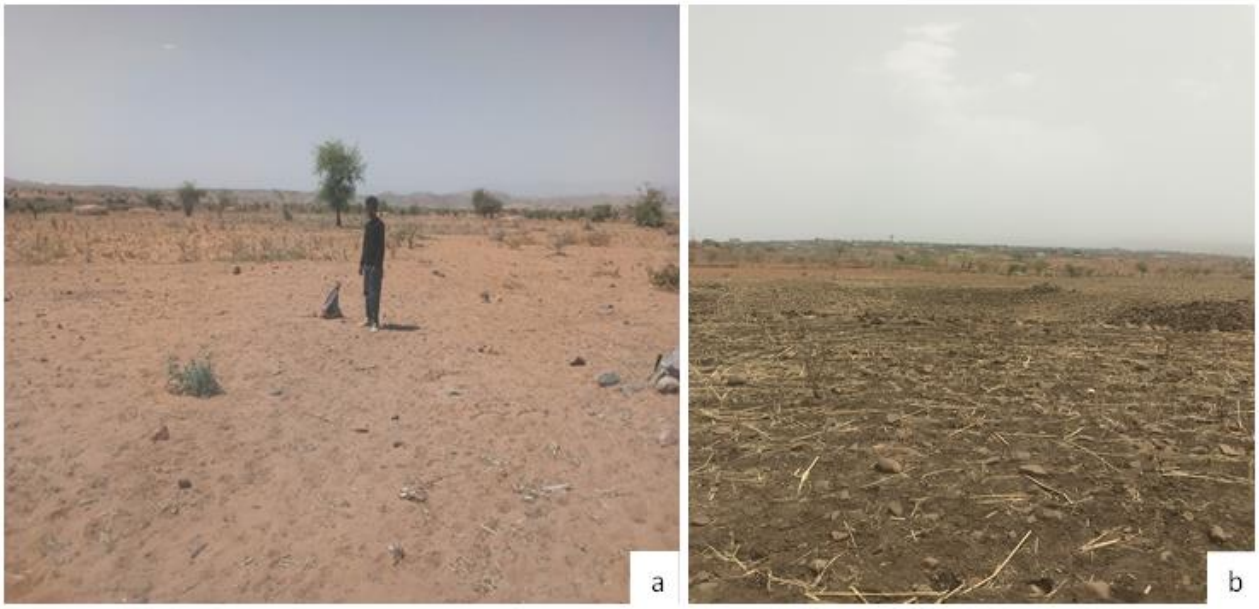

Figure 4.8: Thick alluvial deposits (a) Sand soil from the central part of the study area, (b) Clay soil from the western part of the study area

The Sandy -rich alluvium allows rapid infiltration of rainwater, reducing a runoff loss which is favorable for GWR. Fine silt and clay layers help filter pollutants, improving water quality and good for WH.

CHAPTER FIVE

5. RESULTS AND DISCUSSION

5.1. Textural Description and Classification of the Soils

5.1.1. Fluvial soils

The fluvial (transported) soil deposits are found along the rivers and streams. These soils are dominated by sand which accounts greater than 97% (Table 5.1). The sand deposit is used as water storage that prevents from evaporation just recently observed in the area. The clay and silt soils are very low (<3%) in these deposits as shown in the laboratory result (Table 5.1). The result shows no gravel soil sizes that remained on sieve number 4 (4.75 mm) in the U.S sieve standards. The fines which passed through the sieve number 200 (0.075 mm) are also very low in all samples.

According to Ross et al., (2018), all the stream soils of the area are grouped under HSG A, which has a high rate of infiltration and low runoff potential when thoroughly wet.

Table 5.1 Summary of Laboratory Results and Field Observations on Fluvial Soils

S. Code	Soil color	Sieve Analysis (%)			*Soil Texture	*HSG
		Gravel	Sand	Silt & Clay		
SS1	Red	0	98.3	1.7	Sand	A
SS2	Gray	0	99.75	0.25	Sand	A
SS3	Gray-shining	0	99	1.0	Sand	A
SS4	Gray	0	99.5	0.5	Sand	A
SS5	Light gray	0	97.6	2.4	Sand	A
SS6	Light reddish	0	98.7	1.3	Sand	A
SS7	Gray	0	98	2.0	Sand	A
SS8	Gray	0	98	2.0	Sand	A
SS9	Gray	0	98.7	1.3	Sand	A
SS10	Light gray	0	99	1.0	Sand	A

**Based on Ross et al., (2018)*

5.1.2. Residual Soils

Residual soils are soils formed by the weathering of bedrock in place through physical, chemical, and biological weathering processes. Various soil types, such as clay, sand, silt, loam, sandy loam and clay loam are observed in the area. These soils have their own impacts in water harvesting and groundwater recharge systems. Structures like check dams and farm ponds are better to construct on the impervious clay materials, while percolation tanks must be on pervious materials (sand and sandy loam).

These soils contain sand, sandy loam, silt loam, clay loam and clay with HSG A, B, C, and D respectively.

Table 5.2 Summary of Laboratory Results and Field Observations on Residual Soils

S. Code	Soil color	Sieve Analysis (%)				*Soil Texture	*HSG
		Gravel	Sand	Silt	Clay		
SP1	Light gray	0	43	55	2	Silt Loam	B
SP2	Dark	0	95	4	1	Sand	A
SP3	Red	0	95	3	1	Sand	A
SP4	Gray to black	0	95	3	2	Sand	A
SP5	Red	0	74	20	6	Sandy Loam	A
SP6	Gray to black	0	90	7	3	Sand	A
SP7	Light to dark	0	92	6	2	Sand	A
SP9	Dark	0	31	45	24	Clay Loam	C
SP10	Red	0	97	2	1	Sand	A
SP13	Dark	0	25	30	45	Clay	D

**Based on Ross et al., (2018)*

N.B

HSG	*Description*
A	*Lowest runoff potential. Includes deep sands with very little silt and clay, also deep, rapidly permeable loess*
B	*Moderately low runoff potential. Mostly sandy soils less deep than A, and less deep or less aggregated than A, but the group as a whole has above-average infiltration after thorough wetting*
C	*Moderately high runoff potential. Comprises shallow soils and soils containing considerable clay and colloids, though less than those of group D. The group has below-average infiltration after pre-saturation*
D	*Highest runoff potential: Includes mostly clays of high selling percent, but the group also includes some shallow soils with nearly impermeable sub-horizons near the surface*

SCS hydrologic soil group (USDA 1986)

5.2. Infiltration Rate Results

The study area encounters some different soil types such as sand, clay, silt and loam. Infiltration rate was conducted depending on these soil variations and LULC types using 30 cm diameter and 25 cm high single ring infiltrometer. According to literatures review, the test was conducted at 10 selected sites in the dry season.

The tested results have correlated with the most accepted Infiltration rates Classification standards and literatures (Tables 5.3, 5.4).

Table 5.3 Range and Mean Infiltration rates of the soils of the study area

Test No.	1	2	3	4	5	6	7	8	9	10
Test Location	Takua	Gra-dnkul	Adera-ruba	Eyebela	Durko	Adi-anqeba	Zbla	Baekel	Humer	Chewchew
Soil Type	Loam	Sandy Loam	Sandy Loam	Clayey Loam	Fine Sand	Sand	Clay Loam	Silt Loam	Clay	Sand
I_r Range (cm/hr)	1.3-2.5	2.0-3.4	2.2-3.2	0.2-1.6	1.2-2.8	3.0-3.8	0.4-0.8	1.0-2.3	0.3-0.67	3.2-4.7
Mean I_r (cm/hr)	1.8	2.5	2.8	0.8	1.8	3.4	0.6	1.4	0.4	3.8
*I_r Classification	Moderately Slow	Moderately	Moderately	Moderately Slow	Moderately Slow	Moderately	Moderately Slow	Moderately Slow	Slow	Moderately

**According to Aryanto et al. (2019) as cited in Kiranaratri et al. (2024)*

Table 5.4 Comparison of the standard soil infiltration rates and the current field results

Soil Type	Common Infiltration Rates (Based on many literatures) (cm/hr)	Current Field Average Infiltration Rate Results (cm/hr)
Sand	>3	3.6
Sandy loam	2-3	2.7
Loam	1-2	1.6
Clay loam	0.5-1	0.7
Clay	0.1-0.5	0.4

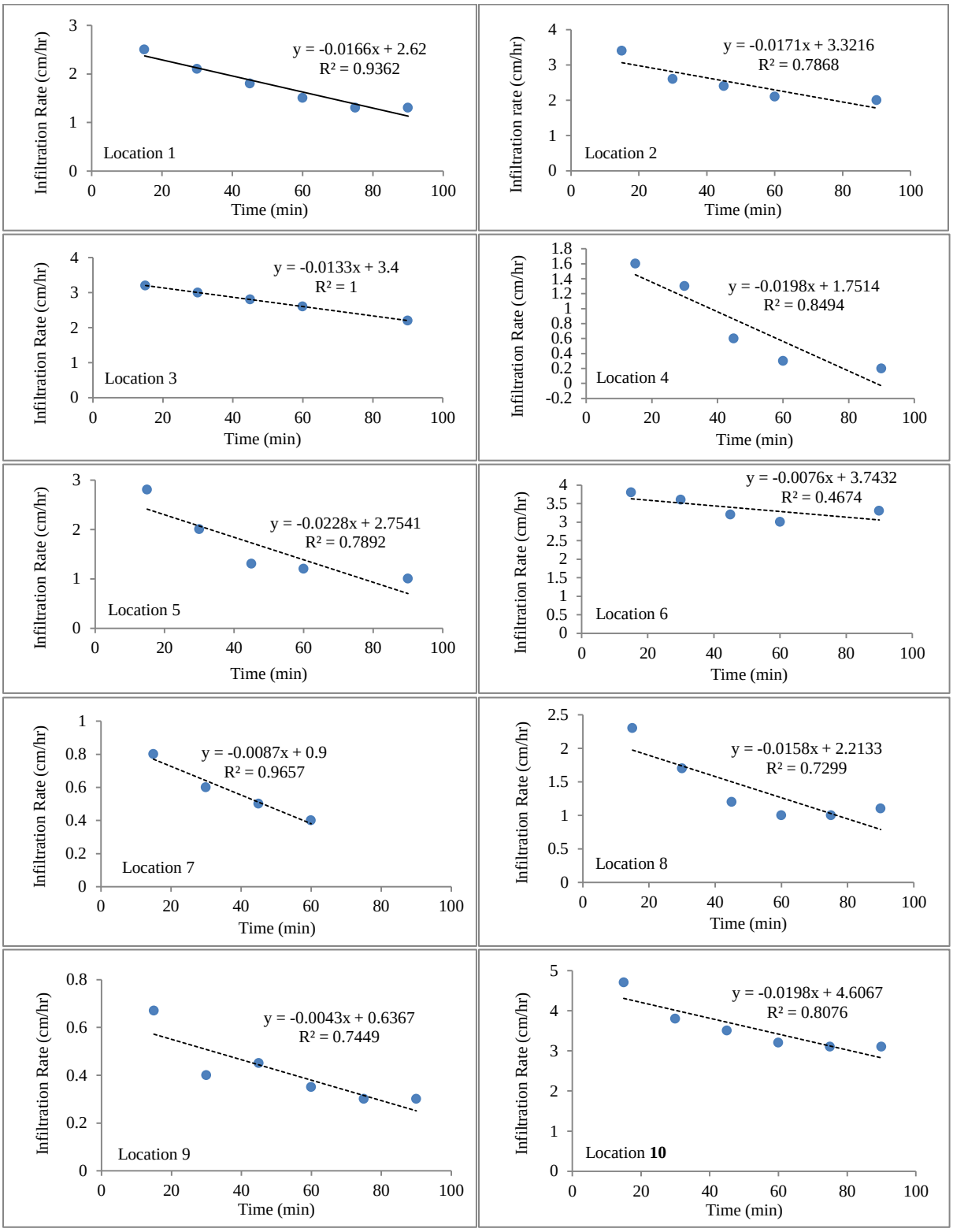

Figure 5.1: Regression Plots created at 10 different locations, Measured and Calculated Infiltration Rates with Regression Coefficients (R^2) and Equations for Each Measurement Point (based on Kiranaratri et al. (2024)

The infiltration rate is influenced by various parameters, including soil density, vegetation, granular compaction, and soil texture. Based on the measured values at different locations (Table 5.3), the lowest infiltration rate recorded was 0.4 cm/hour, classified as slow, corresponding to clay soil type. In contrast, the highest infiltration rate observed was 3.8 cm/hour, classified as medium, associated with sandy soil.

5.3. Rock Mass Characterization

Joint and uniaxial compressive strength (L-Schmidt hammer test) measurements were carried out in all the rock outcrops of the catchment. The measurements were conducted mostly in the flat and gentle topography of the area due to its importance for WH and GWR structures.

The major joint sets in the sandstone exposure, namely J1, J2 and J3 have been identified with strike ranges 280-340, 345-360 and 060-085 respectively. The joints are dipping vertical to sub-vertical angles and varies from closed to opened (approximately 1m) aperture with soils, quartz and calcite infillings. Their persistence ranges from 3m to more than 20m. Bedding is also common in the sandstone rock unit of the area with mostly horizontal and average bedding thickness up to 1.5m except in the cliff forming exposure, which is approximately more than 3m thick. In the Dolerite rock, one joint set with irregular/random joints are observed. The average strike direction of the major joint set ranges 315-350 with vertical/sub-vertical dip angle. The discontinuities in the Basement outcrop are related to foliation and cleavage. Generally, the foliations are trending NNE-SSW direction. The MVs are highly sheared near to the main river with E-W directional force. Three joint sets with some random joints are observed in the granite intrusion with average strike range; 285-330 (J1), 350-360 (J2), 020-045 (J3).

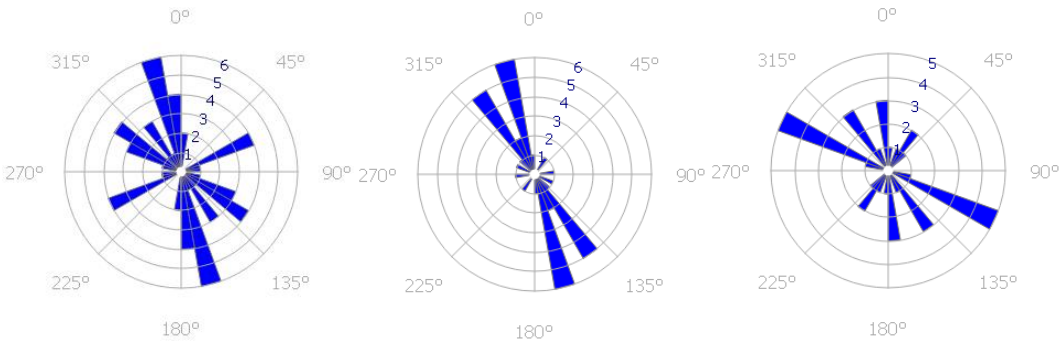

Figure 5.2: Strike class rose diagram of joint measurements for sandstone (left), Dolerite (middle), and Granite (right)

The RQD results for each of the rock units are calculated from volumetric joint count according to ISRM (1981) and Hudson and Harrison (1997) and presented as table 5.5 below.

Table 5.5 Volumetric Joint count (Jv) and average RQD values analyzed from the outcrop discontinuity data of the study area

Lithology/Rock type	Volumetric Joint (Jv)	Jv classification as per Palmström, (1982)	Average RQD
Sandstone	3.3	Moderate (moderately jointed)	100
Dolerite	1.2	Low (weakly jointed)	100
Granite	7.1	Moderate (moderately jointed)	91.6
Basement	3.1	Moderate (moderately jointed)	100

The Schmidt hammer rebound test is a non-destructive method used to assess the hardness and compressive strength of rock surfaces in the field. The test is conducted at about 30 site locations in the study area. In each site location, 20 single rebound impact readings were recorded to ensure accuracy and consistency. According to the guidelines set by the International Society for Rock Mechanics (ISRM, 1978), the readings are arranged in ascending order and discarded the lowest 50% values. Following this, the mean is calculated from the highest 50% rebound values remaining. This average is considered representative of the material's hardness and strength, providing a reliable indicator for further analysis. The uniaxial compressive strength (UCS) is derived from established correlations between hardness numbers and UCS values, typically referenced in charts. This compressive strength value is obtained using the Deer-Miller graph, which illustrates the relationship between rock strength and Schmidt hammer measurements, as shown in Figure 3.1 (refer to methodology). Based on this procedure, the UCS values for the sandstone, dolerite, granite and basement have been calculated and results are presented (refer to Appendix C, Table 1).

Table 5.6 Rock Mass Classification of the Study Area based on Bieniawski's Method (RMR)

No	Parameters		Sandstone	Rating	Dolerite	Rating	Granite	Rating	MV	Rating
1	Rock strength (Schmidt Test) (Mpa)		63	7	126	12	227	12	183	12
2	Average RQD (%)		100	20	100	20	91.6	20	100	20
3	Joints Spacing (m)		1-1.5	15	2	20	0.5	10	0.6	10
4	Condition of joints	Persistence (m)	10-20	1	3-10	2	3-10	2	1-3	4
		Aperture (mm)	50-100	0	5-20	0	8-40	0	5-15	0
		Roughness	Rough	4	Slightly rough	3	Slightly rough	3	Smooth	1
		Infillings	Sandy soils	0	Clay soils	2	Quartz & soils	2	Quartz & calcite	2
		Degree of weathering	Slight	5	Moderate	3	Moderate	3	Slight	5
5	Water situation		Dry	15	Dry	15	Dry	15	Dry	15
6	Joint orientation (dip of joints) Relating to Foundation		Most joints are vertical and some horizontal	-2	Vertical joints	-12	Vertical to sub vertical joints	-7	Vertical to sub vertical joints	-7
	Total RMR			65		65		60		62
	RMR Class		Good Rock		Good Rock		Fair Rock		Good Rock	

Joint spacing, joint conditions (including persistence, aperture, infillings, and degree of weathering), and dip of joints directly influence water percolation. Among the rock outcrops, granite is the most highly fractured; however, its fractures are rendered impermeable due to infillings of quartz veins and clay materials. The basement rock exhibits foliation and shearing, though the foliation is largely surficial and thus has negligible impact on permeability. While shear zones can enhance groundwater movement, their limited extent in the area restricts their overall significance. In contrast, sandstone and dolerite demonstrate relatively higher permeability, as evidenced by favorable joint parameters in these formations.

The joint characteristics is an essential factor to study rock slope, reservoir leakage and as an input for the RMR calculations. The RMR values for the four dominant rock units of the area are calculated according to Bieniawski (1989). The rating of each parameter is summed to get total RMR value (Table 5.6). The Sandstone, Dolerite and MV rock units are classified in the range of

good rock quality and the Granite rock is in the fair rock quality class. Hence, the rock masses of the area can serve as a foundation for the macro and micro reservoirs generally.

5.4. Existed Water Harvesting Practices in the Area

Many traditional and undeveloped WH practices are existed in the area. Hand boring activities in the sand deposited stream beds are very common to extract water for domestic and irrigation purpose. The water and soil conservation practices such as check dams/sand dams, ponds and open shallow wells are observed during the field work. Some local springs are also observed in the contacts between the granite intrusion and MV rock units.

Figure 5.3: Some existed WH structures: (a) Concrete sand dam, (b) Concrete sand dam with multiple gates, (c) Gabion supported stone bund, (d) Pond motor pumping, (e) Hand boring in sand deposited stream bed, (f) Shallow open well, (g) Spring water at the metavolcanic rock, and (h) Water tanks used to collect water through pipe joining from surroundings for water supply to Yechila town; 250,000 m^3 (larger tank) and 100,000 m^3 (smaller tank)

5.5. Water Harvesting and Groundwater Recharge Thematic Maps

5.5.1. Lithology

Lithology is one of the key factors in selecting WH and GWR sites. Particular attention is to be paid to the lithological units as far as the water retention, occurrence, movement and quality of groundwater is concerned (Ahirwar et al., 2020). A detailed geological map for the area is produced using field observations and other map resources. The lithological units exposed in the area include; Alluvial Deposit, Dolerite sill, Trap Basalt, Sandstone, Granite intrusion, Metasediment and Metavolcanic. Alluvial deposits have occupied the southeastern, central and northwestern part of the area with gentle slope. This unit represents very high groundwater formation zone which is suitable for artificial recharge but not for water harvesting due to its highly permeable nature. Most of the area is covered with sandstone, which ranges from steep (small area coverage) to gentle slope, supporting high groundwater recharge suitability. The sandstone rock in the area is affected by joints, bedding, and fractures, as observed during the field. These discontinuities will increase the leakage of water in addition to the good porosity and permeability nature of the rock. Hence, the unit is unsuitable for harvesting water on its surface. The dolerite sill is moderately to highly weathered and covers a gentle to moderate slope. In such a case, it is classified as moderate in both site selection methods. The Basements (MV & MS) are evaluated as high for WH and low for GWR suitability. However, the rock units are highly sheared, foliated, and fractured in some exposures in the area. These rock weaknesses can help to percolate water deep into the underground, which fulfills the groundwater recharge. Granite intrusion is exposed at the northern tip of the area. It is characterized by a slightly to moderately weathered, pinkish color with clear K-feldspar dominant minerals. During the fieldwork, some springs were observed that show water remains very close to the surface in this rock. Due to its hydrogeological properties, it discourages groundwater recharge but supports WH. Trap basalt is exposed in the eastern periphery hilly area with a steep slope supporting less WH, as well as groundwater recharge.

This suitability classification is done using field study, experts and the community opinions, and borehole log data (sourced from Abergelle-Yechilla Wereda Water Supply Office). The distribution of suitability class and area coverage of the rocks is shown in table 5.7.

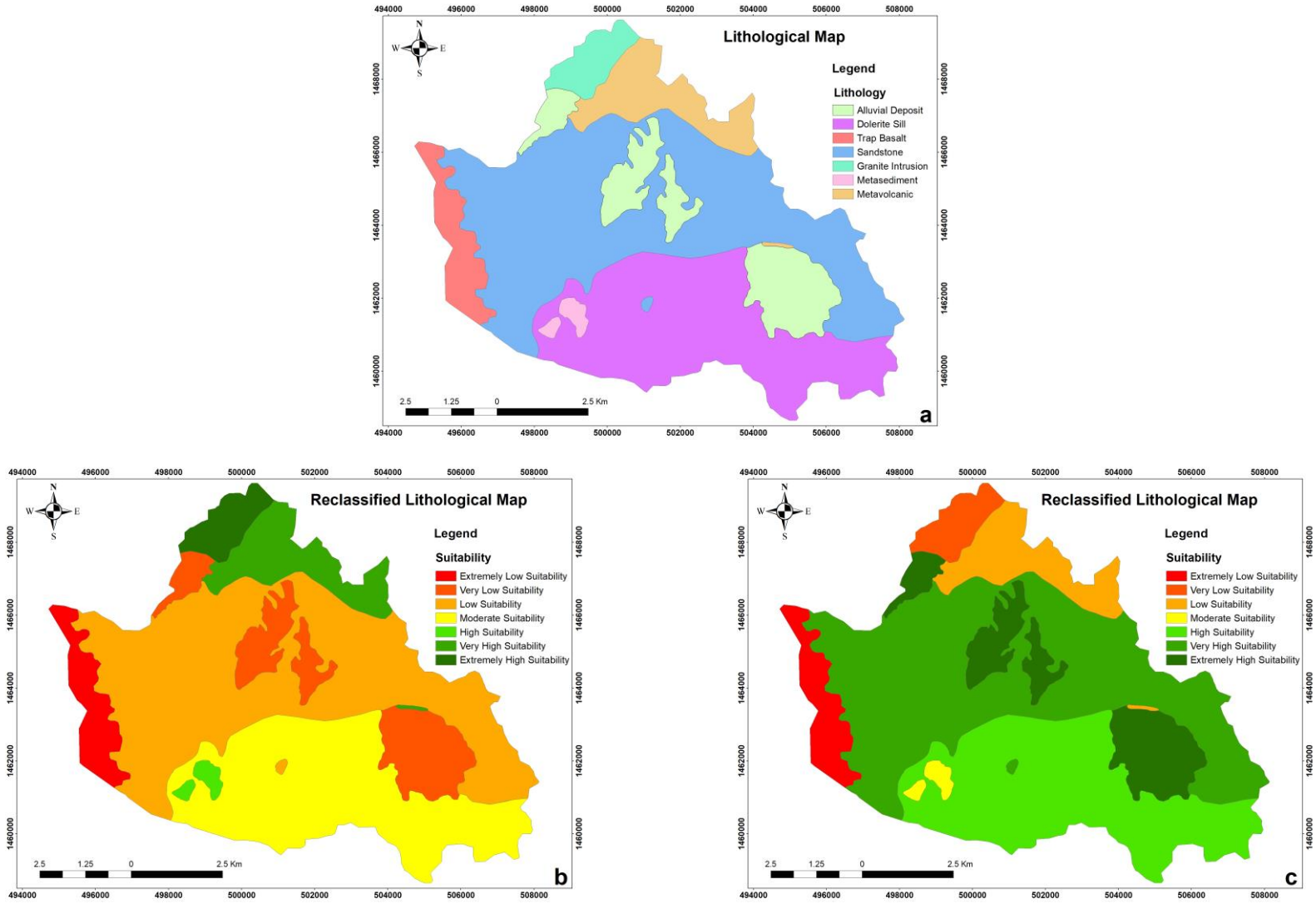

Figure 5.4: (a) Lithological Map, (b) WH Suitability Map and (c) GWR Suitability Map

Table 5.7 Distribution of Lithology suitability classes

Factor	Rock Type	For WH		For GWR		Coverage (km^2)	Coverage (%)
		Rate	Suitability	Rate	Suitability		
Lithology	Trap Basalt	1	Extremely Low	1	Extremely Low	3.82	4.7
	Alluvial Deposit	2	Very Low	7	Extremely High	9.63	11.89
	Sandstone	3	Low	6	Very High	35.3	43.6
	Dolerite Sill	4	Moderate	5	Moderate	22.81	28.2
	Metasediment	5	High	3	Low	0.72	0.89
	Metavolcanic	6	Very High	3	Low	6.13	7.57
	Granite	7	Extremely High	2	Very Low	2.63	3.25

5.5.2. Soil Texture

Fine and medium-textured soils are preferred over coarse soils for rainwater harvesting (RWH) due to their superior water and nutrient retention capacity (White, 2005; Kumar & Jhariya, 2017). The study area consists of clay loam, sand, sandy loam, and coarse fragments/stones (Figure 5.5). Rocky areas (coarse fragments and stones) cover approximately 33.74 km² (41.62%), primarily located along the sloped western to southeastern periphery of the watershed. These areas are unsuitable for both water harvesting (WH) and groundwater recharge (GWR) sites.

Clay loam, the second most dominant soil type, spans 24.87 km² (30.68%) and is found in the central part of the watershed, where slopes are gentler. This soil type is classified as highly suitable for WH and moderately suitable for GWR compared to others. Sand and sandy loams are rated as very high and high suitability, respectively, for GWR site selection. While sandy loam is the second-most preferred soil for WH after clay loam, sand is less favorable for WH due to its high porosity and permeability. However, in this study area, sand is still classified as moderately suitable for WH relative to other soil types.

The infiltration test was used to validate the soil texture suitability model in the study area, with the infiltration rate results (Table 5.3) serving as reliable indicators of soil permeability and

water retention capacity. Clay and clay loam soils, with infiltration rates between 0.4 and 0.8 cm/hr, exhibit high water retention capacity and increased runoff potential, making them favorable for water harvesting (WH). Conversely, sandy and sandy loam soils, with significantly higher infiltration rates ranging from 2.5 to 3.8 cm/hr, demonstrate a greater capacity for water percolation, which is well-suited for groundwater recharge (GWR).

Table 5.8 Distribution of Soil Texture Suitability Classes

Factor	Soil Type	For WH		For GWR		Coverage (km^2)	Coverage (%)
		Rate	Suitability	Rate	Suitability		
Soil Texture	CF and Rocks	1	Low	1	Low	33.74	41.62
	Sand	2	Moderate	4	Very High	17.87	22.05
	Sandy Loam	3	High	3	High	4.58	5.65
	Clay Loam	4	Very High	2	Moderate	24.87	30.68

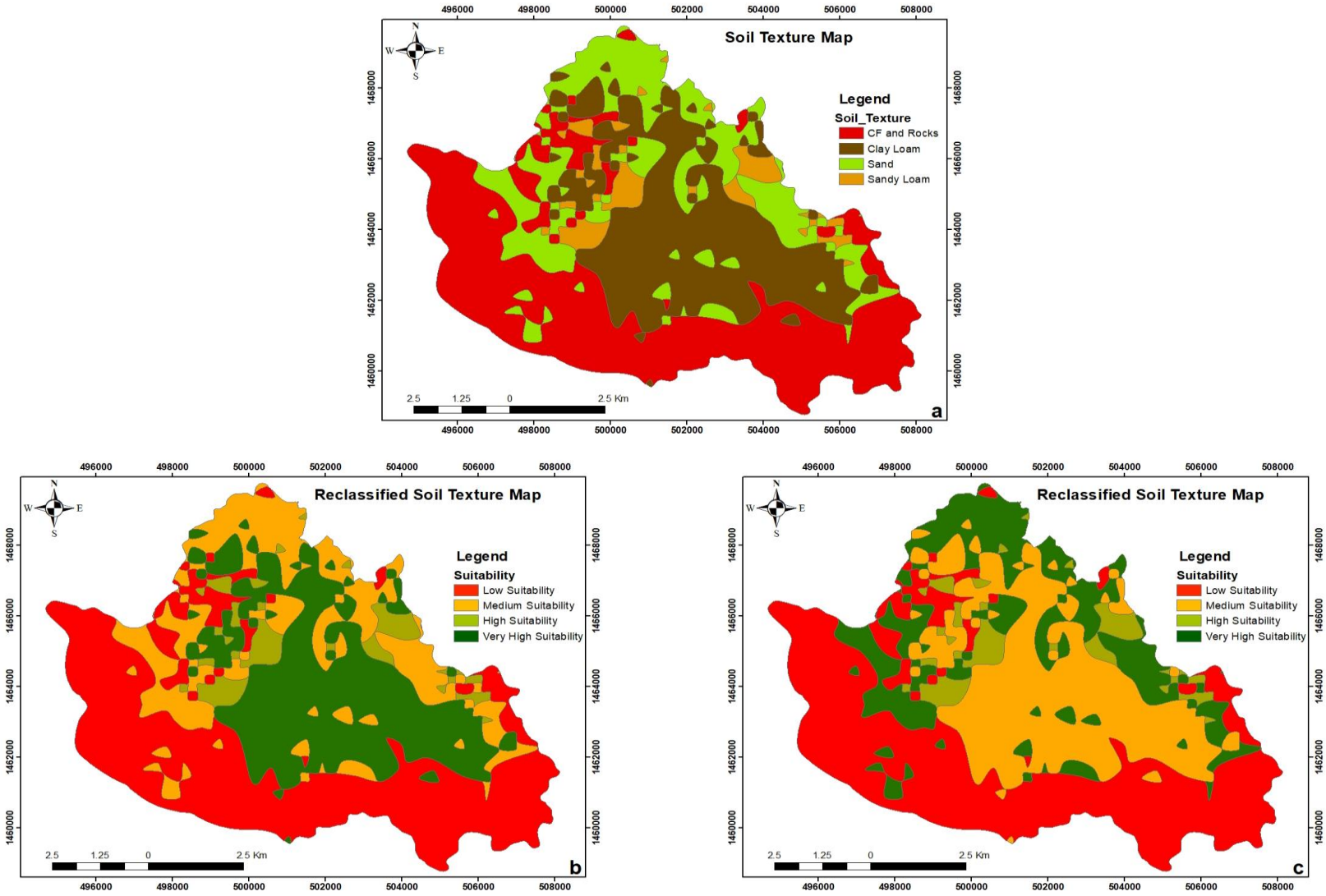

Figure 5.5: (a) Soil Texture Map, (b) WH Suitability Map, (c) GWR Suitability Map

5.5.3. Slope

The study area has a wide range of slopes, from flat to mountainous. Based on literatures review, five categories of slope percentage are distinguished for WH suitability class: flat (0–5%), mild (5–10%), moderate (10–15%), steep (15–30%), and mountainous (>30%). A slope of less than 5% is ideal for WH site selection (Adham et al., 2018). Therefore, a total of 28.1% of the study area is classified as extremely suited for WH, as shown by the slope map (Figure 5.6b). The area coverage for mild and moderate slopes are 35.7% (high suitability) and 13.8% (medium suitability), respectively. The steep and hilly slopes of the area cover 13.4% and 9% respectively, which are least suited areas.

Areas with gentle slopes exhibit moderate surface runoff, facilitating greater water infiltration, whereas regions with steep slopes experience high runoff, resulting in reduced rainwater retention time and consequently moderate infiltration rates (Dassargheya and Panda, 2015). The slope of the area is classified based on GWR suitability class as very high suitability (0-2%), high suitability (2-5%), moderate suitability (5-10%), low suitability (10-15%) and unsuitable (>15%) (Ghayoumian et al., 2007; Ahirwar et al., 2020; Guigui et al., 2021).

Table 5.9 Distribution of slope suitability classes for WH

Factor	Interval	Rate	Suitability	Coverage (km^2)	Coverage (%)
Slope (%)	>30	1	Unsuitable	7.22	9
	15-30	2	Low Suitability	10.73	13.4
	10-15	3	Medium Suitability	11	13.8
	5-10	4	High Suitability	28.5	35.7
	0-5	5	Very High Suitability	22.43	28.1

Table 5.10 Distribution of slope suitability classes for GWR

Factor	Interval	Rate	Suitability	Coverage (km^2)	Coverage (%)
Slope (%)	>15	1	Unsuitable	17.98	22.55
	10-15	2	Low Suitability	10.88	13.65
	5-10	3	Medium Suitability	28.7	36
	2-5	4	High Suitability	18.45	23.14
	0-2	5	Very High Suitability	3.72	4.67

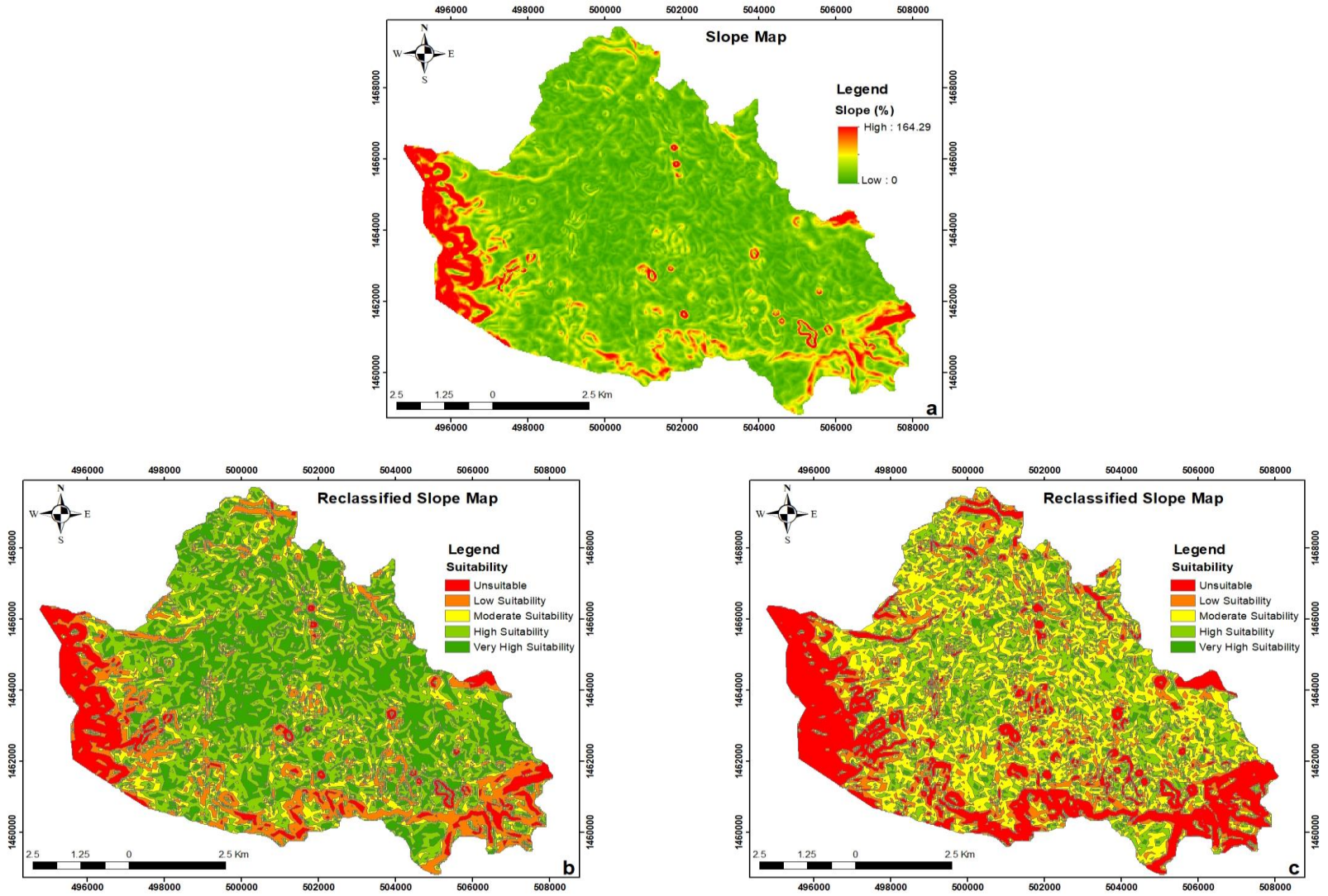

Figure 5.6: (a) Slope Map, (b) WH Slope Suitability Map and (c) GWR Slope Suitability Map

5.5.4. Elevation

The elevation of the study area ranges from 1,491 to 2,265 meters above sea level. Areas above 1,680 meters are generally inaccessible and steep, resulting in rapid runoff and erosion in the area. Constructing water harvesting (WH) and artificial recharge structures in these zones is challenging due to stability issues, requiring advanced engineering solutions.

The majority of the watershed falls under very high and high suitability classes for WH (Table 5.11). The suitability distribution for WH and groundwater recharge (GWR) is detailed in Tables 5.11 and 5.12, respectively.

Table 5.11 Distribution of elevation suitability classes for WH

Factor	Class	Rate	Suitability	Coverage (km^2)	Coverage (%)
Elevation (m)	1715-2265	1	Unsuitable	16.05	19.8
	1690-1715	2	Low Suitability	4.80	5.92
	1650-1690	3	Medium Suitability	13.74	16.95
	1600-1650	4	High Suitability	20.03	24.71
	1491-1600	5	Very High Suitability	26.44	32.62

Table 5.12 Distribution of elevation suitability classes for GWR

Factor	Class	Rate	Suitability	Coverage (km^2)	Coverage (%)
Elevation (m)	1680-2265	1	Unsuitable	23.56	29.07
	1660-1680	2	Low Suitability	7.00	8.64
	1620-1660	3	Medium Suitability	15.33	18.91
	1580-1620	4	High Suitability	17.08	21.07
	1491-1580	5	Very High Suitability	18.08	22.31

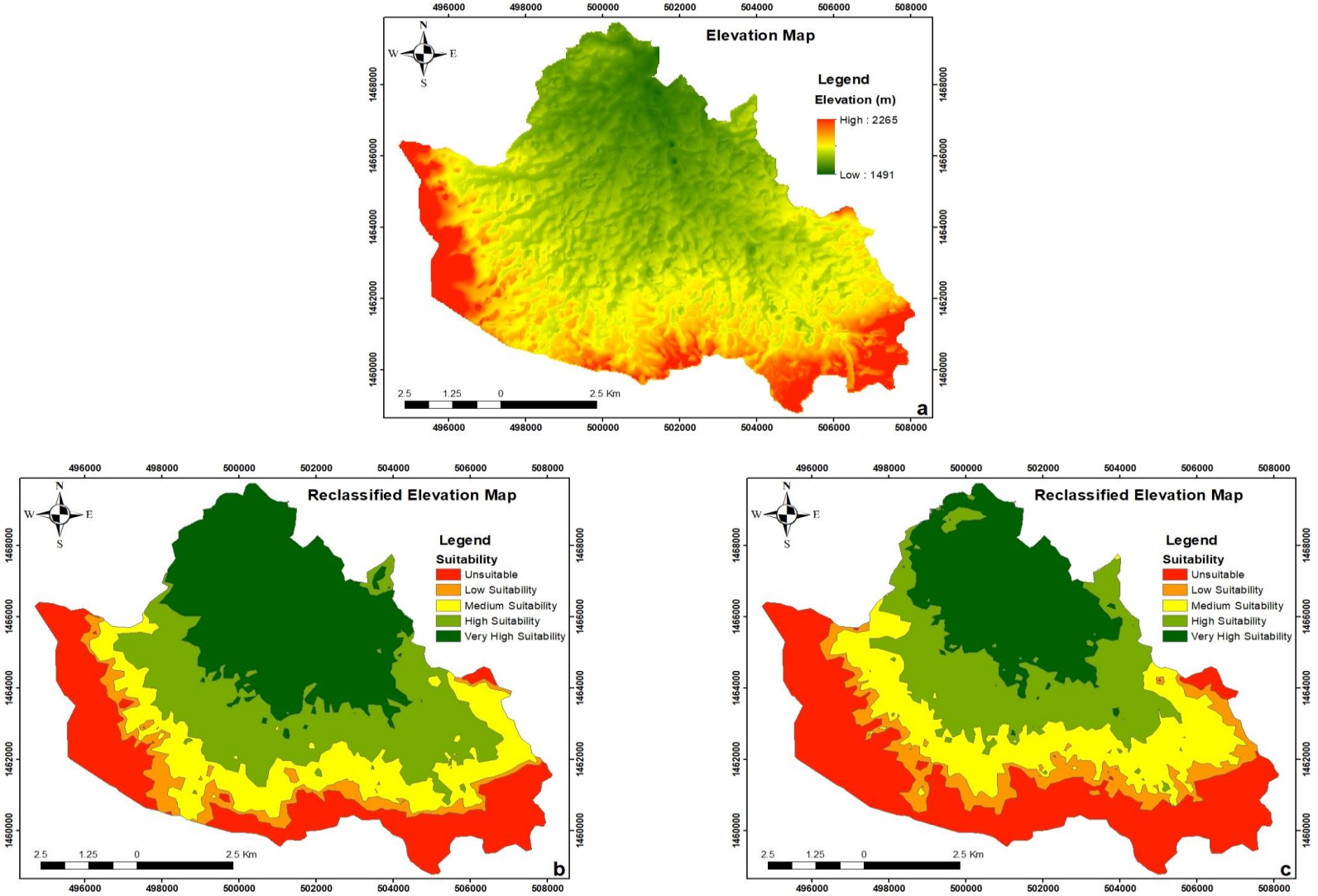

Figure 5.7: (a) Elevation Map, (b) WH Elevation Suitability Map, (c) GWR Elevation Suitability Map

5.5.5. Drainage Density

The study area watershed's drainage density (DD) ranges from 7.99 to 115.75 km/km² (Figure 5.8a). As stated by Agarwal et al. (2013), DD exhibits an inverse relationship with permeability. Mundalik et al. (2018) further highlight its direct influence on land use, topography, and geomorphology. Studies (Ettazarizini & El Mahmouhi, 2004; Abirami & Annadurai, 2016) confirm that higher DD reduces subsurface water infiltration, while lower DD enhances it.

Areas with higher drainage density (DD) are favorable for water harvesting (WH) site selection, as they indicate well-developed surface runoff networks. Conversely, higher DD is unfavorable for groundwater recharge (GWR) due to reduced infiltration capacity, as excessive channelization promotes rapid runoff rather than percolation into the subsurface (Agarwal et al., 2013; Ettazarizini & El Mahmouhi, 2004). According to Preeti et al. (2022), the area is classified in to 5 drainage density suitability classes (Figure 5.8b & c).

Table 5.13 Distribution of Drainage Density suitability classes for WH

Factor	Interval	Rate	Suitability	Coverage (km^2)	Coverage (%)
Drainage Density (km/km^2)	<30	1	Unsuitable	4.44	5.48
	30-40	2	Low Suitability	8.23	10.16
	40-50	3	Medium Suitability	22.82	28.17
	50-60	4	High Suitability	24.85	30.68
	60-115.75	5	Very High Suitability	20.65	25.5

Table 5.14 Distribution of Drainage Density suitability classes for GWR

Factor	Interval	Rate	Suitability	Coverage (km^2)	Coverage (%)
Drainage Density (km/km^2)	>80	1	Unsuitable	4.64	5.72
	70-80	2	Low Suitability	4.62	5.7
	60-70	3	Medium Suitability	11.4	14
	50-60	4	High Suitability	24.87	30.65
	<50	5	Very High Suitability	35.6	43.9

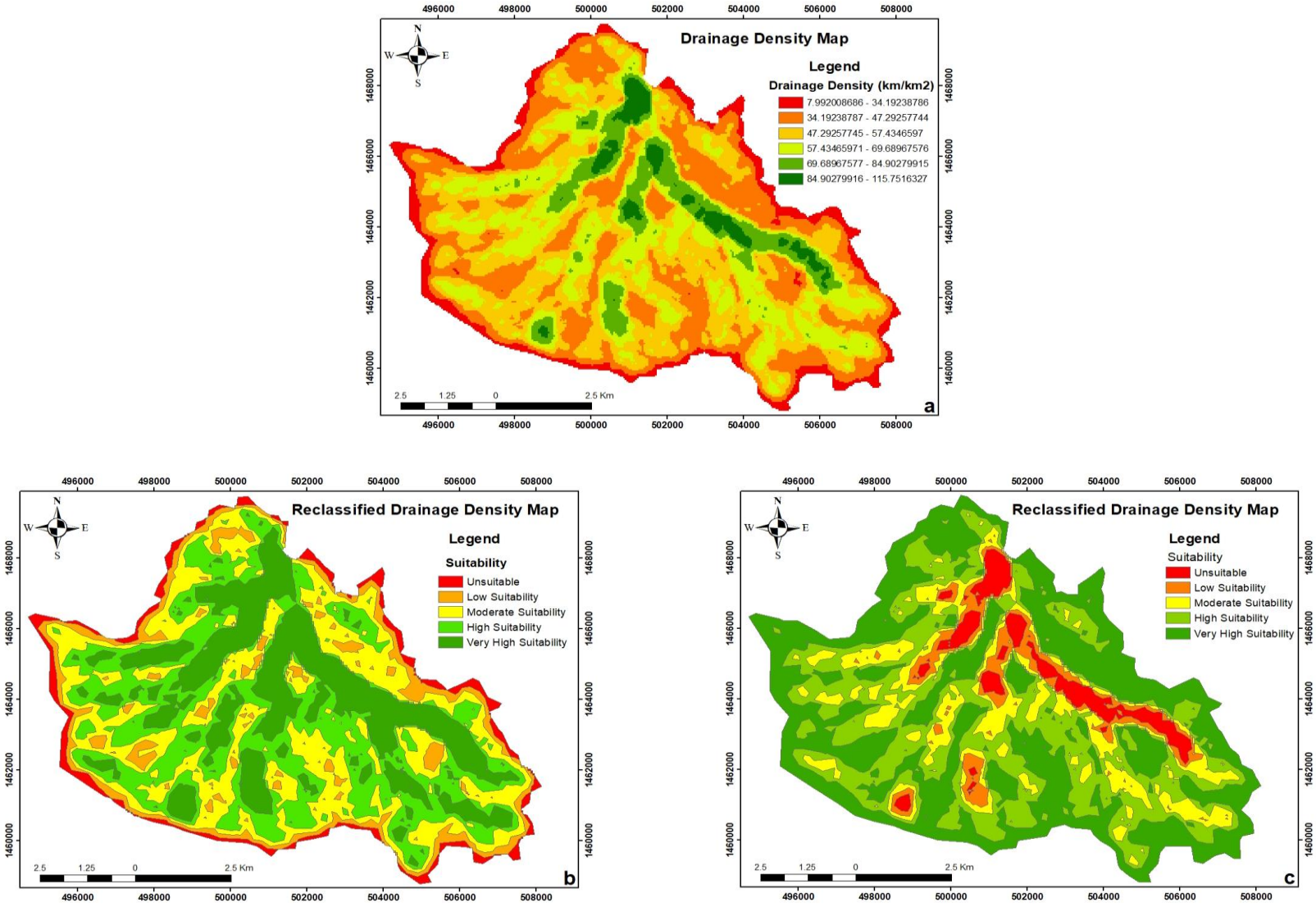

Figure 5.8: (a) Drainage Density Map, (b) WH Drainage Suitability Map and (c) GWR Drainage Suitability Map

5.5.6. Lineament Density

Lineament density (LD) serves as a critical indicator of potential groundwater recharge zones, as it represents areas where water can preferentially infiltrate into subsurface systems (Ghazavi et al., 2018; Mandal et al., 2022; Wijesinghe et al., 2023). This parameter integrates several key geological characteristics associated with structural deformation, particularly fracturing and shearing zones, which significantly influence groundwater potential (Rajasekhar et al., 2021).

The LD range of values of the area is 0 to 5.72 km/km^2 as shown in Figure 5.9a. The lower lineament density area is favorable for WH, but unfavorable for GWR (Figure 5.9b &c).

Table 5.15 Distribution of Lineament Density suitability classes for WH and GWR

Factor	Interval	For WH		For GWR		Coverage (km^2)	Coverage (%)
		Rate	Suitability	Rate	Suitability		
Lineament Density (km/km^2)	3.4-5.7	1	Unsuitable	5	Very High Suitability	3.4	4.2
	2.2-3.4	2	Low Suitability	4	High Suitability	9.76	12
	1.3-2.2	3	Medium Suitability	3	Medium Suitability	21.75	26.8
	0.49-1.3	4	High Suitability	2	Low Suitability	15.65	19.3
	<0.49	5	Very High Suitability	1	Unsuitable	30.47	37.6

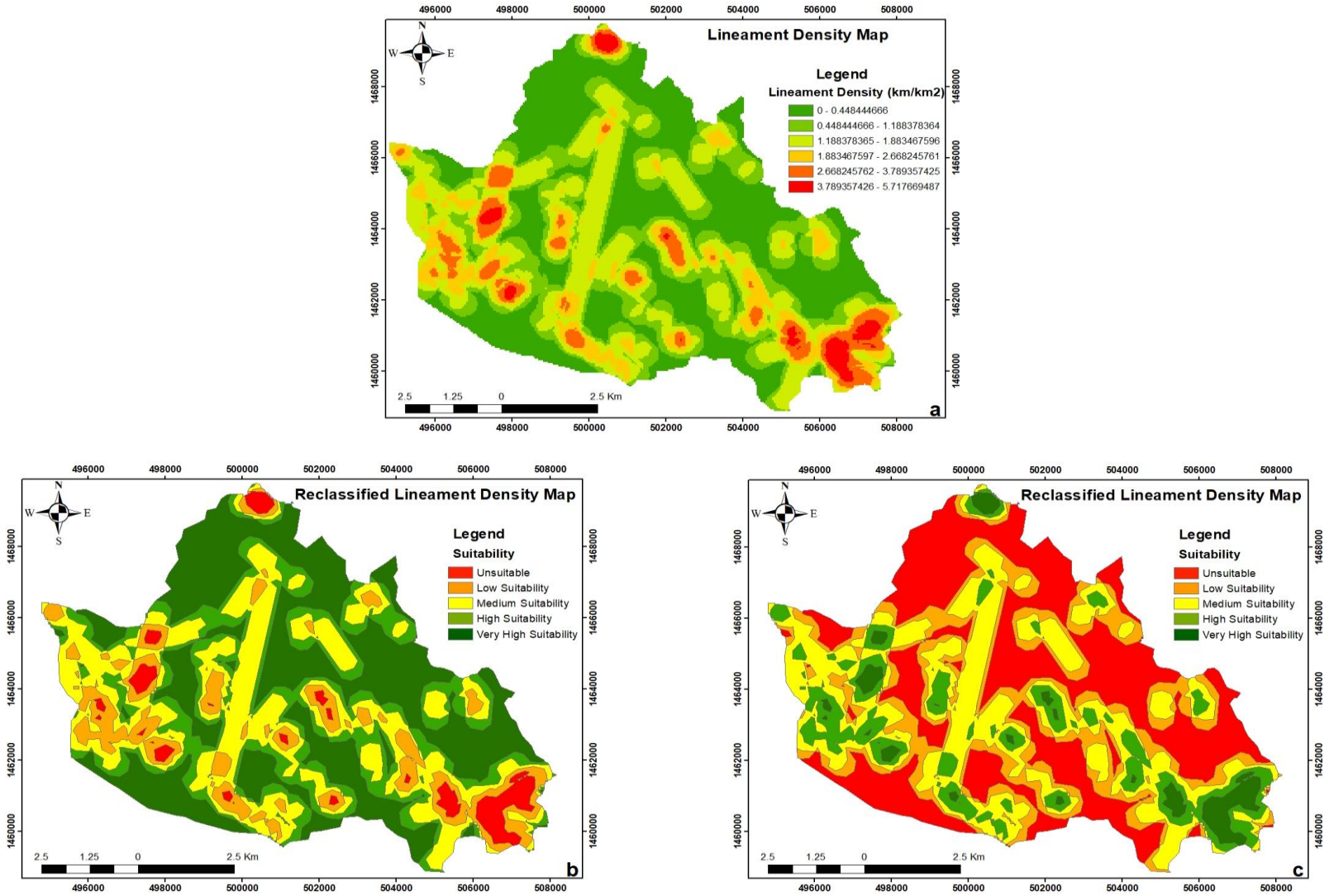

Figure 5.9: (a) Lineament Density Map, (b) WH LD Suitability Map, (c) GWR LD Suitability Map

5.5.7. Rainfall

Figure 5.10 presents a map of the study area's average annual rainfall distribution, showing effective annual rainfall values ranging from 691 mm to 753 mm. Regions with higher effective rainfall (729–753 mm), depicted in deep and light green, are concentrated in the lower-elevation areas along the northeastern and northern borders. In contrast, areas of moderate to high elevation, primarily in the southern and southwestern parts of the study area, receive lower rainfall amounts (691–729 mm). As indicated, the zones of highest rainfall are the most suitable for implementing both water harvesting (WH) and groundwater recharge (GWR) structures.

Increased rainfall promotes rapid groundwater recharge, particularly where macro-pores and preferential pathways enable high infiltration rates (Wittenberg et al., 2019). Conversely, regions with lower effective rainfall, coupled with elevated evapotranspiration, experience constrained groundwater recharge, which subsequently reduces overall water availability (Dey et al., 2020).

Table 5.16 Distribution of Rainfall suitability classes for WH and GWR

Factor	Interval	Rate	Suitability	Coverage (km^2)	Coverage (%)
Rainfall (mm)	<705	1	Unsuitable	7.6	9.4
	705-717	2	Low Suitability	30.62	37.8
	717-728	3	Medium Suitability	12.87	15.9
	728-740	4	High Suitability	19.6	24.2
	>740	5	Very High Suitability	10.4	12.8

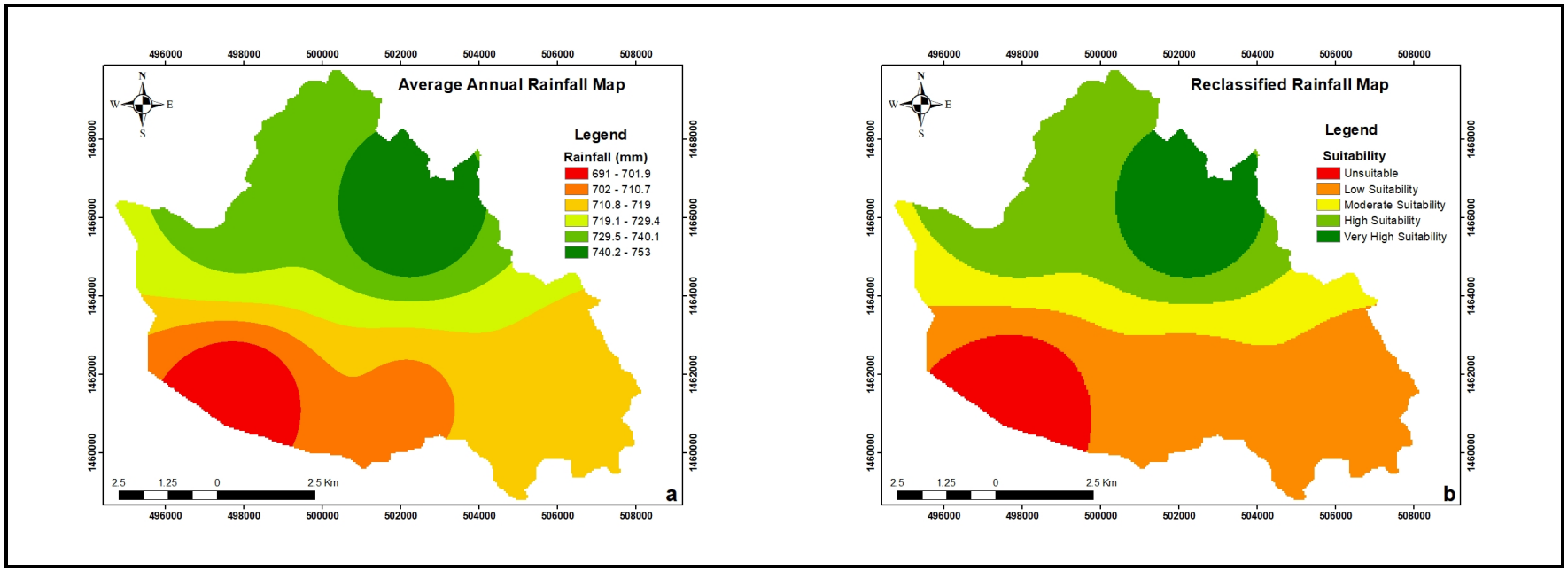

Figure 5.10: (a) Average Annual Rainfall Map, (b) WH and GWR Suitability Map

5.5.8. Land use/land cover (LULC)

The study area is covered with bare land (40.5%), agricultural area (31.1%), stream bed (14%), built up area (10.4%), and vegetation (4%). These classes were verified by field surveying. Streams, bare land and Built up area are recommended for WH zones and structures while agricultural and vegetated lands are for GWR. Human activities in agricultural areas such as plowing, and land cultivation—disturb the soil structure, reducing compaction and increasing infiltration potential. This makes them suitable for managed recharge systems like infiltration basins or recharge wells. Natural vegetation improves soil porosity through root growth and organic matter accumulation, facilitating gradual water percolation. Plant roots also stabilize the soil, minimizing erosion and siltation that could otherwise clog recharge zones. Additionally, vegetation and associated soil microbes act as natural filters, removing pollutants and improving the quality of recharged water. Thus, while agricultural lands benefit from human-induced soil modification, vegetated areas contribute through natural processes that all supporting effective GWR when properly managed.

Table 5.17 Distribution of LULC suitability classes

Factor	Type	WH		GWR		Coverage (km^2)	Coverage (%)
		Rate	Suitability	Rate	Suitability		
LULC	Agricultural	1	Unsuitable	5	Very High	25.22	31.1
	Vegetation	2	Low	4	High	3.25	4
	Built up	3	Medium	1	Unsuitable	8.4	10.4
	Bare land	4	High	3	Medium	32.8	40.5
	Stream bed	5	Very High	2	Low	11.4	14

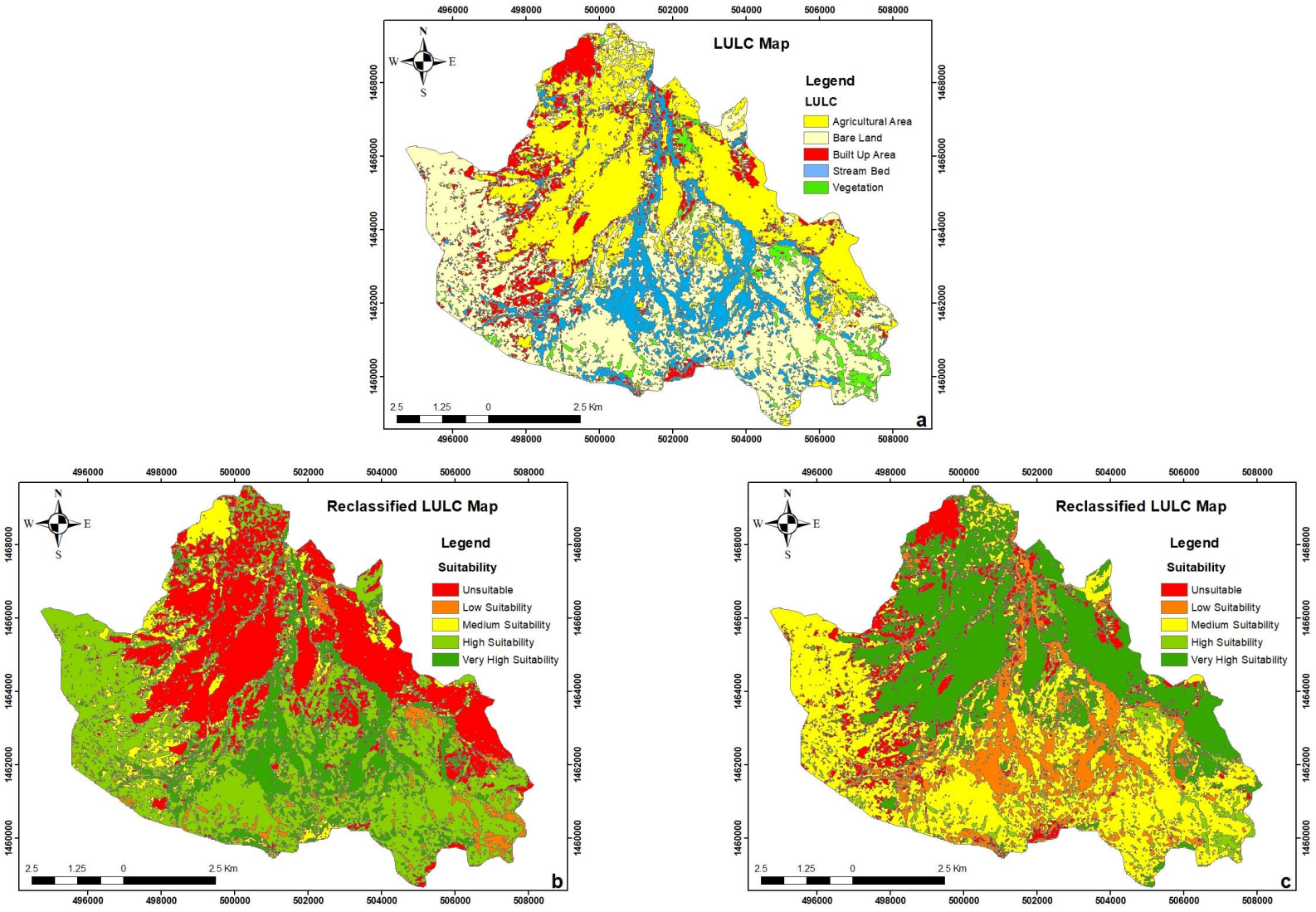

Figure 5.11: (a) LULC Map, (b) WH LULC Suitability Map and (c) GWR LULC Suitability Map

5.6. Overall site suitability map

All the eight criteria are computed using AHP method based on literatures, experts and their current priorities in the area. In this study, the same criteria (i.e., lithology, soil texture, slope, elevation, drainage density, lineament density, rainfall and LULC) were used for both WH and GWR site suitability assessments.

However, the computed weights of the criteria may different for each assessment. WH site suitability in this context is the area where rainwater and flood water can store without percolating and infiltrating to the underground. Conversely, GWR zone is the area of low runoff and high infiltration and percolation rates.

The pairwise comparison, normalized, weighted and overlay analysis are done separately for the proposed two objectives (WH and GWR) in this research.

5.6.1. WH Suitability Map

5.6.1.1. Computing the weights

Tables 5.18 and 5.19 present the results of pairwise comparisons and normalized weights respectively, using the Analytic Hierarchy Process (AHP) in the context of multi-criterion decision-making (MCDM). The calculated Consistency Index (CI) was 0.007, and the resulting Consistency Ratio (CR) of 0.005 was well below the acceptable threshold of 0.1, ensuring the reliability of the assigned weights.

Following the consistency check, the final weights for each criterion were determined and are presented in Table 5.19. The results indicate that soil texture exerts the strongest influence on the selection of suitable sites for water harvesting (WH) structures, followed by rainfall and slope. In contrast, elevation, lineament density (LD), and land use/land cover (LULC) were found to have a relatively minor impact on the site suitability decision-making process.

Table 5.18 Pairwise comparison matrix for main criteria for WH

Criteria	Soil Type	Rainfall	Slope	Lithology	DD	LULC	LD	Elevation
Soil Type	1	1	2	3	4	3	3	5
Rainfall	1	1	2	2	3	3	3	4
Slope	0.5	0.5	1	2	2	4	3	3
Lithology	0.33	0.5	0.5	1	2	2	2	2
DD	0.25	0.33	0.5	0.5	1	2	1	2
LULC	0.33	0.33	0.25	0.5	0.5	1	1	2
LD	0.33	0.33	0.33	0.5	0.5	1	1	1
Elevation	0.2	0.25	0.33	0.5	0.5	0.5	1	1

Table 5.19 Normalized weights of the main criteria for identification of suitable zones for WH

Criteria	Soil Type	Rainfall	Slope	Lithology	DD	LULC	LD	Elev.	Criteria Weight
Soil Type	0.25	0.24	0.29	0.30	0.30	0.18	0.20	0.25	0.25
Rainfall	0.25	0.24	0.29	0.20	0.22	0.18	0.20	0.20	0.22
Slope	0.13	0.12	0.14	0.20	0.15	0.24	0.20	0.15	0.17
Lithology	0.08	0.12	0.07	0.10	0.15	0.12	0.13	0.10	0.11
DD	0.06	0.08	0.07	0.05	0.07	0.12	0.07	0.10	0.08
LULC	0.08	0.08	0.04	0.05	0.04	0.06	0.07	0.10	0.06
LD	0.08	0.08	0.05	0.05	0.04	0.06	0.07	0.05	0.06
Elevation	0.05	0.06	0.05	0.05	0.04	0.03	0.07	0.05	0.05

- $\lambda_{max} = 8.05$
- *Consistency index = 0.007*
- *Random index = 1.41*
- *Consistency ratio = 0.005*

Table 5.20 The rating of the eight criteria selected based on literature review and weights (After Al-Adamat et al., 2010; Al-shabeeb, 2016; Gavhane et al., 2023) for WH

Parameters	Normalized Weight	Sub-class	Rating
Soil Type	0.25	Clay Loam	4
		Sandy Loam	3
		Sand	2
		CF and Rocks	1
Rainfall (mm)	0.22	>740	5
		728-740	4
		717-728	3
		705-717	2
		<705	1
Slope (%)	0.17	<5	5
		5-10	4
		10-15	3
		15-30	2
		>30	1
Lithology	0.11	Granite	6
		Metavolcanic	5
		Metasediment	5
		Dolerite Sill	4
		Sandstone	3
		Alluvial Deposit	2
		Trap Basalt	1
DD (km/km^2)	0.08	>60	5
		50-60	4
		40-50	3
		30-40	2
		<30	1
LULC	0.06	Stream bed	5
		Bare land	4
		Built up area	3
		Vegetation	2
		Agricultural	1

LD (km/km^2)	0.06	<0.49	5
		0.49-1.3	4
		1.3-2.2	3
		2.2-3.4	2
		3.4-5.7	1
Elevation (m)	0.05	1491-1600	5
		1600-1650	4
		1650-1690	3
		1690-1715	2
		1715-2265	1

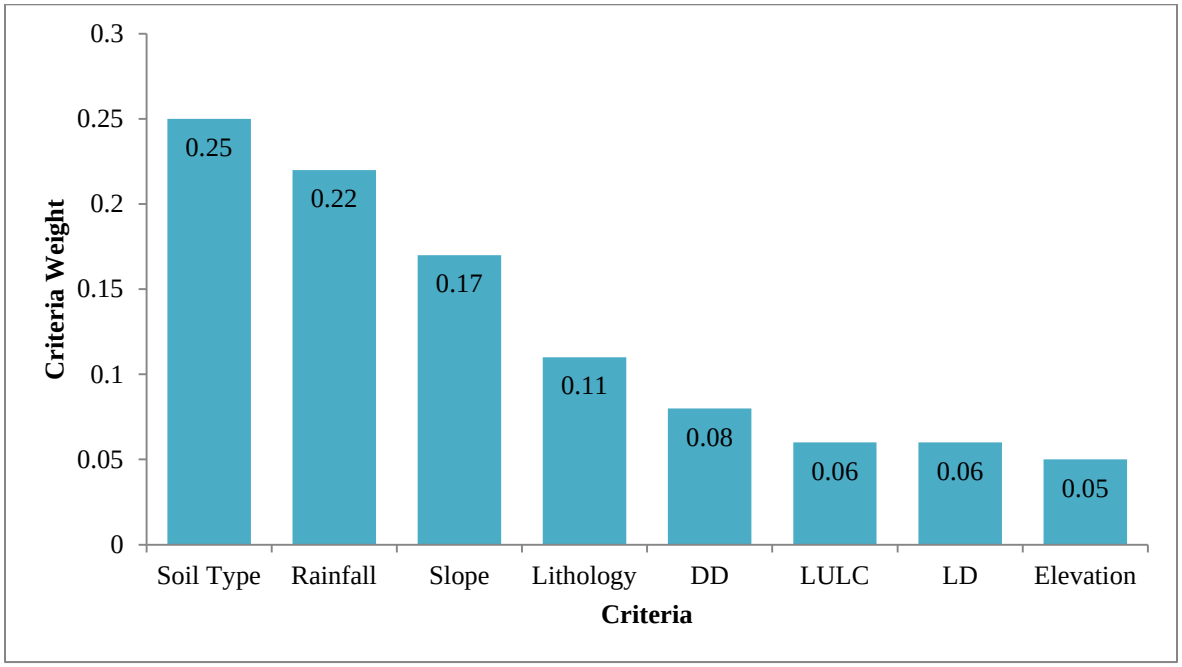

Figure 5.12: Graphs that show weights for the eight selected criteria classes in the WH analysis

5.6.1.2. Weighted Overlay Analysis

The eight criteria layers were integrated using a Weighted Linear Combination (WLC) approach, with the assigned weights applied as illustrated in Figure 5.12. The resulting suitability map, displayed in Figure 5.13, was classified into five distinct categories: (1) very highly suitable, (2) highly suitable, (3) moderately suitable, (4) low suitable, and (5) not suitable. The areal distribution of these classes is summarized in Table 5.21.

Analysis of the suitability map revealed that 14.20% (11.32 km²) of the watershed area was classified as very highly suitable, while 11.90% (9.44 km²) was deemed unsuitable for rainwater harvesting structure (RWHS) construction. The largest portion of the watershed, 29.50% (23.51 km²), fell under the highly suitable category. Meanwhile, moderately suitable and low suitable zones covered 22.00% (17.50 km²) and 22.40% (17.80 km²), respectively.

Table 5.21 The areal distribution of suitability classes for WH of the study area

No.	Suitability Class	Area Coverage	
		Km^2	%
1	Unsuitable	9.44	11.9
2	Low Suitability	17.80	22.4
3	Medium Suitability	17.50	22.00
4	High Suitability	23.51	29.50
5	Very High Suitability	11.32	14.20

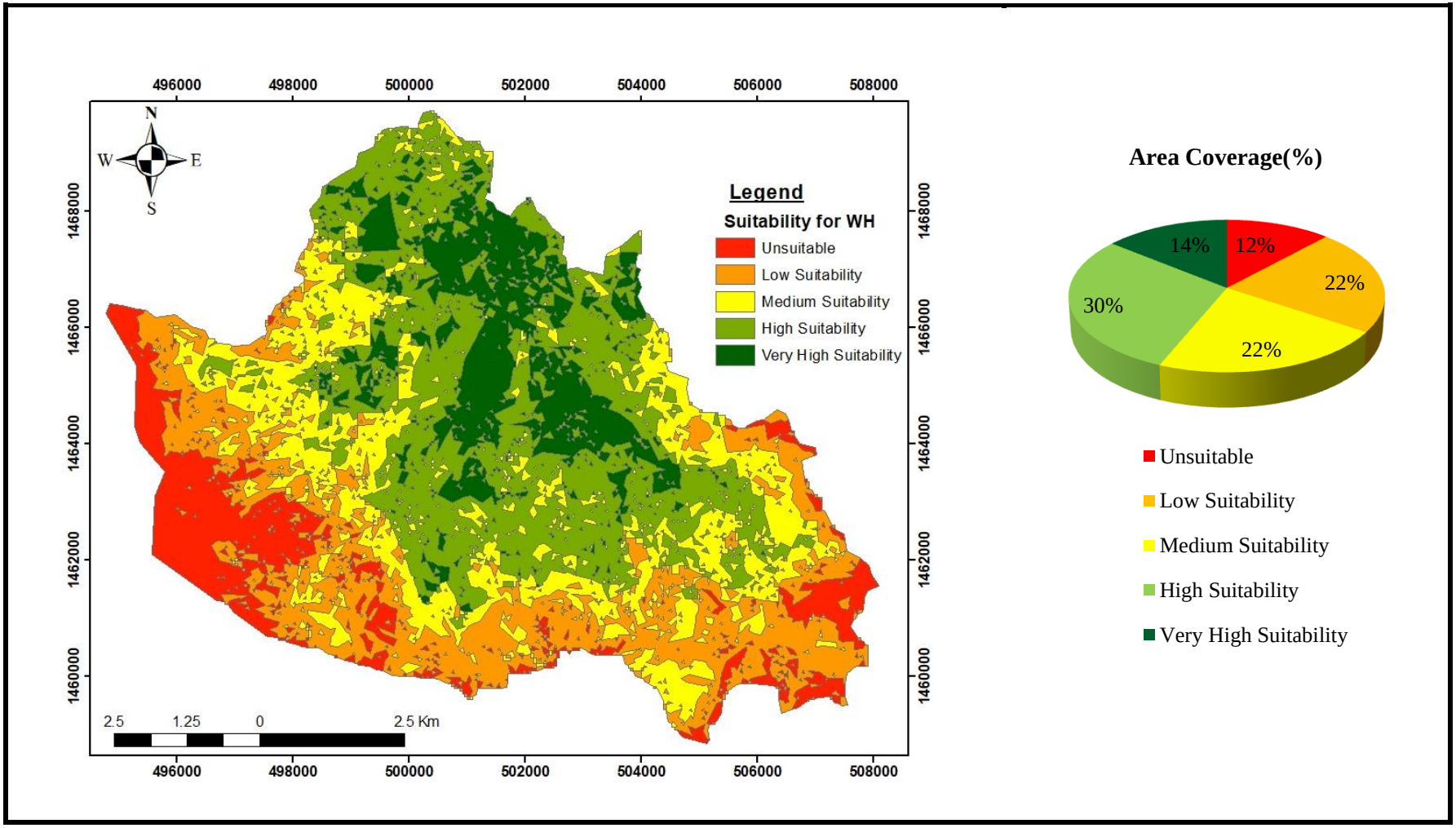

Figure 5.13: Weighted Overlay WH Suitability Map

5.6.2. GWR Suitability Map

5.6.2.1. Computing the weights

Table 5.22 displays the results of pairwise comparisons conducted using the Analytic Hierarchy Process (AHP) as part of a multi-criteria decision-making (MCDM) analysis. The comparison matrix was constructed based on Saaty's nine-point scale to evaluate groundwater availability in the region (Sajad et al., 2021). This matrix captures the relative importance of each factor, derived from local expert judgments and supported by prior research (Rajasekhar et al., 2021).

Table 5.23 presents the normalized matrix of factors along with their derived weights from the comparison matrix. The assigned weights were determined based on each factor's influence on groundwater dynamics and occurrence, informed by expert assessments and supporting literature (Magesh et al., 2012; Nampak et al., 2014; Ibrahim-Bathis & Ahmed, 2016; Andualem & Demeke, 2019; Rajasekhar et al., 2021). The weighted result shows drainage density, slope and rainfall are the most influential parameters, followed by soil type, lineament density and lithology.

Table 5.22 Pairwise comparison matrix for main criteria for GWR

Criteria	DD	Slope	Rainfall	LD	Lithology	Soil Type	Elevation	LULC
DD	1	1	2	3	3	2	4	3
Slope	1	1	2	2	2	1	3	2
Rainfall	0.5	0.5	1	2	3	2	3	2
LD	0.33	0.5	0.5	1	1	2	2	1
Lithology	0.33	0.5	0.33	1	1	0.5	2	2
Soil Type	0.5	1	0.5	0.5	2	1	3	2
Elevation	0.25	0.33	0.33	0.5	0.5	0.33	1	0.5
LULC	0.33	0.5	0.5	1	0.5	0.5	2	1

Table 5.23 Normalized weights of the main criteria for identification of suitable zones for GWR

Criteria	DD	Slope	Rainfall	LD	Lithology	Soil Type	Elev.	LULC	Criteria Weight
DD	0.24	0.19	0.28	0.27	0.23	0.21	0.20	0.22	0.23

Slope	0.24	0.19	0.28	0.18	0.15	0.11	0.15	0.15	0.18
Rainfall	0.12	0.09	0.14	0.18	0.23	0.21	0.15	0.15	0.16
LD	0.08	0.09	0.07	0.09	0.08	0.21	0.10	0.07	0.10
Lithology	0.08	0.09	0.05	0.09	0.08	0.05	0.10	0.15	0.09
Soil Type	0.12	0.19	0.07	0.05	0.15	0.11	0.15	0.15	0.12
Elevation	0.06	0.06	0.05	0.05	0.04	0.04	0.05	0.04	0.05
LULC	0.08	0.09	0.07	0.09	0.04	0.05	0.10	0.07	0.07

- $\lambda_{max} = 8.36$
- *Consistency index = 0.05*
- *Random index = 1.41*
- *Consistency ratio = 0.04*

The weight assigned to each factor reflects its relative influence in identifying potential groundwater zones, with more significant variables receiving higher weights (Yonas & Tesfa, 2021). The calculated Consistency Index (CI) was 0.05, and the derived Consistency Ratio (CR) was 0.04 which is below the acceptable threshold of 0.1, confirming the reliability of the assigned weights.

Table 5.24 The rating of the eight criteria selected based on literature review and weights (After Al-Adamat et al., 2010; Al-shabeeb, 2016; Gavhane et al., 2023) for GWR

Parameters	Normalized Weight	Sub-class	Rating
DD (km/km^2)	0.23	<50	5
		50-60	4
		60-70	3
		70-80	2
		>80	1
Slope (%)	0.18	0-2	5
		2-5	4
		5-10	3
		10-15	2
		>15	1
Rainfall (mm)	0.16	>740	5
		728-740	4

LD (km/km^2)	0.10	717-728	3
		705-717	2
		<705	1
		3.5-5.7	5
		2.2-3.4	4
		1.3-2.2	3
		0.49-1.3	2
		<0.49	1
Lithology	0.09	Alluvial Deposit	6
		Sandstone	5
		Dolerite	4
		Metasediment	3
		Metavolcanic	3
		Granite	2
		Trap Basalt	1
Soil Type	0.12	Sand	4
		Sandy Loam	3
		Clay Loam	2
		CF & Rocks	1
Elevation (m)	0.05	1491-1580	5
		1580-1620	4
		1620-1660	3
		1660-1680	2
		1680-2265	1
LULC	0.07	Built up area	5
		Agricultural	4
		Vegetation	3
		Bare land	2
		Stream bed	1

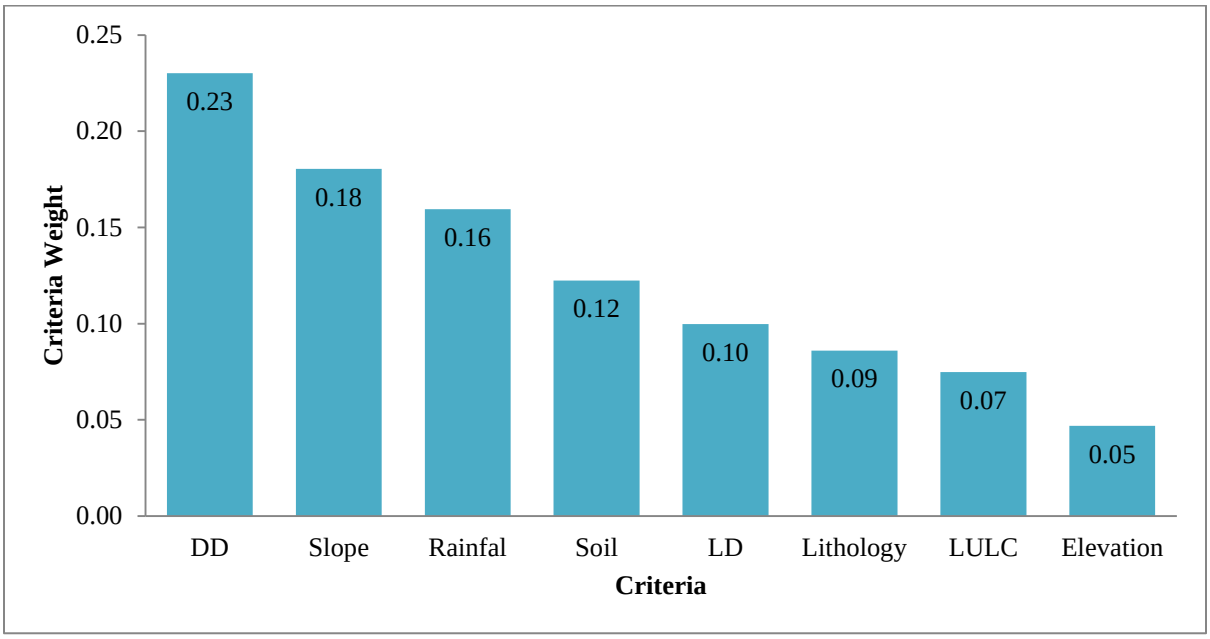

Figure 5.14: Graphs that show weights for the eight selected criteria classes in the GWR analysis

5.6.2.2. Weighted Overlay Analysis

The process of identifying and categorizing potential groundwater recharge zones in the Yechila watershed is visually summarized in Figure 5.15 and quantitatively detailed in Table 5.25. This was accomplished through a weighted overlay analysis in ArcGIS 10.8, which integrated eight distinct thematic layers, each assigned specific weights according to their relative importance.

The groundwater potential zones were classified into five categories based on index values: very high, high, moderate, low, and unsuitable (Khan et al., 2020; Yonas & Tesfa, 2021; Mandal et al., 2022; Wijesinghe et al., 2023).

Table 5.25 the suitability classes and area coverage of the potential GWR zones

No.	Suitability Class	Area Coverage	
		Km^2	%
1	Unsuitable	2.90	3.64
2	Low Suitability	21.40	26.85
3	Medium Suitability	27.00	33.9
4	High Suitability	19.40	24.34
5	Very High Suitability	9.00	11.3

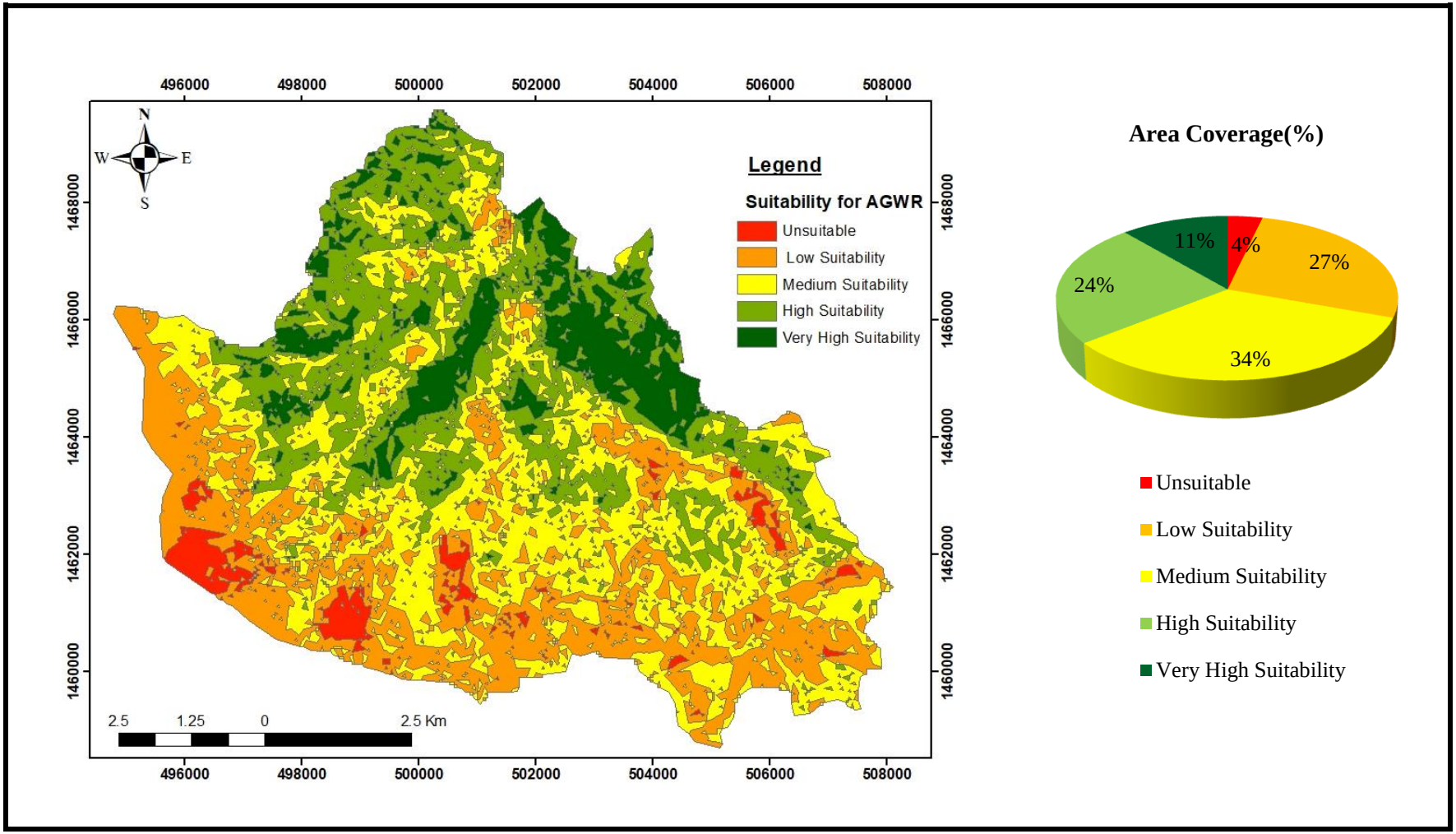

Figure 5.15: Weighted Overlay GWR Suitability Map

5.7. Validation of the delineated WH and GWR Zones

5.7.1. Field Investigation and Assessment

A field survey was conducted during the research period to assess and identify existed and proposed water harvesting (WH) structures and wells, which were then cross-verified with the suitability modeling results.

The survey involved a detailed examination of existing WH infrastructure, including check dams, sand dams, and ponds, with their locations recorded and analyzed. The results confirmed that most of these structures were situated within very high to moderate suitability zones, aligning well with the WH suitability model's predictions. Additionally, based on geological and hydrogeological assessments, potential sites for new WH structures were proposed during the field investigation. This ground-truth exercise reinforced the reliability of the model and provided practical insights for future water resource planning.

The GWR model is also cross checked by assessing the yield of existing wells under current hydrogeological conditions. Data from borehole logs recorded over multiple years were also analyzed to cross-verify the model's predictions. The findings revealed a strong correlation between the modeled potential zones and observed well conditions: productive wells predominantly occur in high and very high potential zones, while damaged and dried wells are located in medium to low potential areas as delineated by the model.

Field surveys incorporating local stakeholder perspectives further validated the study's water harvesting (WH) and groundwater recharge (GWR) suitability assessments. Interviews with regional experts and farmers revealed strong agreement with the model's identified optimal locations. Local respondents consistently reported natural water accumulation patterns during rainy seasons that corresponded precisely with the study's delineated high-potential zones.

These ground-based data are also checked using Area Under the Curve (AUC) method for both suitability models. This validation approach is notably effective for assessing Multi-Criteria Decision Analysis (MCDA) models due to its direct design and comprehensive methodology (Darabi et al., 2021; Rahmati et al., 2019). The ROC plot in Figure 5.17 shows an AUC value of 0.801 (80.10%) for the WH suitability map, while Figure 5.19 displays an AUC value of 0.843

(84.30%) for the GWR potential map. These results underscore the AHP method's strong effectiveness in identifying these potential zones within the study area.

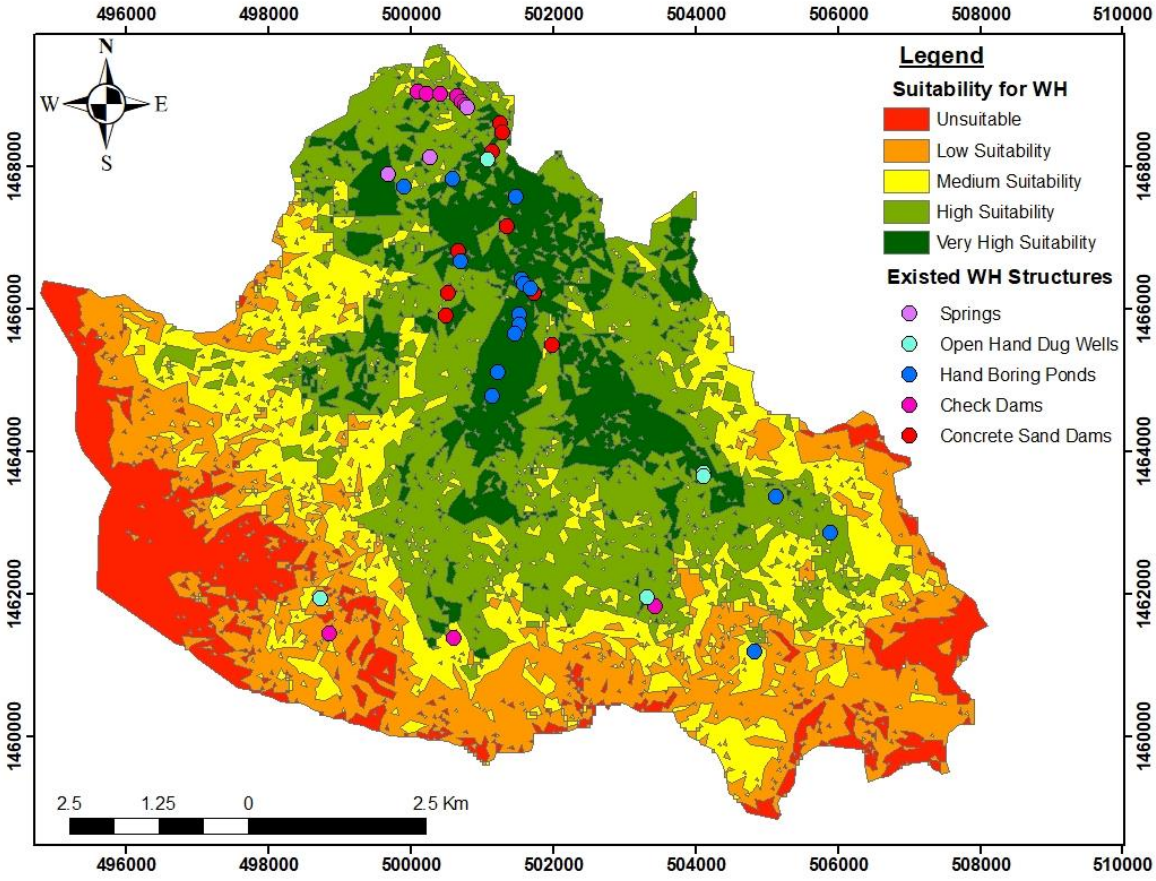

Figure 5.16: Cross checking WH suitability model with existed structures

Table 5.26 Quantitative description of existed WH structures in each suitability zone

S.N	Suitability	WH structures				
		Concrete Sand Dams	Check Dams	Hand Boring Ponds	Open Hand Dug Wells	Springs
1	Unsuitable	0	0	0	0	0
2	Low Suitability	0	1	0	1	0
3	Medium Suitability	2	3	2	0	1
4	High Suitability	2	4	3	2	1
5	Very High Suitability	5	1	10	2	1
	Total	**9**	**9**	**15**	**5**	**3**

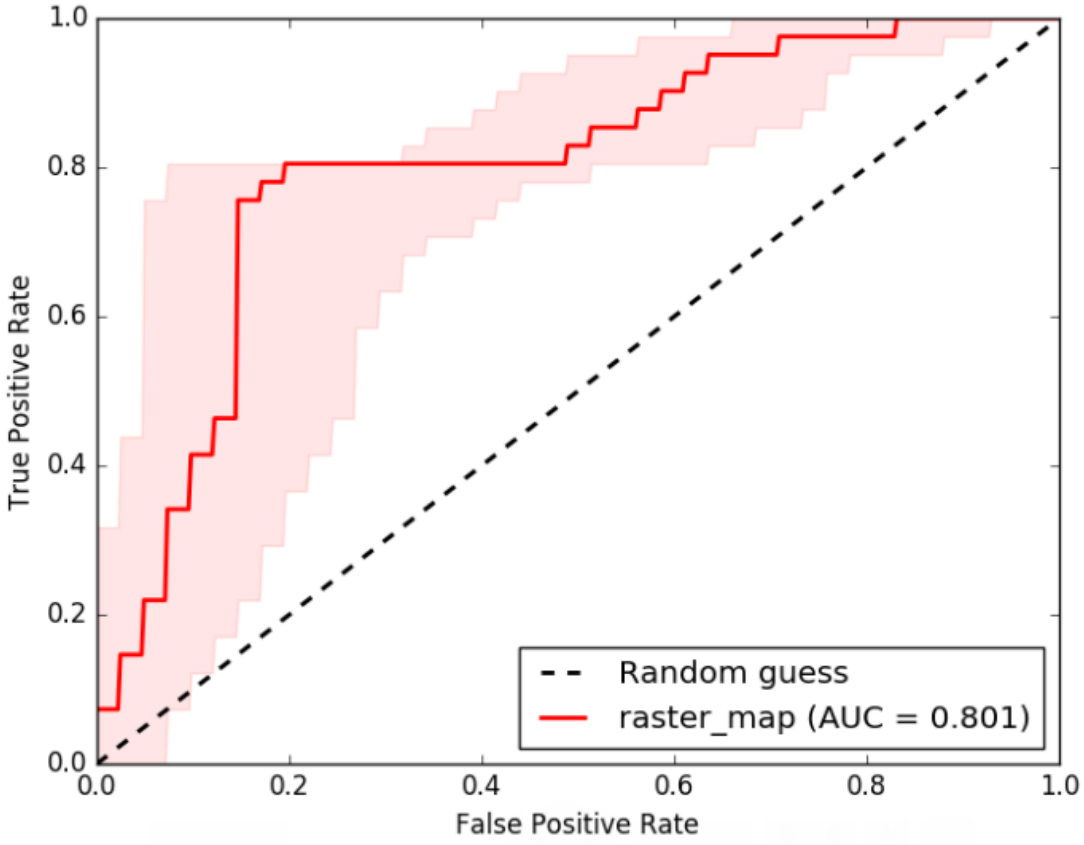

Figure 5.17: ROC curve for validation of the WH potential map

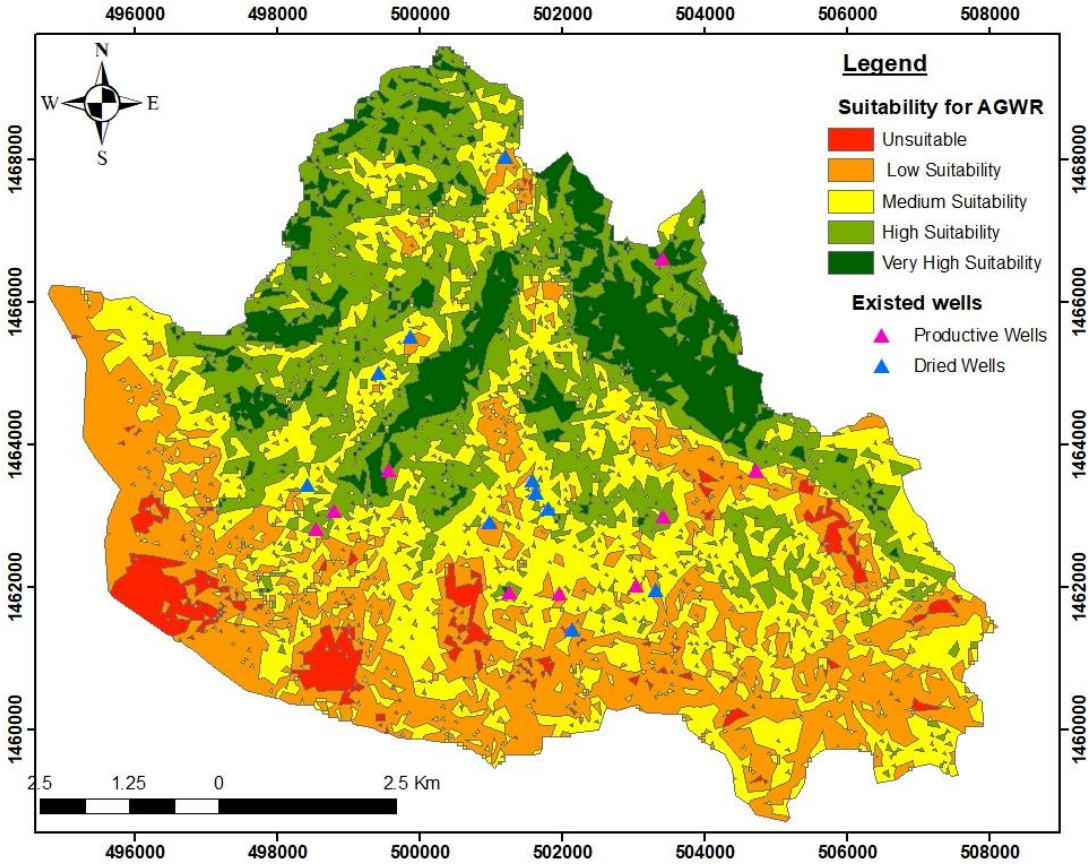

Figure 5.18: Cross checking GWR suitability model with existed wells

Table 5.27 Quantitative description of existed Wells in each GWR suitability zone

S.N	Suitability	Existed Wells	
		Productive	Dried
1	Unsuitable	0	2
2	Low Suitability	0	4
3	Medium Suitability	3	4
4	High Suitability	4	0
5	Very High Suitability	2	0
	Total	**9**	**10**

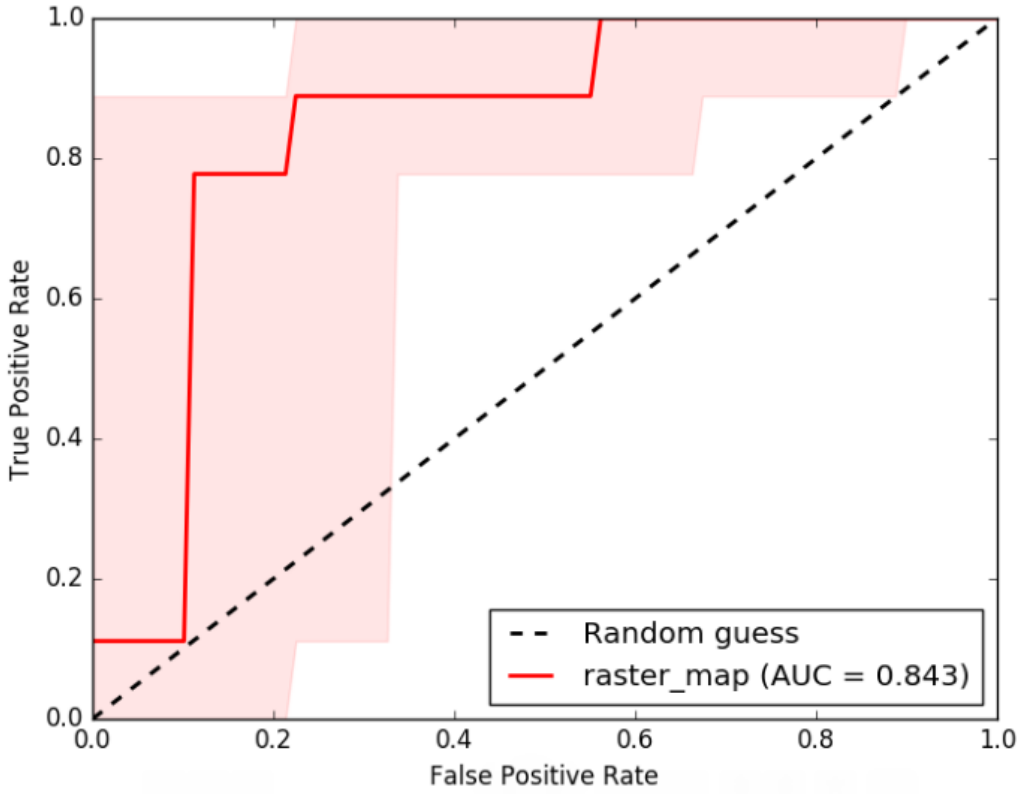

Figure 5.19: ROC curve for validation of the GWR potential map

5.7.2. Google Earth Data

To complement field verification efforts, Google Earth imagery was systematically analyzed to validate the identified water harvesting (WH) and groundwater recharge (GWR) potential zones. The high-resolution satellite data enabled detailed examination of key landscape characteristics, including geomorphological features influencing water accumulation, vegetation patterns indicating moisture availability, settlement distributions and existing water infrastructure, as well as land use characteristics affecting infiltration capacity.

This remote sensing approach provided crucial spatial confirmation of field observations by revealing natural drainage patterns that correlated with high potential zones (for WH), vegetation density variations matching moisture gradients, and existing water management structures located precisely within predicted suitable areas. The integration of these geospatial analysis techniques with ground-truth data significantly enhanced the reliability and accuracy of the suitability assessments across the entire study area, creating multi-method validation framework for the research findings.

CHAPTER SIX

6. CONCLUSION AND RECOMMENDATION

6.1. Conclusion

The geology of the Yechilla Catchment is characterized by seven distinct lithological units, ranging from the oldest metavolcanics (MV) and metasediments (MS) to younger granite intrusions, sandstone, trap basalt, dolerite sills, and alluvial deposits. The study highlights the region's complex geological framework, influenced by tectonic activity, weathering, and erosion. The sandstone and alluvial deposits, with their favorable permeability, are particularly significant for groundwater recharge (GWR), while the impermeable clay-rich layers, granite and basement rocks support water harvesting (WH) initiatives. The study of soil textures in the area reveals distinct characteristics between fluvial and residual soils, which are critical for water management strategies. Fluvial soils, predominantly sandy (≥97%), exhibit high infiltration rates (HSG A), making them ideal for groundwater recharge (GWR). The residual soils, comprising sand, sandy loam, silt loam, clay loam and clay (HSG A-D) have different impact on water retention and recharge due to their variable permeability. The soil infiltration analysis reveals critical variations in water percolation rates across different soil types in the study area. Clay soils exhibit the lowest infiltration rate (0.4 cm/hour), classifying them as slow-permeability surfaces ideal for water retention structures like ponds and check dams. Conversely, sandy soils demonstrate the highest infiltration capacity (3.8 cm/hour); making them optimal zones for groundwater recharges initiatives.

The study successfully generated water harvesting (WH) and groundwater recharge (GWR) suitability maps that effectively identify optimal locations for enhancing water supply through irrigation and aquifer replenishment. These spatial distributions of suitable sites were derived through a comprehensive evaluation of eight weighted criteria: geology, soil texture, slope, elevation, drainage density, lineament density, rainfall, and land use/land cover (LULC). The research employed Geographic Information Systems (GIS) and Multi-Criteria Decision Making (MCDM) techniques, with criteria weights determined using the Analytical Hierarchy Process

(AHP). The validity of these weight assignments was confirmed through a consistency ratio below 10%, demonstrating appropriate and reliable comparisons between criteria.

For water harvesting suitability, the AHP analysis revealed that soil texture, rainfall, slope, geology, and drainage density emerged as the five most influential factors. The resulting suitability assessment classified 14.20% (11.32 km²) of the watershed as very highly suitable and 29.50% (23.51 km²) as highly suitable, indicating that approximately 44% of the total area presents favorable conditions for rainwater harvesting structure (RWHS) implementation. The remaining areas were categorized as moderately suitable (22.00% or 17.50 km²), low suitable (22.40% or 17.80 km²), and unsuitable (11.90% or 9.44 km²). Similarly, the groundwater recharge potential assessment effectively categorized the study area into five distinct zones. The analysis identified 11.30% of the watershed as having very high recharge potential and 24.34% as high potential, collectively representing over 35% of the area as highly conducive to groundwater recharge. Moderate potential zones constituted the largest proportion at 33.90%, followed by low potential areas (26.85%), with only 3.64% classified as poor or unsuitable for recharge activities. Drainage density, slope and rainfall are the most influential parameters, followed by soil, lineament density and lithology based on the AHP analysis for GWR potential zone.

The current study is validated by field investigations, stakeholder input, and remote sensing analysis. Field surveys confirmed that proposed and existed WH structures predominantly align with high to moderate suitability zones, while well yield data reinforced the accuracy of the GWR potential classification. Local knowledge further supported the model's predictions, with natural water accumulation patterns matching the identified high-potential areas. The validation of the suitability models using the AUC method demonstrates the AHP method's effectiveness, with AUC values of 0.801 for the WH suitability map and 0.843 for the GWR potential map. This highlights strong capability of Multi-Criteria Decision Analysis (MCDA) in accurately identifying potential zones within the study area. The integration of Google Earth imagery provided additional spatial validation, revealing strong correlations between modeled suitability zones and real-ground hydrological features. These multi-method verification techniques enhance the reliability of the findings, offering a scientifically grounded and community-informed framework for sustainable water resource planning.

6.2. Recommendation

The findings of this study provide policymakers with critical insights to develop effective water management strategies and optimize resource allocation. The study not only delivers a scientifically defensible suitability map but also provides practical policy guidance. It is recommended that the Tigray Bureau of Water Resources and the Yechilla local administration prioritize the high-potential sites for pilot implementation, supported by the proposed institutional framework and community engagement strategies. By identifying the most suitable sites for (WH) and (GWR), the research supports the adoption of these practices as sustainable alternative water sources in Yechilla and other water-scarce regions facing similar challenges.

While the current study has successfully identified and prioritized potential (WH) and (GWR) sites, further research will enhance the robustness, feasibility, and long-term sustainability of the proposed interventions. The following future studies are recommended to build upon the findings of this work:

- Geophysical investigation: This method provides critical subsurface characterization by identifying aquifer thickness, saturation zones, permeable areas, and fracture networks - all essential for understanding water storage and movement dynamics. Given its effectiveness in mapping underground water systems, geophysical studies should be systematically employed to enhance site assessment accuracy and project outcomes.
- Water quality assessment: This must be assessed in detail because it ensures that harvested or recharged water is safe, sustainable, and suitable for its intended use. High sediment/turbidity in harvested water can clog infiltration basins or injection wells, reducing efficiency.
- Dynamic hydrological processes: Future studies must incorporate temporal changes in rainfall patterns, temperature fluctuations, and anthropogenic impacts, as these directly influence groundwater recharge. Enhanced modeling approaches should utilize time-series data to assess dynamic recharge variations, while integrating long-term hydrological records and seasonal climate forecasts.
- Environmental and socio-economic studies: To ensure sustainable, equitable, and effective WH/GWR projects, environmental and socio-economic studies are as critical as technical investigations.

REFERENCES

Abadi, B., Sadeghfam, S., Ehsanitabar, A., & Nadiri, A. A. (2023). Investigating socio-economic and hydrological sustainability of ancient Qanat water systems in arid regions of central Iran. *Groundwater for Sustainable Development*, 23, 100988.

Abd-Elaty, I., Kuriqi, A., Ahmed, A., Ramadan, E.M. (2024). Enhanced groundwater availability through rainwater harvesting and managed aquifer recharge in arid regions. *Appl.Water Sci.*, 14, 121.

Abdelaziz, Z., Radwan, A. W., & Mohamed, A. (2006). Water Harvesting Techniques in the Arab Region. UNESCO/G-WADI Workshop on Water Harvesting, 20-22 November, Aleppo, Syria.

Abdulla, F. (2020). Rainwater harvesting in Jordan: potential water saving, optimal tank sizing and economic analysis. *Urban Water Journal*, 17(5), 446-456.

Abdullah, M., Al-Ansari, N., & Laue, J. (2020). Water harvesting in Iraq: status and opportunities. *Journal of Earth Sciences and Geotechnical Engineering*, 10(1), 199-217.

Abirami C, Annadurai R (2016) Identification of groundwater potential zones using the GIS-based Multi-Criteria Technique: A case study on the Bhavani watershed, Erode district, Tamilnadu, Southern India. *Int J Eng Res Technol (IJERT).* , ISSN: 2278 – 0181

Abraham, M., Mohan, S. (2015). Effectiveness of artificial recharge structures in enhancing groundwater storage: A case study. *Indian J. Sci. Technol.*, 8, 1–10.

Abu-Taleb, M.F. (2003). Recharge of groundwater through multi-stage reservoirs in a desert basin. *Environ. Geol.*, 44, 379–390.

Adham, A., Sayl, K.N., Abed, R., Abdeladhim, M.A., Wesseling, J.G., Riksen, M., Ritsema, C.J. (2018). A GIS-based approach for identifying potential sites for harvesting rainwater in the Western Desert of Iraq. *Int. Soil Water Conserv. Res.*, 6, 297–304.

Adhikari, R.N., Singh, A.K., Math, S.K.N., Raizada, A., Mishra, P.K., Reddy, K.K. (2013). Augmentation of groundwater recharges and water quality improvement by water harvesting structures in the semi-arid Deccan. *Curr. Sci.*, 104, 1534–1542.

Agarwal E, Agarwal R, Garg RD, Garg PK (2013) Delineation of the groundwater potential zone: an AHP/ANP approach. *J Earth Syst Sci.*, 122(3):887–898

Ahirwar, S., Malik, M.S., Ahirwar, R., ShuklaL J.P. (2020). Identification of suitable sites and structures for artificial groundwater recharge for sustainable groundwater resource development and management. *Groundwater for Sustainable Development*, 11,100388. https://doi.org/10.1016/j.gsd.2020.100388

Ahmed, I., Umar, R. (2008). Hydrogeological framework and water balance studies in parts of Krishni–Yamuna interstream area, Western Uttar Pradesh, India. *Environ. Geol.*, 53, 1723–1730.

Ahmed, S., Jesson, M., Sharifi, S. (2023). Selection frameworks for potential rainwater harvesting sites in arid and semi-arid regions: A systematic literature review. *Water*, 15, 2782.

Al-Adamat, R. (2008). GIS as a decision support system for siting water harvesting ponds in the Basalt Aquifer/NE Jordan. *Journal of Environmental Assessment Policy and Management*, 10(02), 189-206.

Al-Adamat, R., Diabat, A., Shatnawi, G. (2010). Combining GIS with Multi-criteria Decision Making for Siting Water Harvesting Ponds in Northern Jordan. *Journal of Arid Environments*, 74, 1471-1477. http://dx.doi.org/10.1016/j.jaridenv.2010.07.001

Alam, S., Borthakur, A., Ravi, S., Gebremichael, M., Mohanty, S.K. (2021). Managed aquifer recharge implementation criteria to achieve water sustainability. *Sci. Total Environ.*, 768, 144992.

Alataway, A., El Alfy, M. (2019). Rainwater harvesting and artificial groundwater recharge in arid areas: Case study in Wadi Al-Alb, Saudi Arabia. *J. Water Res. Plan. Manag.*, 145, 05018017.

Alemohammad, S. H., & Gharari, S. (2017). Qanat: An ancient invention for water management in Iran. In found in Proceedings of Water History Conference, Delft, The Netherlands.

Alkhaddar, R. (2003). Water harvesting in Jordan using earth ponds. *Waterlines*, 19-21.

Al-shabeeb, A.R. (2016). The Use of AHP within GIS in Selecting Potential Sites for Water Harvesting Sites in the Azraq Basin—Jordan. *Journal of Geographic Information System*, 8, 73-88. http://dx.doi.org/10.4236/jgis.2016.81008

AL-Shammari, M. M., AL-Shamma'a, A. M., Al Maliki, A., Hussain, H. M., Yaseen, Z. M., & Armanuos, A. M. (2021). Integrated water harvesting and aquifer recharge evaluation methodology based on remote sensing and geographical information system: Case study in Iraq. *Natural Resources Research*, 30(3), 2119-2143.

Ammar, A., Riksen, M., Ouessar, M., Ritsema, C. (2016). Identification of suitable sites for rainwater harvesting structures in arid and semi-arid regions: A review. *Int. Soil Water Conserv. Res.*, 4, 108–120.

Andualem, T.G., Demeke, G.G. (2019). Groundwater potential assessment using GIS and remote sensing: a case study of the Guna Tana landscape, upper Blue Nile basin. *Ethiopia Hydrology*, 24:100610.

Arkin, Y., Beyth, M., Dow, D.B., Levitte, D., Temesgen, H., Tsegaye, H. (1971). Geological map of Mekelle sheet area, ND 37–11 Tigray province. Ministry of Mines. Geol Survey of Ethiopia, Addis Ababa.

Aroka, N. (2010). Rainwater Harvesting in Rural Kenya Reliability in a Variable and Changing Climate, Master thesis. Stockholm University.

Asif, M., Yaseen, M., Shahid, S. U., Latif, Y., Anwar, S., & Abbas, S. (2024). Geospatial identification of possible rainwater harvesting locations within a high-altitude Gilgit River basin, Pakistan. *Theoretical and Applied Climatology*, 155(8), 7991-8004.

ASTM D422-63. (2007). Standard Test Method for Particle-Size Analysis of Soils. ASTM International, 100 Barr Harbor Drive, PO Box C700, West Conshohocken, PA 19428-2959. United States.

Azis, A., Yusuf, H., Faisal, Z., Suradi, M. (2015). Water turbidity impact on discharge decrease of groundwater recharge in recharge reservoir. *Procedia Eng*., 125, 199–206.

Barry, B., Olaleye, A.O., Fatondji, D. (2008). Rainwater harvesting technologies in the Sahelian

Zone of West Africa and the potential for outscaling. In IWMI Working Paper.

Barry, B., Olaleye, A.O., Fatondji, D. (2008). Rainwater harvesting technologies in the Sahelian Zone of West Africa and the potential for outscaling. In IWMI Working Paper.

Barthel, R., Stangefelt, M., Giese, M., Nygren, M., Seftigen, K., Chen, D. (2021). Current understanding of groundwater recharge and groundwater drought in Sweden compared to countries with similar geology and climate. *Geogr. Ann. A Phys. Geogr*., 103, 323–345.

Benítez, J., Delgado-Galván, X., Izquierdo, J., Pérez-García, R. (2012). Improving consistency in AHP decision-making processes. *Appl. Math. Comput*., 219(5):24322441. https://doi.org/10.1016/j.amc.2012.08.079

Berhane, G. (2016). Micro-Dam Reservoir Leakage and Hydrogeological Setting in Tigray, Northern Ethiopia. PhD dissertation, Ghent University.

Beyth, M. (1972). Palaeozoic–Mesozoic sedimentary basin of Mekelle outlier, northern Ethiopia. AAm Assoc Pet Geol Bull, 56,2426–2439.

Bhattacharya, A.K. (2010). Artificial ground water recharge with a special reference to India. *Int. J. Recent. Res. Appl. Stud.*, 4, 214–221.

Bhattacharya, S. (2015). Traditional water harvesting structures and sustainable water management in India: A socio-hydrological review. *International Letters of Natural Sciences*, 37.

Bhattacharya, S., Dasgupta, A., Mahansaria, R., Ghosh, S., Chattopadhyay, D., & Mukhopadhyay, A. (2011). Traditional rainwater harvesting in India: Historical perspectives, present scenario and Future prospects.

Bieniawski, Z.T. (1989). Engineering rock mass classifications. Wiley, New York, p 251

Booman, G., Leiker, S. (2021). Soil Sampling Guide; Document ID: RND_SSG_001; Regen Network Development, Inc.: Northfield, MA, USA.

Bouwer, H. (2002). Artificial recharge of groundwater: Hydrogeology and engineering. *Hydrogeol. J*., 10, 121–142.

Brown, R.F., Signor, D.C. (1974). Artificial Recharge-State of the Art. *Groundwater*, 12, 152–160.

Burnett, K., Wada, C.A. (2014). Optimal groundwater management when recharge is declining: A method for valuing the recharge benefits of watershed conservation. *Environ. Econ. Policy Stud*., 16, 263–278.

Cambraia Neto, A.J., Rodrigues, L.N. (2020). Evaluations of groundwater recharge estimation methods in a watershed in the Brazilian Savannah. *Environ. Earth Sci*., 79, 140.

Chakava, Y., Franceys, R., Parker, A. (2014). Private Boreholes for Nairobi's urban poor: The stop-gap or the solution? *Habitat. Int*., 43, 108–116.

Darabi, M., Majeed, H., Diehl, A., Norton, J., Zhang, Y. (2021). A review of micro-plastics in aquatic sediments: occurrence, fate, transport, and ecological impact. *Curr Pollution Rep*, 7(1):40–53.

Dassargheya, R., Panda, S.K. (2015). Artificial groundwater recharges potential in a hard rock terrain using GIS and remote sensing techniques. *Water Resour Manage*, 29(2):411–423. https://doi.org/10.1007/s11269-014-0792-1)

Davis, R. O. E. (1927). Grouping of soils on the basis of mechanical analysis (Vol. 419). US Department of Agriculture.

Deere, D.U and Miller, R.P. (1966). Engineering classification and index properties for intact rock. Air Force Weapons Laboratory Technical Report (AFWL-TR).

Denison, J.A., Wotshela, L. (2012). An overview of indigenous, indigenised and contemporary water harvesting and conservation practices in South Africa. *Irrigation and Drainage*, 61(SUPPL.2), 7–23. DOI: 10.1002/ird.1689

Dey, S., Bhatt, D., Haq, S., Mall, R.K. (2020). Potential impact of rainfall variability on groundwater resources: A case study in Uttar Pradesh, India. *Arab. J. Geosci*., 13, 114.

Dillon, P., Stuyfzand, P., Grischek, T., Lluria, M., Pyne, R.D.G., Jain, R.C., Sapiano, M. (2019). Sixty years of global progress in managed aquifer recharge. *Hydrogeol. J*., 27, 1–30.

Dweiri, F., Kumar, S., Khan, S.A., Jain, V. (2016). Designing an integrated AHP based decision

support system for supplier selection in automotive industry. *Expert Syst Appl*, 62:273–283. https://doi.org/ 10. 1016/j.eswa.2016.06.030

Emrouznejad, A., Ho, W. (2017). Fuzzy analytic hierarchy process. CRC Press

Ertop, H., Kocięcka, J., Atilgan, A., Liberacki, D., Niemiec, M., Rolbiecki, R. (2023). The importance of rainwater harvesting and its usage possibilities: Antalya example (Turkey). *Water*, 15(12),2194. https://doi.org/10.3390/w15122194

Ettazarizini, S., El Mahmouhi, N. (2004). Vulnerability mapping of the turonian limestone aquifer in the phosphate plateau (Morocco). *Environ. Geol.,* 46:113–117. https://doiorg/101007/ s00254-004-1022-3

FAO. (2003). Training Course on Water Harvesting: Land and Water Digital Media Series; Food and Agriculture Organization of the United Nations (FAO): Rome, Italy.

Fathy, I., Ahmed, A., Elhamid, H.F. (2021). Integrated management of surface water and groundwater to mitigate flood risks and water scarcity in arid and semi-arid regions. *J. Flood Risk Manag*., 14, e12720.

Fawcett, T. (2006). An introduction to ROC analysis. *Pattern Recogn Lett*, 27(8):861–874.

Fuentes, I., van Ogtrop, F., Vervoort, R.W. (2020). Long-term surface water trends and relationship with open water evaporation losses in the Namoi catchment, Australia. *J. Hydrol*., 584, 124714.

Gavhane, K.P., Mishra, A.K., Sarangi, A., Singh, D.K., Sudhishri, S. (2023). Targeting of rainwater harvesting structures using geospatial tools and analytical hierarchy process (AHP) in the semi-arid region of Rajasthan (India). *Environmental Science and Pollution Research*, 30:61682–61709. https://doi.org/10.1007/s11356-023-26289-7

Gebru, T.A., Brhane, G.K., Gebremedhin, Y.G. (2021). Contributions of water harvesting technologies intervention in arid and semi-arid regions of Ethiopia, in ensuring households' food security, Tigray in focus. *Journal of Arid Environments*, 185,104373. https://doi.org/10.1016/j.jaridenv.2020.104373

Gee, G.W., Hillel, D. (1988). Groundwater recharge in arid regions: Review and critique of

estimation methods. *Hydrol. Process*, 2, 255–266.

Ghanbarpour, M. R., Ahmadi, E., & Gholami, S. (2007). Evaluation of different traditional water management systems in semi-arid regions (case study from Iran). *Options Méditerranéennes: Série B. Etudes et Recherches*, 3(56), 133-139.

Ghayoumian, J., Saravi, M.M., Feiznia, S., Nouri, B., Malekian, A. (2007). Application of GIS techniques to determine the areas most suitable for artificial groundwater recharge in a coastal aquifer in Southern Iran. *J Asian Earth Sci*., 30(2),364–374.

Ghazavi, R., Babaei, S., Erfanian, M. (2018). Recharge well site selection for artificial groundwater recharge in an urban area using the fuzzy logic technique. *Water Resour Manag*, 32(12),3821–3834.

Gontia, N.K., Patil, P.Y. (2012). Assessment of groundwater recharge through rainfall and water harvesting structures in Jamka micro-watershed using remote sensing and GIS. *J. Indian Soc. Remote Sens*., 40, 639–648.

Guigui, X., Xiaosi, S., Yiwu, Z., Bing, Y. (2021). Identifying potential sites for artificial recharge in the plain area of the Daqing river catchment using GIS-based multi-criteria analysis. *Sustainability*, 13, 3978. https://doi.org/10.3390/su13073978

Gwenzi, W., Nyamadzawo, G. (2014). Hydrological impacts of urbanization and urban roof water harvesting in water-limited catchments: A review. *Environ. Process*, 1, 573–593.

Haile, G., Suryabhagavan, K. V. (2019). GIS-based approach for identification of potential rainwater harvesting sites in Arsi Zone, Central Ethiopia. *Modeling Earth Systems and Environment*, 5,353–367. https://doi.org/10.1007/s40808-018-0537-7

Hashemi, H., Berndtsson, R., Kompani-Zare, M., Persson, M. (2013). Natural vs. artificial groundwater recharge, quantification through inverse modeling. *Hydrol. Earth Sys Sci*., 17, 637–650.

Hassan, W.H., Mahdi, K., Kadhim, Z.K. (2025). GIS-based multi-criteria decision making for identifying rainwater harvesting sites. *Applied Water Science*, 15,45. https://doi.org/10.1007/s13201-025-02378-5

Hassan, W.H., Mahdi, K., Kadhim, Z.K. (2025). Optimal rainwater harvesting locations for arid and semi-arid regions by using MCDM-based GIS techniques. *Heliyon*, 11, e42090, 2405-8440.

Huang, Z., Nya, E.L., Rahman, M.A., Mwamila, T.B., Cao, V., Gwenzi, W., Noubactep, C. (2021). Integrated water resource management: Rethinking the contribution of rainwater harvesting. *Sustainability*, 13, 8338.

Hussain, F., Hussain, R., Wu, R.S., Abbas, T. (2019). Rainwater harvesting potential and utilization for artificial recharge of groundwater using recharge wells. *Processes*, 7, 623.

Ibrahim-Bathis, K., & Ahmed, S. A. (2016). Geospatial technology for delineating groundwater potential zones in Doddahalla watershed of Chitradurga district, India. *The Egyptian Journal of Remote Sensing and Space Science*, 19(2), 223-234.

Islam, S., Singh, R. K., & Khan, R. A. (2015). Methods of estimating ground water recharge. *International Journal of Engineering Associates*, 5(2), 6-9.

Jamali, B., Bach, P. M., & Deletic, A. (2020). Rainwater harvesting for urban flood management–An integrated modelling framework. *Water research*, 171, 115372.

Jebamalar, A., Ravikumar, G., Meiyappan, G. (2012). Groundwater storage through rain water harvesting (RWH). *Clean Soil Air Water*, 40, 624–629.

Kebede, M.M., Kumar, M., Mekonnen, M.M., Clement, T.P. (2024). Enhancing Groundwater Recharge through Nature-Based Solutions: Benefits and Barriers. *Hydrology*, 11, 195.

Khan, A., Govil, H., Taloor, A. K., & Kumar, G. (2020). Identification of artificial groundwater recharge sites in parts of Yamuna River basin India based on Remote Sensing and Geographical Information System. *Groundwater for Sustainable Development*, 11, 100415.

Kiranaratri, A. H., Bisri, M., & Asmaranto, R. (2024, March). Correlational of soil permeability and infiltration rate at the ITERA infiltration drainage development plan. In *IOP conference series: earth and environmental science* (Vol. 1311, No. 1, p. 012023). IOP Publishing.

Kubler S, Derigent W, Voisin A, Robert J, Le Traon Y, Viedma EH (2018) Measuring inconsistency and deriving priorities from fuzzy pairwise comparison matrices using the

knowledge-based consistency index. *Knowl-Based Syst*, 162:147–160. https:// doi.org/ 10.1016/j. knosys.2018.09.015

Kumar, P.J., Schneider, M., Elango, L. (2021). The state-of-the-art estimation of groundwater recharge and water balance with a special emphasis on India: A critical review. *Sustainability*, 14, 340.

Kumar, S., Bhadra, B.K., Paliwal, R. (2017). Evaluating the impact of artificial groundwater recharge structures using geo-spatial techniques in the hard-rock terrain of Rajasthan, India. *Environ. Earth Sci*., 76, 613.

Kurttila, M., Pesonen, M., Kangas, J., Kajanus, M. (2000). Utilizing the analytic hierarchy process (AHP) in SWOT analysis—a hybrid method and its application to a forest-certification case. *Forest Policy Econ.*, 1(1),41–52. https://doi.org/10.1016/ S1389-9341(99) 00004-0

Lall, U., Josset, L., Russo, T. (2020). A snapshot of the world's groundwater challenges. *Ann. Rev. Environ. Resour*., 45, 171–194.

Lasage, R., Verburg, P.H. (2015). Evaluation of small scale water harvesting techniques for semi-arid environments. *J. Arid. Environ*., 118, 48–57.

Magesh, N.S., Chandrasekar, N., Soundranayagam, J.P. (2012). Delineation of the groundwater potential zones in Theni district, Tamil Nadu, using remote sensing, GIS, and MIF techniques. *Geoscience Front*, 3(2):189–196. https://doi.org/101016/j gsf201110007

Mahmood, K., Qaiser, A., Farooq, S., Nisa, M. (2020). RS- and GIS-based modeling for optimum site selection in rain water harvesting system: an SCS-CN approach. *Acta Geophysica*, 68:1175–1185. https://doi.org/10.1007/s11600-020-00460-x

Mandal, P., Maiti, A., Paul, S., Bhattacharya, S., Paul, S. (2022). Mapping the multi-hazards risk index for the coastal block of Sundarban, India using AHP and machine learning algorithms. *Trop Cyclone Res. Rev*., 11(4):225–243

Manisha, M., Verma, K., Narayanaswamy, R., Marigoudar, S.R., Hoysall, N.C., Rao, L. (2024). Role of indirect groundwater recharge using recycled water in promoting food security in

semi-arid regions. *Environment, Development and Sustainability*, Springer. https://doi.org/10.1007/s10668-024-05249-2

Monir, M.M., Sarker, S.C., Islam, A.R.M.T. (2024). A critical review on groundwater level depletion monitoring based on GIS and data-driven models: Global perspectives and future challenges. *Hydro Res*., 7, 285–300.

Mukherjee, D. (2016). A review on artificial groundwater recharge in India. *Int. J. Civ. Eng*., 3, 60–65.

Mundalik, V., Fernes, C., Kadam, A.K., Umrikar, B.N. (2018). Integrated geomorphological, Geospatial, and AHP techniques for groundwater prospect mapping in the basaltic terrain. *Hydrology Spat Anal*., 2(1):16–27. https://doi.org/10.21523/gcj3.1802010.2

Nachshon, U., Netzer, L., Livshitz, Y. (2016). Land cover properties and rain water harvesting in urban environments. *Sustain. Cities Soc*., 27, 398–406.

Naghibi, S.A., Pourghasemi, H.R., Dixon, B. (2016). GIS-based groundwa¬ter potential mapping using boosted regression tree, classification and regression tree, and random forest machine learning models in Iran. *Environ. Monit Assess*., 188:44,1–27.

Naghibi, S.A., Pourghasemi, H.R., Pourtaghi, Z.S., Rezaei, A. (2015). Groundwater potential mapping using the frequency ratio and Shannon's entropy models in the Moghan watershed. *Iran Earth Sci. Inf*., 8:171–186.

Nampak, H., Pradhan, B., Manap, M.A. (2014). Application of the GIS based data-driven evidential belief function model to predict groundwater potential zonation. *J Hydrol* 513:283–300. https://doi.org/10.1016/j.jhydrol.2014.02.053

Nandi, A., Shakoor, A. (2009). A GIS-based landslide susceptibility evaluation using bivariate and multivariate statistical analyses. *Eng. Geol*., 110 (2009) 11–20.

Nandi, S., Gonela, V. (2022). Rainwater harvesting for domestic use: A systematic review and outlook from the utility policy and management perspectives. Util. Policy, 77, 101383.

Nijhof, S., Jantowski, B., Meerman, R., Schoemaker, A.R.D. (2010). Rainwater harvesting in challenging environments: Towards institutional frameworks for sustainable domestic water

supply. *Waterlines*, 29(3), 209–219. DOI: 10.3362/1756-3488.2010.022

Noori, A.R., Singh, S.K. (2023). Rainfall Assessment and Water Harvesting Potential in an urban area for artificial groundwater recharge with land use and land cover approach. *Water Resour. Manag*., 37, 5215–5234.

Oduor, A.R., Gadain, H.M. (2007). Potential of Rainwater Harvesting in Somalia, A Planning, Design, Implementation and Monitoring Framework, Technical Report NoW-09, 2007, FAO-SWALIM, Nairobi, Kenya.

Ouali, L., Hssaisoune, M., Kabiri, L., Slimani, M.M., El Mouquaddam, K., Namous, M., Arioua, A., Ben Moussa, A., Benqlilou, H., Bouchaou, L. (2022). Mapping of potential sites for rainwater harvesting structures using GIS and MCDM approaches: Case study of the Toudgha watershed, Morocco. *Euro-Mediterranean Journal for Environmental Integration*, 7(1), 49–64. DOI: 10.1007/ s41207-022-00294-7

Oweis, T., Oberle, A., Prinz, D. (1998). Determination of potential sites and methods for water harvesting in central Syria. *Adv. GeoEcology*, 31, 83–88.

Oweis, T.Y. (2012). Improving agricultural water productivity: A viable response to water scarcity in the dry areas, 39–55. In: Integrated Water Resources Management in the Mediterranean Region, Eds. R. Choukr-Allah, R. Ragab, R. Rodriguez-Clemente. Springer: Dordrecht. DOI: 10.1007/978-94-007-4756-2

Ozdemir, A., Altural, T. (2013). A comparative study of the frequency ratio, weights of evidence, and logistic regression methods for landslide susceptibility mapping: Sultan Mountains, SW Turkey. *J Asian Earth Sci*, 64:180–197.

Palmstrom, A. (1982). The volumetric joint count—a useful and simple measure of the degree of rock mass jointing. IVth International congress. IAEG, New Delhi, India, 4 (pp. 221-228).

Patel, A., Chaudhari, N. (2023). Enhancing water security through site selection of water harvesting structures in semi-arid regions: A GIS-based multiple criteria decision analysis. *Water Supply*, 10, 4149–4165.

Patel, A., Chaudhari, N. (2023). Enhancing water security through site selection of water

harvesting structures in semi-arid regions: a GIS-based multiple criteria decision analysis. *Water Supply*, 0(1), 6822-7883. doi: 10.2166/ws.2023.257

Perez-Aguilar, L. Y., Plata-Rocha, W., Monjardin-Armenta, S. A., Franco-Ochoa, C., & Zambrano-Medina, Y. G. (2021). The identification and classification of arid zones through multicriteria evaluation and geographic information systems—case study: arid regions of northwest Mexico. *ISPRS International Journal of Geo-Information*, 10(11), 720.

Pourghasemi, H.R., Moradi, H.R., Fatemi Aghda, S.M. (2013a). GIS-based landslide susceptibility mapping with probabilistic likelihood ratio and spatial multi-criteria evaluation models (North of Tehran, Iran). *Arab J Geosci*., doi:10.1007/s12517-012-0825-x

Prinz, D. (1996). Water harvesting-past and future. In *Sustainability of irrigated agriculture* (pp. 137-168). Dordrecht: Springer Netherlands.

Qadir, M., Boers, T.M., Schubert, S., Ghafoor, A., Murtaza, G. (2003). Agricultural water management in water-starved countries: Challenges and opportunities. *Agric. Water Manag*., 62, 165–185.

Rahmati, O., Falah, F., Dayal, K., Deo, R.C., Mohammadi, F., Biggs, T., Bui, D.T. (2019). Machine learning approaches for the Spatial modeling of agricultural droughts in the Southeast region of Queensland Australia. *Sci. Total Environ*.,134230. https://doi.org/10.1016/j.scitotenv.2019.1342

Raimondi, A., Quinn, R., Abhijith, G.R., Becciu, G., Ostfeld, A. (2023). Rainwater harvesting and treatment: State of the art and perspectives. Water, 15, 1518.

Rajasekhar, M., Ajaykumar, K., Sudarsana, R.G., Vijay, B. (2021). Identification of artificial groundwater recharge zones in the semi-arid region of Southern India using Geospatial and integrated decision- making approaches. *Environ Challenges*, 5:100278.

Remini, B., Kechad, R., Achour, B. (2014). The collecting of groundwater by the qanats: A millennium technique decaying. *Larhyss J*., 20, 2521–9782.

RockWare Inc. (1983-2020). RockWorks. [Software]. RockWare, Incorporation, Golden

Ross, C. W., Prihodko, L., Anchang, J., Kumar, S., Ji, W., & Hanan, N. P. (2018).

HYSOGs250m, global gridded hydrologic soil groups for curve-number-based runoff modeling. Scientific data, 5(1), 1-9.

Saaty, T.L. (1980). The Analytic Hierarchy Process: Planning, Priority Setting, Resource Allocation. 2nd edition, McGraw-Hill International Co., ISBN: 9780070543713, 287p.

Saaty, T.L. (2000). The fundamentals of decision making and priority theory with the analytic hierarchy process. 2nd edition, RWS Publications, Pittsburg, 478p.

Saaty, T.L. (2008). 'Decision making with the analytic hierarchy process. *International Journal of Services Sciences*, 1(1):83–98.

Saha, D., Sikka, A.K., Goklani, R. (2022). Artificial recharge endeavours in India: A review. *Water Secur*., 16, 100121.

Sajad, A.M., Bhat, M.S., Rather, G.M., Durdanah, M. (2021). Groundwater potential zonation using integration of remote sensing and AHP/ANP approach in North Kashmir, Western himalaya India. *Remote Sens Land*, 5(1):41–58

Sembroni, A., Molin, P., Dramis, F., & Abebe, B. (2017). Geology of the Tekeze river basin (northern Ethiopia). *Journal of Maps*, 13(2), 621-631.

Şener, Ş., Şener, E., Nas, B., & Karagüzel, R. (2010). Combining AHP with GIS for landfill site selection: a case study in the Lake Beyşehir catchment area (Konya, Turkey). *Waste management*, 30(11), 2037-2046. doi:10.1016/ j.wasman.2010.05.024

Sharma, R., Kumar, R., Agrawal, P.R., Ittishree, Chankit, Gupta, G. (2021). Groundwater extractions and climate change. In Water Conservation in the Era of Global Climate Change; Thokchom, B., Qiu, P., Singh, P., Parameswar, K.I., Eds.; Elsevier: Amsterdam, the Netherlands, pp. 23–45.

Shemer, H., Wald, S., Semiat, R. (2023). Challenges and Solutions for Global Water Scarcity. *Membranes*, 13, 612.

Sibanda, T., Nonner, J.C., Uhlenbrook, S. (2009). Comparisons of groundwater recharge estimation methods for the semi-arid Nyamandhlovu area, Zimbabwe. *Hydrogeol. J.*, 17, 1427.

Singh, A., Panda, S.N., Uzokwe, V.N., Krause, P. (2019). An assessment of groundwater recharges estimation techniques for sustainable resource management. *Groundw. Sustain. Dev*., 9, 100218.

Sun, J., Li, B., Wang, W., Yan, X., Li, Q., Li, Z. (2024). Variations and controls on groundwater recharge estimated by combining the water-table fluctuation method and Darcy's law in a loess tableland in China. *Hydrogeol. J*., 32, 379–394.

Tamagnone, P., Comino, E., Rosso, M. (2020). Rainwater harvesting techniques as an adaptation strategy for flood mitigation. *J. Hydrol*., 586, 124880.

Teston, A., Scolaro, T.P., Maykot, J.K., Ghisi, E. (2022). Comprehensive Environmental Assessment of Rainwater Harvesting Systems: A Literature Review. *Water*, 14, 2716.

Umukiza, E., Abagale, F.K., Apusiga Adongo, T., Petroselli, A. (2024). Suitability Assessment and Optimization of Small Dams and Reservoirs in Northern Ghana. *Hydrology*, 11, 166.

Umukiza, E., Ntole, R., Chikavumbwa, S.R., Bwambale, E., Sibale, D., Jeremaih, Z., Petroselli, A. (2023). Rainwater harvesting in arid and semi-arid lands of Africa: Challenges and opportunities. *Acta Sci. Pol-Form. C*., 22(2), 41–52.

Vema, V., Sudheer, K.P., Chaubey, I. (2018). Hydrologic design of water harvesting structures through simulation-optimization framework. *Journal of Hydrology*, 563, 460–469. DOI:10.1016/j.jhydrol.2018.06.020

Wang, W., Zaiyong, Z., Lihe, Y., Lei, D., Jinting, H. (2021). Topical Collection: Groundwater recharge and discharge in arid and semi-arid areas of China. *Hydrogeol. J*., 29, 521–524.

Wartalska, K., Grzegorzek, M., Bełcik, M., Wdowikowski, M., Kolanek, A., Niemierka, E., Ka´zmierczak, B. (2024). The Potential of Rain Water Harvesting Systems in Europe–Current State of Art and Future Perspectives. *Water Resour. Manag*., 38, 4657–4683.

Wijesinghe, C., Mishra, K., Withanage, C., Abdelrahman, K., Mishra, V., Tripathi, S., Fnais, M.S. (2023). Application of GIS, Multi-Criteria Decision-Making techniques for mapping groundwater potential zones: A case study of Thalawa division, Sri Lanka. *Water*, 15(19):1–20.

Wittenberg, H., Aksoy, H., Miegel, K. (2019). Fast response of groundwater to heavy rainfall. *J. Hydrol.,* 571, 837–842.

Woldearegay, K., Tamene, L., Mekonnen, K., Kizito, F., & Bossio, D. (2017). Fostering food security and climate resilience through integrated landscape restoration practices and rainwater harvesting/management in arid and semi-arid areas of Ethiopia. In *Rainwater-smart agriculture in arid and semi-arid areas: fostering the use of rainwater for food security, poverty alleviation, landscape restoration and climate resilience* (pp. 37-57). Cham: Springer International Publishing.

World Economic Forum Water Initiative. (2011). Water security: the water-food-energy-climate nexus. Island Press.

Yannopoulos, S., Giannopoulou, I., Kaiafa-Saropoulou, M. (2019). Investigation of the Current Situation and Prospects for the Developmen of Rainwater Harvesting as a Tool to Confront Water Scarcity Worldwide. *Water,* 11, 2168.

Yonas, G.H., Tesfa, G.A. (2021). Geospatial and multi-criteria decision approach for the groundwater potential zone identification in the Cuma sub-basin, South Ethiopia. *Heliyon*, 7:1–7

Zhang, H., Xu, Y., Kanyerere, T. (2020). A review of the managed aquifer recharge: Historical development, current situation and perspectives. *Phys. Chem. Earth*, 118–119, 102887.

Zhao, Y., Zhang, M., Liu, Z., Ma, J., Yang, F., Guo, H., Fu, Q. (2024). How Human Activities Affect Groundwater Storage. *Research*, 7, 0369.

Zhou, J., Pang, Y., Fu, G., Wang, H., Zhang, Y., & Memon, F. A. (2023). A review of urban rainwater harvesting in China. *Water Reuse*, 13(1), 1-17.

APPENDICES

Appendix A: Infiltration Test Data for 10 Selected Site Locations of the Study Area

Table 1: Infiltration test for location 1

Project name and test location				Constants		Ring Data		Liquid Containers	
Takua GPS (UTM: Adindan, 37 N X=504137, Y=1463208, Z=1596						Ring Area, A_r (cm^2)	Depth of Liquid (cm)	Reservoir Container Volume, V_r (cm^3/cm)	
						707	4	78.54	
Test by:	Hailay G/slassie		USCS Class:	Loam	Penetration of Ring in to soil (cm):			7.5	
Liquid Used:	Deep well Water		PH:		Ground Temp. (°C):			at Depth:	
Date of Test:	10/04/2025	Depth to Water Table:							
Liquid Level Maintained by using:		( ) Flow valve (*) Float valve ( ) Mariotte Tube ( ) Other:							
Additional Comments	Dry Ground								

Trial No		Time (hr:min)	Elapsed Time: Δ/Total (min)	Flow Reading		Liquid Temp. (°C)	Infiltration Rate, I** (cm/hr)	Remarks
				Elev., H (cm)	ΔH (cm) & Q_t* (cm^3)			
1	S	12:08	15	3	5.7		2.5	
	E	12:23	(15)	8.7	448			
2	S	12:23	15	8.7	4.8		2.1	
	E	12:38	(30)	13.5	377			
3	S	12:38	15	13.5	4.1		1.8	
	E	12:53	(45)	17.6	322			
4	S	12:53	15	17.6	3.4		1.5	
	E	01:08	(60)	21	267			

Table 2: Infiltration test for location 2

Project name and test location				Constants		Ring Data		Liquid Containers	
Gra-Dnkul GPS (UTM: Adindan, 37 N X=503741, Y=1463358, Z=1594						Ring Area, A_r (cm^2)	Depth of Liquid (cm)	Reservoir Container Volume, V_r (cm^3/cm)	
						707	4	78.54	
Test by:	Hailay G/slassie		USCS Class:	Loam	Penetration of Ring in to soil (cm):			7.5	
Liquid Used:	Deep well Water		PH:		Ground Temp. (°C):			at Depth:	
Date of Test:	10/04/2025	Depth to Water Table:							
Liquid Level Maintained by using:		( ) Flow valve (*) Float valve ( ) Mariotte Tube ( ) Other:							
Additional Comments	Dry Ground								

Trial No		Time (hr:min)	Elapsed Time: Δ/Total (min)	Flow Reading		Liquid Temp. (°C)	Infiltration Rate, I** (cm/hr)	Remarks
				Elev., H (cm)	ΔH (cm) & Q_t* (cm^3)			
1	S	01:30	15	0	7.6		3.4	
	E	01:45	(15)	7.6	597			
2	S	01:45	15	7.6	5.8		2.6	
	E	02:00	(30)	13.4	456			
3	S	02:00	15	13.4	5.4		2.4	
	E	02:15	(45)	18.8	424			
4	S	02:15	15	18.8	4.7		2.1	
	E	02:30	(60)	23.5	369			

Table 3: Infiltration test for location 3

Project name and test location				Constants		Ring Data		Liquid Containers	
Adera-Ruba GPS (UTM: Adindan, 37 N X=503247, Y=1462316, Z=1632						Ring Area, A_r (cm^2)	Depth of Liquid (cm)	Reservoir Container Volume, V_r (cm^3/cm)	
						707	4	78.54	
Test by:	Hailay G/slassie		USCS Class:	Loam	Penetration of Ring in to soil (cm):			7.5	
Liquid Used:	Open well Water		PH:		Ground Temp. (°C):			at Depth:	
Date of Test:	10/04/2025		Depth to Water Table:						
Liquid Level Maintained by using:		( ) Flow valve (*) Float valve ( ) Mariotte Tube ( ) Other:							
Additional Comments	Dry Ground								

Trial No		Time (hr:min)	Elapsed Time: Δ/Total (min)	Flow Reading		Liquid Temp. (°C)	Infiltration Rate, I** (cm/hr)	Remarks
				Elev., H (cm)	ΔH (cm) & Q_t* (cm^3)			
1	S	02:50	15	0	7.3		3.2	
	E	03:05	(15)	7.3	573			
2	S	03:05	15	7.3	6.9		3	
	E	03:20	(30)	14.2	542			
3	S	03:20	15	14.2	6.2		2.8	
	E	03:35	(45)	20.4	487			
4	S	03:35	15	20.4	5.9		2.6	
	E	03:50	(60)	26.3	463			

Table 4: Infiltration test for location 4

Project name and test location				SINGLE RING INFILTROMETER TEST DATA		Ring Data		Liquid Containers	
Eyebela GPS (UTM: Adindan, 37 N X=503800, Y=1462368, Z=1625				Constants		Ring Area, A_r (cm^2)	Depth of Liquid (cm)	Reservoir Container Volume, V_r (cm^3/cm)	
						707	4	78.54	
Test by:	Hailay G/slassie		USCS Class:	Clay	Penetration of Ring in to soil (cm):			7.5	
Liquid Used:	Open well Water		PH:		Ground Temp. (°C):			at Depth:	
Date of Test:	11/04/2025		Depth to Water Table:						
Liquid Level Maintained by using:		( ) Flow valve (*) Float valve ( ) Mariotte Tube ( ) Other:							
Additional Comments	Dry Ground								

Trial No		Time (hr:min)	Elapsed Time: Δ/Total (min)	Flow Reading		Liquid Temp. (°C)	Infiltration Rate, I** (cm/hr)	Remarks
				Elev., H (cm)	ΔH (cm) & Q_t* (cm^3)			
1	S	09:15	15	0	3.5		1.6	
	E	09:30	(15)	3.5	275			
2	S	09:30	15	3.5	2.9		1.3	
	E	09:45	(30)	6.4	228			
3	S	09:45	15	6.4	1.4		0.6	
	E	10:00	(45)	7.8	110			
4	S	10:00	15	7.8	0.7		0.3	
	E	10:15	(60)	8.5	55			

Table 5: Infiltration test for location 5

Project name and test location				Constants		Ring Data		Liquid Containers	
Durko GPS (UTM: Adindan, 37 N X=504372, Y=1463698, Z=1600						Ring Area, A_r (cm^2)	Depth of Liquid (cm)	Reservoir Container Volume, V_r (cm^3/cm)	
						707	4	78.54	
Test by:	Hailay G/slassie		USCS Class:	Sand	Penetration of Ring in to soil (cm):			7.5	
Liquid Used:	Hand pump well Water		PH:		Ground Temp. (°C):			at Depth:	
Date of Test:	11/04/2025	Depth to Water Table:							
Liquid Level Maintained by using:	( ) Flow valve (*) Float valve ( ) Mariotte Tube ( ) Other:								
Additional Comments	Dry Ground								

Trial No		Time (hr:min)	Elapsed Time: Δ/Total (min)	Flow Reading		Liquid Temp. (°C)	Infiltration Rate, I** (cm/hr)	Remarks
				Elev., H (cm)	ΔH (cm) & Q_t* (cm^3)			
1	S	10:42	15	0	6.4		2.8	
	E	10:57	(15)	6.4	503			
2	S	10:57	15	6.4	4.6		2	
	E	11:12	(30)	11	361			
3	S	11:12	15	11	3		1.3	
	E	11:27	(45)	14	236			
4	S	11:27	15	14	2.8		1.2	
	E	11:42	(60)	16.8	220			

Table 6: Infiltration test for location 6

Project name and test location				Constants		Ring Data		Liquid Containers	
Adi-Angeba GPS (UTM: Adindan, 37 N X=503843, Y=1464696, Z=1590						Ring Area, A_r (cm^2)	Depth of Liquid (cm)	Reservoir Container Volume, V_r (cm^3/cm)	
						707	4	78.54	
Test by:	Hailay G/slassie		USCS Class:	Sand	Penetration of Ring in to soil (cm):			7.5	
Liquid Used:	Tanker Water		PH:		Ground Temp. (°C):			at Depth:	
Date of Test:	11/04/2025	Depth to Water Table:							
Liquid Level Maintained by using:	( ) Flow valve (*) Float valve ( ) Mariotte Tube ( ) Other:								
Additional Comments	Dry Ground								

Trial No		Time (hr:min)	Elapsed Time: Δ/Total (min)	Flow Reading		Liquid Temp. (°C)	Infiltration Rate, I** (cm/hr)	Remarks
				Elev., H (cm)	ΔH (cm) & Q_t* (cm^3)			
1	S	12:40	15	0	8.5		3.8	
	E	12:55	(15)	8.5	668			
2	S	12:55	15	8.5	8		3.6	
	E	01:10	(30)	16.5	628			
3	S	01:10	15	16.5	7.3		3.2	
	E	01:25	(45)	23.8	573			
4	S	01:25	15	23.8	6.9		3	
	E	01:40	(60)	30.7	542			

Table 7: Infiltration test for location 7

Project name and test location				Constants		Ring Data		Liquid Containers	
Zbla GPS (UTM: Adindan, 37 N X=501976, Y=1466241, Z=1553						Ring Area, A_r (cm^2)	Depth of Liquid (cm)	Reservoir Container Volume, V_r (cm^3/cm)	
						707	4	78.54	
Test by:	Hailay G/slassie		USCS Class:	Clay and Silt	Penetration of Ring in to soil (cm):			7.5	
Liquid Used:	Pond Water		PH:		Ground Temp. (°C):			at Depth:	
Date of Test:	11/04/2025	Depth to Water Table:							
Liquid Level Maintained by using:	( ) Flow valve (*) Float valve ( ) Mariotte Tube ( ) Other:								
Additional Comments	Dry Ground								

Trial No		Time (hr:min)	Elapsed Time: Δ/Total (min)	Flow Reading		Liquid Temp. (°C)	Infiltration Rate, I** (cm/hr)	Remarks
				Elev., H (cm)	ΔH (cm) & Q_t* (cm^3)			
1	S	02:14	15	0	1.8		0.8	
	E	02:29	(15)	1.8	141			
2	S	02:29	15	1.8	1.3		0.6	
	E	02:44	(30)	3.1	102			
3	S	02:44	15	3.1	1.2		0.5	
	E	02:59	(45)	4.3	94			
4	S	02:59	15	4.3	0.9		0.4	
	E	03:14	(60)	5.2	71			

Table 8: Infiltration test for location 8

Project name and test location				Constants		Ring Data		Liquid Containers	
Baekel GPS (UTM: Adindan, 37 N X=501134, Y=1467701, Z=1515						Ring Area, A_r (cm^2)	Depth of Liquid (cm)	Reservoir Container Volume, V_r (cm^3/cm)	
						707	4	78.54	
Test by:	Hailay G/slassie		USCS Class:	Silt	Penetration of Ring in to soil (cm):			7.5	
Liquid Used:	Pond Water		PH:		Ground Temp. (°C):			at Depth:	
Date of Test:	11/04/2025	Depth to Water Table:							
Liquid Level Maintained by using:	( ) Flow valve (*) Float valve ( ) Mariotte Tube ( ) Other:								
Additional Comments	Dry Ground								

Trial No		Time (hr:min)	Elapsed Time: Δ/Total (min)	Flow Reading		Liquid Temp. (°C)	Infiltration Rate, I** (cm/hr)	Remarks
				Elev., H (cm)	ΔH (cm) & Q_t* (cm^3)			
1	S	04:40	15	0	5.1		2.3	
	E	04:55	(15)	5.1	401			
2	S	04:55	15	5.1	3.9		1.7	
	E	05:10	(30)	9	306			
3	S	05:10	15	9	2.8		1.2	
	E	05:25	(45)	11.8	220			
4	S	05:25	15	11.8	2.2		1	
	E	05:40	(60)	14	173			

Table 9: Infiltration test for location 9

Project name and test location				Constants		Ring Data		Liquid Containers
Humer GPS (UTM: Adindan, 37 N X=498941, Y=1467546, Z=1572						Ring Area, A_r (cm^2)	Depth of Liquid (cm)	Reservoir Container Volume, V_r (cm^3/cm)
						707	4	78.54
Test by:	Hailay G/slassie		USCS Class:	Clay	Penetration of Ring in to soil (cm):			7.5
Liquid Used:	Tanker Water		PH:		Ground Temp. (°C):		at Depth:	
Date of Test:	12/04/2025	Depth to Water Table:						
Liquid Level Maintained by using:	( ) Flow valve (*) Float valve ( ) Mariotte Tube ( ) Other:							
Additional Comments	Dry Ground							

Trial No		Time (hr:min)	Elapsed Time: Δ/Total (min)	Flow Reading		Liquid Temp. (°C)	Infiltration Rate, I** (cm/hr)	Remarks
				Elev., H (cm)	ΔH (cm) & Q_t* (cm^3)			
1	S	11:12	15	0	1.5		0.67	
	E	11:27	(15)	1.5	118			
2	S	11:27	15	1.5	0.9		0.4	
	E	11:42	(30)	2.4	71			
3	S	11:42	15	2.4	1		0.45	
	E	11:57	(45)	3.4	79			
4	S	11:57	15	3.4	0.8		0.35	
	E	12:12	(60)	4.2	63			

Table 10: Infiltration test for location 10

Project name and test location				Constants		Ring Data		Liquid Containers
Chewchew GPS (UTM: Adindan, 37 N X=500056, Y=1465995, Z=1565						Ring Area, A_r (cm^2)	Depth of Liquid (cm)	Reservoir Container Volume, V_r (cm^3/cm)
						707	4	78.54
Test by:	Hailay G/slassie		USCS Class:	Sand	Penetration of Ring in to soil (cm):			7.5
Liquid Used:	Tanker Water		PH:		Ground Temp. (°C):		at Depth:	
Date of Test:	12/04/2025	Depth to Water Table:						
Liquid Level Maintained by using:	( ) Flow valve (*) Float valve ( ) Mariotte Tube ( ) Other:							
Additional Comments	Dry Ground							

Trial No		Time (hr:min)	Elapsed Time: Δ/Total (min)	Flow Reading		Liquid Temp. (°C)	Infiltration Rate, I** (cm/hr)	Remarks
				Elev., H (cm)	ΔH (cm) & Q_t* (cm^3)			
1	S	01:10	15	0	10.5		4.7	
	E	01:25	(15)	10.5	825			
2	S	01:25	15	10.5	8.6		3.8	
	E	01:40	(30)	19.1	675			
3	S	01:40	15	19.1	7.9		3.5	
	E	01:55	(45)	27	620			
4	S	01:55	15	27	7.2		3.2	
	E	02:10	(60)	34.2	565			

Appendix B: Discontinuity Measurements

Table 1: Joint Measurements

S.N	GPS (UTM Zone: 37, Datum: Adindan			Joint set	Orientation	S. N	GPS (UTM Zone: 37, Datum: Adindan			Joint set	Orientation
	X	Y	Z				X	Y	Z		
1	506968	1463403	1672	1	280/vertical-subvertical	17	500374	1467594	1531	1	030/80 NW
				2	360/vertical-subvertical	18	498104	1461694	1689	1	295/subvertical
										2	030/ subvertical
										3	065/90
				3	085/vertical-subvertical	19	498875	1460380	1701	1	315/90
2	506590	1463820	1678	1	300/90	20	498584	1463224	1658	`1	320/subvertical
				2	360/90					2	345/ subvertical
				3	060/90					3	050/ subvertical
3	497571	1466061	1640	1	300/90	21	498060	1465131	1629	1	340/ subvertical
				2	345/90	22	499134	1462519	1623	1	335/ subvertical
				3	070/90					2	015/ subvertical
4	497195	1465272	1626	1	320/90					3	060/90
5	498324	1463501	1628		310/90	23	498882	1462257	1649	1	340/90
6	499964	1468528	1552	1	290/72 NE					2	025/90
				2	350/80 E	24	498733	1461422	1660	1	285/ subvertical
7	500360	1468057	1516	1	300/38 NW					2	018/ subvertical
				2	025/75 SE	25	498770	1466369	1590	1	300/90
8	500378	1467602	1521	1	015/55W					2	355/90
9	499902	1465658	1559	1	320/90					3	060/90
10	500077	1463920	1601	1	320/65 SW	26	499277	1463924	1622	1	330/subvertical
11	499400	1462127	1631	1	345/90	27	501178	1461857	1674	1	320/subvertical
12	498938	1461334	1664	1	340/90					2	345/90
13	500768	1469016	1523	1	285/subvertical	28	503617	1466225	1571	1	288/ subvertical
				2	045/subvertical					2	060/ subvertical
14	501228	1467886	1510	1	330/subvertical					3	350/ subvertical
				2	060/subvertical	29	497748	1461802	1720	1	300/ subvertical
				3	050/subvertical					2	045/subvertical
15	501232	1464881	1569	1	320/subvertical					3	070/90
				2	010/subvertical	30	497964	1462494	1698	1	345/90
16	501056	1464075	1575	1	340/subvertical					2	360/90

Table 2: Normal Fault measurements

S.N	GPS (UTM Zone: 37, Datum: Adindan			Strike	Dip	Dip Direction
	X	Y	Z			
1	505002	1463583	1625	354	66	86SW
2	505589	1463719	1633	340	67	70SW
3	505716	1463937	1652	340	60	70SW
4	505734	1464082	1662	346	85	76SW
5	505701	1464206	1687	300	89	30SW
6	505472	1464195	1684	354	75	84NE

Table 3: Summary of Results of discontinuity data measured at the four dominant rock units of the area

Lithology	Joint Set	Strike Range (deg.)	Dip amount (deg.)	Av. spacing (m)	Av. opening (cm)	Av. frequency (m)	Persistence (m)	Infillings	Remark
Sandstone	J1	280-340	Vertical/ Sub-vertical	1.5	5-10 (av.=7.5)	0.67	15-20	Soils/open	Rough , undulating, Slightly to Moderately weathered
	J2	345-360	Vertical/ Sub-vertical	1	2.5-5 (av.=3.8	1	10-15	Soils/open	Rough , undulating, Slightly to Moderately weathered
	J3	060-085	Vertical/ Sub-vertical	1	1-1.5 (av.=1.3)	1	3-5	Soils/open	Rough , undulating, Slightly to Moderately weathered
	B	Horizontal		1.5	5-10 (av.=7.5)	0.67	>20	Soils	Rough , Slightly to Moderately weathered
Dolerite	J1	315-350	Vertical/ Sub-vertical	1.6	1-3 (av.=2)	0.63	5-10	Soils/closed	Rough, moderately to highly weathered
	3 random joints	-	-	5*	0.3-0.7 (av.=0.5)	0.6	1-3	Soils	Rough, Highly weathered
Granite	J1	285-330	Vertical/ Sub-vertical	0.5	2-3 (av.=2.5)	2	5-10	Quartz and soils	Rough, Moderately to highly weathered
	J2	350-360	Vertical/ Sub-vertical	0.4	3-5 (av.=4)	2.5	3-5	Quartz and soils	Rough, Moderately to highly weathered
	J3	020-045	Vertical/ Sub-vertical	0.46	2-3 (av.=2.5)	2.2	5-10	Quartz and soils	Rough, Moderately weathered
	2 random joints	-	-	5*	0.5-1 (av.=0.8)	0.4	2-5	Quartz and soils	Rough, Moderately to highly weathered
Basement	J1	300-330	Sub-vertical	0.6	0.7-1.5 (av.=1.1)	1.7	3	Quartz and calcite	Smooth, Slightly weathered
	J2	025-060	Sub-vertical	0.7	0.5-5 (av.=2.8)	1.4	2	Quartz and calcite	Smooth, Slightly weathered
	F	040-060	40-75	-	-	-	0.5-1	Quart and calcite	Wavy, Smooth, Slightly weathered
	Sh	015-060	Sub-vertical	-	-	-	>20	Quartz and calcite	Rough, stepped, mineral stain alteration

J1-Joint set 1, J2-Joint set 2, J3-Joint set 3, F-Foliation, Sh- Shearing, B-Bedding, 5-spacing of random joints*

Appendix C: Uniaxial Compressive Strength (Schmidt hammer) tests

Table 1: Summary of Results of L-type Schmidt hammer Test for the study area

Test No	Location (UTM Zone: 37, Datum: Adindan)			Lithology	Mean Rebound	Average UCS (Mpa)	*Qualitative Strength
	X	Y	Z				
1	506968	1463403	1672	Sandstone	36	58	Moderately Strong
2	506590	1463820	1678	Sandstone	29	41	Moderately Strong
3	500768	1469016	1523	Granite	59	260	Extremely Strong
4	501499	1468709	1501	MV	53	230	Extremely Strong
5	501253	1468149	1509	MV	48	180	Very Strong
6	501228	1467886	1510	MV	42	140	Very Strong
7	501287	1465674	1559	Sandstone	40	69	Moderately Strong
8	501232	1464881	1569	Sandstone	38	65	Moderately Strong
9	501056	1464075	1575	Sandstone	45	89	Moderately Strong
10	501036	1462454	1634	Sandstone	48	102	Strong
11	501102	1462161	1641	Dolerite	50	175	Very Strong
12	500362	1461836	1648	Dolerite	41	102	Strong
13	499126	1462020	1670	Slate-phyllite	47	140	Very Strong
14	498983	1462114	1653	Slate-phyllite	42	105	Strong
15	500493	1467785	1523	MV	48	180	Very Strong
16	499954	1465491	1557	Sandstone	34	52	Moderately Strong
17	501621	1462024	1646	Dolerite	30	56	Moderately Strong
18	500624	1461381	1638	Dolerite	51	180	Very Strong
19	498829	1461470	1641	Dolerite	48	160	Very Strong
20	500152	1469145	1542	Granite	54	200	Very Strong
21	497571	1466061	1640	Sandstone	30	43	Moderately Strong
22	497195	1465272	1626	Sandstone	25	33	Moderately Strong
23	498324	1463501	1628	Sandstone	40	69	Moderately Strong
24	499313	1464662	1583	Sandstone	38	65	Moderately Strong
25	499964	1468528	1552	Granite	56	220	Very Strong
26	504660	1461175	1643	Dolerite	22	28	Moderately Strong
27	503531	1461544	1653	Dolerite	45	130	Very Strong
28	503324	1461958	1636	Dolerite	49	165	Very Strong
29	502067	1461789	1646	Dolerite	46	135	Very Strong
30	501881	1463517	1596	Sandstone	39	67	Moderately Strong

** Based on IAEG Classification system as cited in Berhane and Ayenew (2010).*

Appendix D: Laboratory Soil Texture Analysis

Table 1: Sieve Analysis Results for Fluvial Soils

S.Code	U.S Sieve	Opening (mm)	Wt. sieve + soil (g)	Wt. sieve (g)	Wt. soil (g)	Cumulative Wt. retained above each sieve (g)	% finer
SS1	4	4.75	414.9	414.9	0	0	100
	10	2	385.55	384.72	0.83	0.83	99.83
	20	0.85	484.93	474.83	10.1	10.93	97.81
	40	0.425	489.68	422.18	67.5	78.43	84.31
	60	0.25	597.91	393.64	204.27	282.7	43.46
	80	0.18	510.97	398.25	112.72	395.42	20.91
	100	0.15	467.35	428.88	38.47	433.89	13.22
	200	0.075	444.41	387.04	57.37	491.26	1.74
	pan	-	533.73	525.01	8.72	499.98	0
SS2	4	4.75	414.9	414.9	0	0	100
	10	2	386.58	384.72	1.86	1.86	99.6
	20	0.85	528.07	474.83	53.24	55.1	89
	40	0.425	579.17	422.18	156.99	212.09	57.6
	60	0.25	609.84	393.64	216.2	428.29	14.5
	80	0.18	444.79	398.25	46.54	474.8	5.2
	100	0.15	441.87	428.88	12.99	487.79	2.6
	200	0.075	398.73	387.04	11.69	499.48	0.25
	pan	-	526.27	525.01	1.26	500.74	0
SS4	4	4.75	414.9	414.9	0	0	100
	10	2	385.39	384.72	0.67	0.67	99.9
	20	0.85	494.24	474.83	19.41	20.08	96
	40	0.425	517.87	422.18	95.69	115.77	69
	60	0.25	604.88	393.64	211.24	327.01	34.7
	80	0.18	508.25	398.25	110	437.01	12.7
	100	0.15	462.90	428.89	34.01	471.02	6
	200	0.075	414.36	387.04	27.32	498.34	0.5
	pan	-	527.41	525.01	2.4	500.74	0
SS5	4	4.75	414.9	414.9	0	0	100
	10	2	418.96	384.72	34.24	34.24	93.2
	20	0.85	592.04	474.80	117.24	151.48	69.8
	40	0.425	526.20	422.15	104.05	255.53	49
	60	0.25	509.43	393.60	115.83	371.36	26
	80	0.18	453.04	398.25	54.79	426.15	15
	100	0.15	451.08	428.88	22.2	448.35	10.5
	200	0.075	427.84	387.05	40.79	489.14	2.4
	pan	-	536.89	525.00	11.89	5001.03	0
SS6	4	4.75	414.9	414.9	0	0	100
	10	2	388.53	384.26	4.27	4.27	99
	20	0.85	509.77	474.88	34.89	39.16	92.2
	40	0.425	533.77	422.40	111.37	150.53	70
	60	0.25	579.29	393.69	185.60	336.13	33
	80	0.18	480.88	398.03	82.85	418.98	16.5
	100	0.15	457.00	428.67	28.33	447.31	11
	200	0.075	434.72	386.65	48.07	495.38	1.3
	pan	-	531.60	525.01	6.59	501.97	0
SS8	4	4.75	414.9	414.9	0	0	100
	10	2	392.03	384.26	7.77	7.77	98.5
	20	0.85	689.38	474.88	214.50	221.86	55.8
	40	0.425	571.20	422.39	148.81	370.88	26
	60	0.25	476.22	393.69	82.53	453.46	9.6
	80	0.18	418.68	398.03	20.65	473.89	5.5
	100	0.15	436.09	428.67	7.42	481.1	4
	200	0.075	398.45	386.65	11.8	493.48	1.6
	pan	-	532.93	525.01	7.92	501.40	0
SS10	4	4.75	414.9	414.9	0	0	100
	10	2	399.68	384.72	14.96	14.96	97
	20	0.85	665.56	474.83	190.73	205.69	59
	40	0.425	534.91	422.18	112.73	318.42	36.5
	60	0.25	493.64	393.64	100	418.42	16.6

	80	0.18	439.30	398.25	41.05	459.47	8.4
	100	0.15	444.96	428.88	16.08	475.55	5.2
	200	0.075	408.96	387.04	21.92	497.47	0.8
	pan	-	529.04	525.01	4.03	501.5	0

Table 2: Sieve Analysis Results for Residual Soils

S.Code	U.S Sieve	Opening (mm)	Wt. sieve + soil (g)	Wt. sieve (g)	Wt. soil (g)	Cumulative Wt. retained above each sieve (g)	% finer
SP1	4	4.75	455.12	415.06	40.06	40.06	92
	10	2	418.23	384.26	33.97	74.03	85.2
	20	0.85	522.96	474.58	48.38	122.41	75.5
	40	0.425	455.38	422.67	32.71	155.12	69
	60	0.25	450.14	393.64	56.5	211.62	57.6
	80	0.18	436.94	398.23	38.71	250.33	50
	100	0.15	443.31	428.82	14.49	264.82	47
	200	0.075	439.31	386.58	52.73	317.55	36.5
	pan	-	544.24	362.02	182.22	499.77	0
SP2	4	4.75	415.06	415.06	0	0	100
	10	2	385.70	384.26	1.44	1.44	99.7
	20	0.85	522.79	474.58	48.21	49.65	90
	40	0.425	542.51	422.67	119.84	169.49	66
	60	0.25	546.15	393.64	152.51	322	35.6
	80	0.18	473.98	398.23	75.75	397.75	20.4
	100	0.15	458.54	428.82	29.72	427.47	14.5
	200	0.075	434.80	386.58	48.22	475.69	4.8
	pan	-	549.06	525.01	24.05	499.74	0
SP3	4	4.75	418.52	415.02	3.5	3.5	99.3
	10	2	390.74	384.36	6.38	9.88	98
	20	0.85	512.63	475.05	37.58	47.46	90.5
	40	0.425	471.72	422.55	49.17	96.63	80.7
	60	0.25	469.71	393.99	75.72	172.35	65.5
	80	0.18	523.11	398.47	124.64	296.99	40.6
	100	0.15	517.54	428.88	88.66	385.65	22.8
	200	0.075	476.75	386.68	90.07	475.72	4.8
	pan	-	548.34	524.49	23.85	499.57	0
SP4	4	4.75	418.26	414.97	3.29	3.29	99
	10	2	393.69	384.26	9.43	12.72	97.5
	20	0.85	524.54	474.95	49.59	62.31	87.5
	40	0.425	564.14	422.81	141.33	20.64	59.3
	60	0.25	560.09	393.83	166.26	369.9	26.26
	80	0.18	428.63	398.17	30.46	400.36	20
	100	0.15	465.02	428.69	36.33	436.69	12.6
	200	0.075	429.57	386.61	42.96	479.65	4
	pan	-	544.54	524.42	20.12	499.77	0
SP5	4	4.75	416.79	416.79	0	0	100
	10	2	385.03	384.09	0.93	0.93	99.8
	20	0.85	493.16	479.22	13.94	14.87	97
	40	0.425	576.92	430.69	146.23	161.1	67.8
	60	0.25	533.17	401.64	131.53	292.63	41.5
	80	0.18	451.87	403.47	48.4	341.03	31.8
	100	0.15	439.63	435.43	4.2	345.23	31
	200	0.075	414.38	390.84	23.54	368.77	26.3
	pan	-	658.60	526.99	131.61	500.38	0
SP6	4	4.75	422.03	415.01	7.02	7.02	98.6
	10	2	401.00	384.33	16.67	23.69	95.3
	20	0.85	556.00	475.06	80.94	104.63	79
	40	0.425	503.15	422.38	80.77	185.4	63
	60	0.25	492.11	393.70	98.41	283.81	43.3
	80	0.18	458.33	398.17	60.16	343.97	31.2
	100	0.15	459.66	428.61	31.05	375.02	25
	200	0.075	463.59	386.68	76.91	451.93	9.6
	pan	-	572.71	524.35	48.36	500.29	0
SP7	4	4.75	415.51	414.90	0.61	0.61	99.9

	10	2	392.38	384.26	8.12	8.73	98.3
	20	0.85	555.35	474.80	80.55	89.28	82.2
	40	0.425	528.16	422.39	105.77	195.05	61
	60	0.25	509.37	393.69	115.68	310.73	37.9
	80	0.18	458.58	398.03	60.55	371.28	25.8
	100	0.15	457.13	428.67	28.46	399.74	20
	200	0.075	445.51	386.65	58.86	458.60	8.3
	pan	-	565.96	524.39	41.57	500.17	0
SP8	4	4.75	414.90	414.90	0	0	100
	10	2	390.24	384.26	5.98	5.98	98.8
	20	0.85	497.15	474.80	22.35	28.33	94.3
	40	0.425	443.41	422.39	21.02	49.35	90.1
	60	0.25	427.05	393.69	33.36	82.71	83.4
	80	0.18	409.82	398.03	11.79	94.50	81
	100	0.15	440.26	428.67	11.59	106.09	78.8
	200	0.075	434.65	386.65	48	154.09	69.1
	pan	-	862.45	517.12	345.33	499.42	0
SP9	4	4.75	414.90	414.90	0	0	100
	10	2	390.24	384.26	5.98	5.98	98.8
	20	0.85	497.15	474.80	22.35	28.33	94.3
	40	0.425	443.41	422.39	21.02	49.35	90.1
	60	0.25	427.05	393.69	33.36	82.71	83.4
	80	0.18	409.82	398.03	11.79	94.50	81
	100	0.15	440.26	428.67	11.59	106.09	78.8
	200	0.075	434.65	386.65	48	154.09	69.1
	pan	-	862.45	517.12	345.33	499.42	0
SP13	4	4.75	414.9	414.9	0	0	100
	10	2	403.17	384.72	6.33	6.33	98.8
	20	0.85	495.05	474.83	20.22	26.55	94.8
	40	0.425	440.97	422.18	18.79	45.34	91.2
	60	0.25	424.08	393.64	30.44	75.78	85.2
	80	0.18	410.49	398.26	12.23	88.01	82.8
	100	0.15	439.54	428.88	10.66	98.67	80.8
	200	0.075	417.31	386.58	30.73	129.4	74.8
	pan	-	908.19	525.01	383.18	512.58	0

Table 3: Soil Hydrometer analysis results

Input Parameters	
viscosity of water at 25oC temperature	0.00000922g s/cm2
Gs	2.65
Wieght of dry soil	60g
Zero correction	2g
Mniscous correction	1

S.C	Time (min)	Ra	T	Tc	Rc = Ra-Zc+Tc	%Finer = (Rc*a)/Ws	R corrected for miniscous	L = 16.3-0.164R	K = √(30η/(Gs-1))	D(mm) = K(L/t)^(1/2)	Actual % finer wrt to total fines in soil mass
										0.075	**36.5**
	0.5	40	22	0.4	38.4	64.00	41	9.6	0.0133	0.058	23.36
	1	25	22	0.4	23.4	39.00	26	12.0	0.0133	0.046	14.24
	2	7	22	0.4	5.4	9.00	8	15.0	0.0133	0.036	3.29
	4	6	22	0.4	4.4	7.33	7	15.2	0.0133	0.026	2.68
	8	5	22	0.4	3.4	5.67	6	15.3	0.0133	0.018	2.07
SP1	15	5	22	0.4	3.4	5.67	6	15.3	0.0133	0.013	2.07
	30	5	22	0.4	3.4	5.67	6	15.3	0.0133	0.010	2.07
	60	5	22	0.4	3.4	5.67	6	15.3	0.0133	0.007	2.07
	120	4	22	0.4	2.4	4.00	5	15.5	0.0133	0.005	1.46
	240	4	23	0.7	2.7	4.50	5	15.5	0.0132	0.003	1.64
	480	3	23	0.7	1.7	2.83	4	15.6	0.0132	0.002	1.03
	1440	3	21	0.2	1.2	2.00	4	15.6	0.0135	0.001	0.73

SP5										**0.075**	**26.3**
	0.5	27	22	0.4	25.4	42.33	28	11.7	0.0133	0.064	11.13
	1	25	22	0.4	23.4	39.00	26	12.0	0.0133	0.046	10.26
	2	20	22	0.4	18.4	30.67	21	12.9	0.0133	0.034	8.07
	4	10	22	0.4	8.4	14.00	11	14.5	0.0133	0.025	3.68
	8	9	22	0.4	7.4	12.33	10	14.7	0.0133	0.018	3.24
	15	8	22	0.4	6.4	10.67	9	14.8	0.0133	0.013	2.81
	30	7	22	0.4	5.4	9.00	8	15.0	0.0133	0.009	2.37
	60	7	22	0.4	5.4	9.00	8	15.0	0.0133	0.007	2.37
	120	6	22	0.4	4.4	7.33	7	15.2	0.0133	0.005	1.93
	240	5	23	0.7	3.7	6.17	6	15.3	0.0132	0.003	1.62
	480	5	23	0.7	3.7	6.17	6	15.3	0.0132	0.002	1.62
	1440	4	21	0.2	2.2	3.67	5	15.5	0.0135	0.001	0.96
SP9										**0.075**	**69.1**
	0.5	6	22	0.4	4.4	7.33	7	15.2	0.0133	0.073	5.07
	1	5	22	0.4	3.4	5.67	6	15.3	0.0133	0.052	3.92
	2	5	22	0.4	3.4	5.67	6	15.3	0.0133	0.037	3.92
	4	4	22	0.4	2.4	4.00	5	15.5	0.0133	0.026	2.76
	8	4	22	0.4	2.4	4.00	5	15.5	0.0133	0.019	2.76
	15	4	22	0.4	2.4	4.00	5	15.5	0.0133	0.014	2.76
	30	4	22	0.4	2.4	4.00	5	15.5	0.0133	0.010	2.76
	60	4	22	0.4	2.4	4.00	5	15.5	0.0133	0.007	2.76
	120	3	22	0.4	1.4	2.33	4	15.6	0.0133	0.005	1.61
	240	3	23	0.7	1.7	2.83	4	15.6	0.0132	0.003	1.96
	480	3	23	0.7	1.7	2.83	4	15.6	0.0132	0.002	1.96
	1440	2	21	0.2	0.2	0.33	3	15.8	0.0135	0.001	0.23
SP13										**0.075**	**74.8**
	0.5	40	22	0.4	38.4	64.00	41	9.6	0.0133	0.058	47.87
	1	35	22	0.4	33.4	55.67	36	10.4	0.0133	0.043	41.64
	2	25	22	0.4	23.4	39.00	26	12.0	0.0133	0.033	29.17
	4	16	22	0.4	14.4	24.00	17	13.5	0.0133	0.024	17.95
	8	8	22	0.4	6.4	10.67	9	14.8	0.0133	0.018	7.98
	15	6	22	0.4	4.4	7.33	7	15.2	0.0133	0.013	5.49
	30	4	22	0.4	2.4	4.00	5	15.5	0.0133	0.010	2.99
	60	3	22	0.4	1.4	2.33	4	15.6	0.0133	0.007	1.75
	120	3	22	0.4	1.4	2.33	4	15.6	0.0133	0.005	1.75
	240	2	23	0.7	0.7	1.17	3	15.8	0.0132	0.003	0.87
	480	2	23	0.7	0.7	1.17	3	15.8	0.0132	0.002	0.87
	1440	2	21	0.2	0.2	0.33	3	15.8	0.0135	0.001	0.25